DBS DYNAMICS OF MEMRISTIVE LIF NEURON SYSTEM

PROJECT REPORT

Submitted by

ANNA JOY

Register No: AM20PHY002

Under the guidance of

DR. MARY VINAYA

In partial fulfillment of the requirement for the award

Of

MASTERS DEGREE OF SCIENCE IN

PHYSICS

ST.TERESA'S COLLEGE (AUTONOMOUS),

ERNAKULAM, KOCHI-682011

ST. TERESAS COLLEGE, ERNAKULAM

MSc PHYSICS
PROJECT REPORT

Name : ANNA JOY

Register No. : AM20PHY002

Year of work : 2020-2022

This is to certify that the project "DBS DYNAMICS OF MEMRISTIVE LIF NEURON SYSTEM" was done by ANNA JOY.

Staff member in charge
Dr. Mary Vinaya

Head of the Department
Priya

Submitted for the university examination held in St. Teresa's College (Autonomous), Ernakulam.

Examiners 1) Dr. Issac Paul,

2) Dr. Grichamol Mathew

Date: 13.06.2022

ST.TERESA'S COLLEGE

(AUTONOMOUS)

ERNAKULAM

CERTIFICATE

This is to certify that the project report title **"DBS DYNAMICS OF MEMRISTIVE LIF NEURON SYSTEM"** submitted by **ANNA JOY**, towards partial fulfillment of the requirements for the award of the degree of Master of Physics is a record of bonafide work carried out by them during the academic year 2020-2022.

Supervising guide

Dr. Mary Vinaya

Assistant professor

Department of Physics

Head of the department

Dr. Priya Parvathi Ameena Jose

Associate Professor

Department of Physics

PLACE: Ernakulam

DATE: 13-06-2022

DECLARATION

I, ANNA JOY, Register No. AM20PHY002, Department of Physics, St. Teresa's College (Autonomous), Ernakulam do hereby declare that this project work entitled **"DBS DYNAMICS OF MEMRISTIVE LIF NEURON SYSTEM"** submitted to Mahatma Gandhi University, Kottayam in partial fulfillment of the requirements for the award of the degree of Master of Science in Physics is a record of original work done by us under the supervision of Dr. Mary Vinaya, Assistant Professor, St. Teresa's College (Autonomous), Ernakulam.

Place: Ernakulam

Date:13/06/2022

ACKNOWLEDGEMENT

Every project big or small is successful largely due to the effort of a number of wonderful people who have always given their valuable or extensive cooperation.

First and foremost we would like to thank God Almighty for showering his blessings on us in this endeavor.

We express our sincere gratitude to Dr. Mary Vinaya, Assistant Professor, Department of Physics, St. Teresa'a College (Autonomous), Ernakulam, under whose able guidance and supervision, we could complete our project. Her extensive cooperation and valuable guidance were the light in the dark for us in the course of this project.

We take this opportunity to thank Dr. Priya Parvathy Ameena Jose, Head of the Physics Departmet for the generous concern and support given to us. We express our sincere sense of gratitude to both teaching and non-teaching staffs of Department of Physics, St. Teresas College (Autonomous), Ernakulam, for extending facilities required from time to time.

We would like to thank each and every one who has contributed to this work by their unfailing support throughout the preparation of the project.

DBS DYNAMICS OF MEMRISTIVE LIF NEURON SYSTEM

CONTENTS

Abstract……...1

Chapter 1: NON LINEAR DYNAMICS

1.1 Dynamical systems……...2

1.2 Linearity versus Non linearity ……3

1.3 Nonlinear systems……4

1.4 Characteristics of nonlinear systems……5

1.5 Characterization of nonlinear systems…….9

Chapter 2: NEURAL NETWORK

2.1 What is a Neuron?.....10

2.2 Structure of a Neuron……..11

2.3 What is Synapse?.....12

2.4 Neurotransmitters and Action potential……..14

2.5 Communication of Neurons……15

Chapter 3: REVIEW OF BRAIN STIMULATION ON TM MODEL

3.1 Deep Brain Stimulation……..17

3.2 Tsodyks-Markram (TM) model……19

3.3 Synaptic response to DBS……...……...21

Chapter 4: THE LIF SPIKING NEURON MODEL

4.1 Introduction……..……...……..……..24

4.2 Post-synaptic neuron firing…….26

4.3 Result……..27

Chapter 5: DYNAMICS OF MEMRISTIVE LIF MODEL UNDER DEEP BRAIN STIMULATION

5.1 Introduction……38

5.2 Memristor properties……..40

5.3 The Memristive LIF (MLIF) spiking neuron model……..44

5.4 Result…….…..…46

Chapter 6: DISCUSSION…….…67

MATLAB code for TM Model……69

MATLAB code for LIF Neuron Model……...73

MATLAB code for MLIF Neuron Model……...…78

REFERENCES……84

ABSTRACT

Deep brain stimulation (DBS) is a successful clinical therapy for a wide range of neurological disorders; however, the physiological mechanisms of DBS remain unresolved. While many different hypotheses currently exist, our analyses suggest that high frequency (130 Hz) stimulation-induced synaptic suppression represents the most basic concept that can be directly reconciled with experimental recordings of spiking activity in neurons that are being driven by DBS inputs.

The goal of this project was to develop a simple model system to characterize the excitatory post-synaptic currents (EPSCs) and action potential signaling generated in a neuron that is strongly connected to pre-synaptic glutamatergic inputs that are being directly activated by DBS.

We used the Tsodyks-Markram (TM) phenomenological synapse model to represent depressing, facilitating, and pseudo-linear synapses driven by DBS over a wide range of stimulation frequencies. The EPSCs were then used as inputs to a leaky integrate-and-fire neuron model (LIF) and later to a memristor leaky integrate-and-fire neuron model (MLIF) in order to measure the DBS-triggered post-synaptic spiking activity.

The result we obtained is that the synaptic suppression was a robust feature of high frequency stimulation, independent of the synapse type and MLIF neuron model exhibits greater spiking activity than LIF neuron model.

CHAPTER 1

NON-LINEAR DYNAMICS

1.1 Dynamical systems

Dynamical systems are found all around us. A dynamical system is a system whose state is distinctively specified by a set of variables and whose behavior is outlined by certain predefined rules. Some examples of dynamical systems are population growth, a swinging pendulum, the motions of celestial bodies, and the behavior of "rational" individuals playing a negotiation game, to name a few. If you assume that individuals make decisions always perfectly rationally, then the decision making process becomes deterministic, and therefore the interactions among them may be modeled as a deterministic dynamical system. Of course, this doesn't guarantee whether it is a good model or not [1]. The main reason behind studying dynamic systems is to predict system behavior and to control it.

Dynamical systems first developed from the geometry of Newton's equations and the question of the stability of the solar system motivated further researches inspired by celestial mechanics. Then dynamical systems developed intensively from stability theory (Lyapunov's theory) to generic properties (based on functional analysis techniques,) hyperbolic structures and to perturbation theory [2].

Dynamical systems are deterministic mathematical models, where time can be either a continuous or a discrete variable. Both qualitative and quantitative properties of such models are of interest to researchers [3]. Dynamical systems are usually studied in order to figure out their complex behaviors such as chaos, hyperchaos, transient chaos, bursting oscillations, mixed mode oscillations, multistability and extreme multistability [4].

The equations representing a dynamical system describe the change in time of variables taken to adequately describe the target system and these equations are referred to as dynamical or evolution equations. A complete specification of the initial state of such equations is referred to as the initial conditions for the model, while a characterization of the boundaries for the model domain are

known as the boundary conditions. A simple example of a dynamical system would be the equations modelling a particular chemical reaction, where a set of equations relates the temperature, pressure, amounts of the various compounds and their reaction rates. The boundary condition might be that the container walls are maintained at a fixed temperature. The initial conditions would be the starting concentrations of the chemical compounds. The dynamical system would then be taken to describe the behavior of the chemical mixture over time [3].

The variables that completely describe the state of the dynamical system are called the state variables. The set of all the possible values of the state variables is the state space. An instantaneous state is taken to be characterized by the instantaneous values of the variables considered crucial for a complete description of the state. The state space can be discrete, consisting of isolated points, such as if the state variables could only take on integer values. It could be continuous, consisting of a smooth set of points, such as if the state variables could take on any real value. The number of state variables is the dimension of the dynamical system. The state space can also be infinite-dimensional. When the state of the system is fully characterized by position and momentum variables, the resulting space is often called a phase space. A model can be studied in state space by following its trajectory, which is a history of the model's behavior in terms of its state transitions from the initial state to some chosen final state [3, 4].

1.2 Linearity Versus Non linearity

Linear systems are rare in nature. A linear system is one in which the cause produces a constant proportionality effect. The dynamics of a linear system can be reconstructed by summing up the individual causes acting on a single component. Small initial errors in prediction or from a random measurement grow linearly over time. Linear phenomena are concerned with inter relationship between cause and effect, which can be determined with great accuracy.

A linear system can be characterized in several different ways. Its dynamics can be represented by a system of linear differential equations (for continuous-time systems) or linear difference equations (for discrete-time systems). It has a

transfer function and obeys the law of superposition. A sinusoidal input produces a sinusoidal output of the same frequency. One of the most common ways to test for a system's linearity is by verifying if it follows the law of superposition. Superposition is composed of two parts, scaling and additively.

Nonlinear systems are ubiquitous in nature. A nonlinear system is simply one that is not linear. However, there are several reasons why a system might be nonlinear, and different classes of nonlinearities come about because of different physical reasons.

1.3 Nonlinear systems

A nonlinear system is a system in which the variation in the output is not proportional to the variations occurring in the input. As most real physical systems are inherently nonlinear in nature, nonlinear systems are of great interest to physicists, engineers and mathematicians [5]. For a nonlinear system a small change in a parameter may cause sudden and dramatic changes, resulting in a complex and unpredictable trajectory. A curve for a nonlinear system consists of a smooth curve, wiggles, an abrupt cut-off or any number of different types of lines. That is a nonlinear system can be considered as a sum of its parts. A small initial error in prediction or from a random measurement grows exponentially over time. A large scale deviation and huge unpredictable effects can take place from small initial changes.

The behavior of a nonlinear system is described in mathematics by a nonlinear system of equations. In a nonlinear system of equations, the equation(s) to be solved cannot be written as a linear combination of the unknown variables or functions that appear in them. Non-linear dynamic systems do not obey superposition principle. They have multiple isolated equilibrium points. The state of an unstable nonlinear system can reach up to infinity in finite time [6]. Nonlinear equations are difficult to be solved by analytical methods and give rise to interesting phenomena such as bifurcation, limit cycle and chaos.

The purpose of nonlinear dynamic systems is twofold. To begin with, it serves as an instrument to analyze information (e.g., EEG rhythms, eye developments, and so on). Second, it is utilized to show the various areas being scrutinized

(from neuroscience to imagination). Time and change are the two factors behind the strength of the nonlinear dynamic systems approach [7]. Nonlinearity might stay inactive or, lead to subjective changes of conduct contingent upon the values of the control parameters portraying the manner in which a framework has been at first ready or is being permanently requested by the external world [8].

1.4 Characteristics of nonlinear systems

1.4.1 Limit cycle

One peculiar behavior exhibited by nonlinear systems is a limit cycle. Although linear systems may oscillate, this oscillatory behavior cannot be explained in terms of linear theory. It is characterized by a constant amplitude and frequency determined by the nonlinear properties of the system irrespective of the initial conditions, external data inputs, or perturbations [9, 10].

A limit cycle is a closed trajectory in phase space exhibiting the property that at least one other trajectory spirals into it either as time approaches infinity or as time approaches negative infinity [10]. A limit cycle is said to be asymptotic stable if all trajectories nearby the limit cycle converge to it ast $\rightarrow \infty$. Otherwise the limit cycle is said semi-stable or unstable, that is, all neighboring trajectories approach it as time approaches negative infinity [11].

Stable limit cycles are vital scientifically, since they model systems that display self-sustained oscillations, for example systems which oscillate even without any external driving force (e.g. thumping of a heart, rhythms in body heat level, chemical discharge). In the event that the system is perturbed marginally, it always gets back to the stable limit cycle. If a system has a stable limit cycle, the system will tend to fall into the limit cycle, with the output approaching the amplitude of that limit cycle regardless of the initial condition and forcing function.

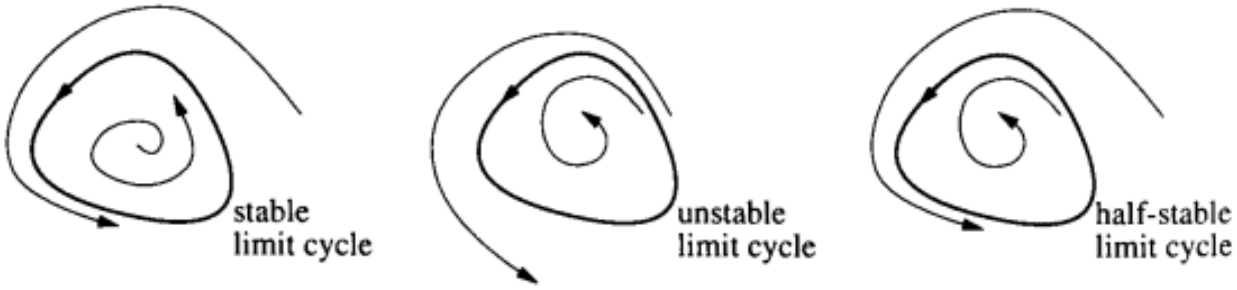

Fig. 1.1 Different types of Limit cycles

1.4.2 Bifurcation

As we mentioned earlier, a system's nonlinearities are not awakened gradually rather it involves a succession of explosive events in the form of instabilities. When the constraints exerted by environment reach certain threshold, small perturbation or small spontaneously arising fluctuations become amplified the system moves out from its basic state and is pushed toward a new regime called bifurcation.

Bifurcation in a nonlinear system can be defined as a change in behavior resulting from a small change in a parameter. By behavior, we mean a change in the number equilibrium points, a change in the type of equilibrium points (stable or unstable), or the emergence of a limit cycle. By small change in a parameter, we mean that there is a threshold above which the system exhibits one type of behavior and below it exhibits another [9].

When the initial state become unstable, it is replaced by a multitude of stable regimes that are accessible simultaneously. To decide which particular branch will be followed is decided by chance in the form of critical variation at that moment. This makes the system sensitive to parameters which controls the position of bifurcation point since two macroscopically indiscernible systems at same constraints follow entirely different path.

As system undergoes not just a single transition but a whole sequence of transition as the constraints are varied and its characteristics depend on the nature of nonlinearities present. One such phenomenon is deterministic chaos, where the transition eliminates in regime which is characterized by as irregular evolution of the variables in space and time.

1.4.3 Chaos

Chaos is the phenomenon of occurrence of bounded non periodic evolution, deterministic but not predictable, nonlinear dynamical systems with very high sensitive dependence on initial conditions. If we begin a system at two different initial conditions then the trajectories resulting from each initial condition may be extremely different from each other. Whereas in linear systems, two initial conditions that start close to each other will have trajectories that behave similarly and stay relatively close to each other.

The idea of Chaos theory was acquainted with the cutting edge world by Edward Lorenz in 1972 with conceptualization of "Butterfly Effect". A butterfly flapping its wings causes a hurricane on the other side of the world. The relatively small amplitude of butterfly wings is equivalent to a small change in initial condition. Surely a butterfly can't have much of an effect on atmospheric conditions. But even this small change is enough to make the difference between a nice sunny day and a storm (weather trajectory) in another part of the world. Knowledge of this hypothesis will assist with making a complex system more predictable [9].

In theoretical physics, chaos is a kind of moderated randomness that, unlike true randomness, contains complex patterns that are mostly unknown. The first evidence for an underlying design in chaos was observed by American physicist Mitchell Feigenbaum, who in 1976 discovered that when an ordered system begins to break down into chaos, a consistent pattern of rate doubling occurs [1]. In 1975, Yorke and Li showed a sustained periodic behavior could be found in 1-D maps. They coined the term chaos for the various phenomena that showed a periodicity along with sensitive dependence on initial conditions. In addition to showing that the existence of a periodic three orbit in 1-D continuous map implies sensitive dependence, they showed another remarkable consequence: the existence of infinitely many other periodic orbits.

If the equations governing a chaotic system and the initial conditions are known, then the behavior can be predicted by simple iteration. In practice, however, the initial condition can never be specified to 100% accuracy. This initial uncertainty, coupled with the sensitive dependence, means that such attempts at prediction are futile.

Other hallmarks of chaos include the existence of a dense set of unstable periodic orbits in its regime[12], positive Lyapunov exponents or finite Kolmogorov-Sinai entropy[13], continuous power spectrum, non-ergodicity, mixing (Arnold's cut map), as well as some other limiting properties [1].

Chaos is "ubiquitous". Interesting chaotic dynamical systems include:

- Hamiltonian systems of many different kinds,
- Digital filters, electrical and electronics systems,
- Celestial mechanics (the three-body problem),
- Laser, plasmas, solid state, and quantum mechanics,
- Nonlinear optics,
- Chemical reactions,
- Power systems,
- Neural networks,
- Economic behaviour, and
- Biological systems (heart, brain, population, etc.).

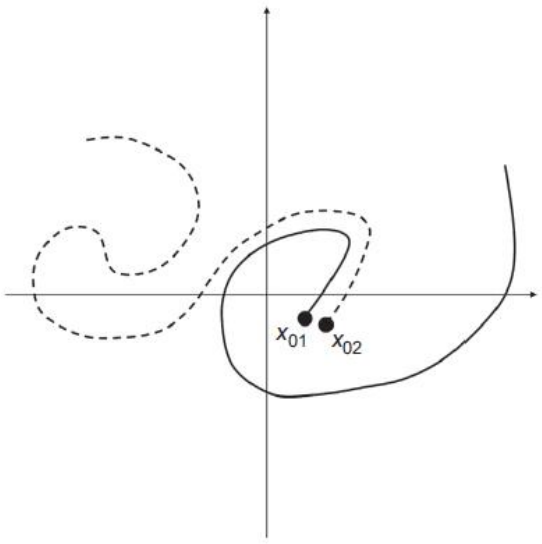

Fig.1.2 Trajectories in a chaotic system may diverge from each other even if the initial conditions are close.

1.5 Characterization of nonlinear systems

Consider a system with finite set of observables such as temperature, chemical composition, flow velocity, pressure etc. The evolution into the abstract space spanned by all these variables is phase space. In this space, an instantaneous state of the system is represented by a point. As the time goes on, the point follows a curve called phase trajectory. By following these trajectories from different initial states, a phase portrait is obtained which provides a valuable qualitative idea of system potentialities. For every natural system the phase trajectory will converge to an object in phase space which is referred to as the attractor.

In recent years, it has been realized that ordinary systems obeying nonlinear laws leads to complexity associated with abrupt transitions, multiplicity of states referred to as deterministic chaos. Thermal convection in a fluid layer heated from below, turbulence etc. provide well established example of property of nonlinear systems which is referred to as self-organization. The self-organization become a powerful tool for analyzing complex systems, mainly biological systems and systems encountered in environmental science.

CHAPTER - 2

NEURAL NETWORK

2.1 What is a neuron?

Human brain consists of neurons or nerve cells which transmit and process the information received from our senses. They use electrical impulses and chemical signals to transmit information between different areas of the brain, and between the brain and the rest of the nervous system. Everything we think and feel and do would be impossible without the work of neurons and their support cells, the glial cells [14]. Many such nerve cells are arranged together in our brain and they form a network of nerves. They pass electrical impulses i.e. the excitation from one neuron to the other.

The dendrites receive the impulse from synapse of an adjoining neuron. These dendrites carry the impulse to the nucleus of the nerve cells which is called as soma. The electrical impulse is processed here and the passed on to the axon. The axon is the longer branch among the dendrites which carries the impulse from the soma to the synapse. The synapse then passes the impulse to dendrites of the second neuron. A complex network of neuron is thus created in the human brain.

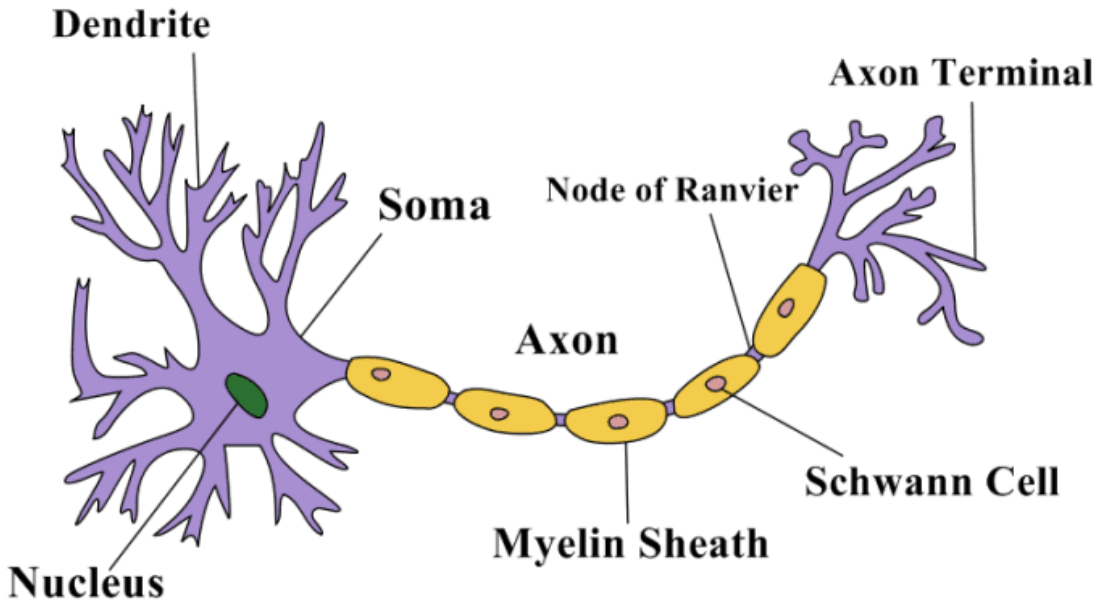

Fig. 2.1 Structure of a Neuron

The basic building block of the brain and central nervous system is the neuron. They are specialized cells that transmit chemical and electrical signals. The brain is made up of neurons and glial cells. Glial cells are non-neuronal cells which provide structure and support for the neurons. Nearly there are 86 billion neurons work together within the nervous system to communicate with the rest of the body. They control everything from consciousness and thought to pain and hunger. There are three primary types of neuron: sensory neurons, motor neurons and inter-neurons.

Sensory neurons respond to stimuli such as touch, sound, or light that affect the cells of the sensory organs, and they send signals to the spinal cord or brain.

Motor neurons receive signals from the brain and spinal cord to control everything from muscle contractions to glandular output.

Inter-neurons connect neurons to other neurons within the same region of the brain or spinal cord. When multiple neurons are connected together they form what is called a neural circuit.

2.2 Structure of neuron

Neurons contain unique structure for receiving and sending the electrical signals that make neuronal communication possible. They consist of a nucleus, cell body, axon, dendrite and a myelin sheath.

Dendrite

Dendrites are branch-like structure extending away from the cell body. Their job is to receive message from other neurons and allow those messages to travel to the cell body. Although some neurons do not have any dendrites, other types of neurons have multiple dendrites.

Cell Body

Each neuron has a cell body (or soma) that contains a nucleus, smooth and endoplasmic reticulum, Golgi apparatus, mitochondria, and other cellular components. They control the functions of a cell. They contain different organelles which help them to do its job.

Axon

An axon is a tube like structure that carries an electrical impulse from the cell body (or from another cell's dendrites) to the structure at opposite end of the neuron i.e. axon terminals, which then pass the impulse to another neuron.

Synapse

The synapse is a chemical junction between the axon terminals of one neuron and the dendrites of the next. It is a gap where chemical interactions can occur. Its function is to transfer electrical activity (information) from one cell to another.

2.3 What is synapse?

"Coming together" is the meaning of the word synapse. A synapse is formed when two structures or entities come together. Although the term synapse can refer to any cellular junction, it is most commonly used in physiology to refer to the junction of two neurons, the junction of a neuron and a target cell (ex. the neuromuscular junction), or the interface between adjacent cardiac muscle cells or adjacent smooth muscle cells. A synapse is a structure in the nervous system that permits a neuron to send an electrical or chemical signal to another cell.

Synapse cell

The presynaptic cell is the cell that sends the signal to the synapse. The postsynaptic cell is the cell that receives the signal after it crosses the synapse. A postsynaptic neuron at one synapse may become the presynaptic neuron for another cell downstream since most brain pathways contain several neurons.

With a postsynaptic neuron, a presynaptic neuron can make one of three types of synapses. The axon of the presynaptic neuron synapses with a dendrite of the postsynaptic neuron in an axodendritic synapse, which is the most frequent form of synapse. An axosomatic synapse occurs when the presynaptic neuron synapses with the postsynaptic neuron's soma, while an axoaxonic synapse occurs when it synapses with the postsynaptic cell's axon.

Synapse Transmission

In your body, there are two types of synapses: electrical and chemical. Electrical synapses allow ions and signalling molecules to move directly from one cell to the next. Chemical synapses, on the other hand, do not transmit signals directly from the presynaptic cell to the postsynaptic cell. An action potential in the presynaptic neuron causes the release of a chemical message known as a neurotransmitter in a chemical synapse. The neurotransmitter then diffuses across the synapse and binds to postsynaptic cell receptors. When a neurotransmitter binds to a receptor, an electrical signal is produced in the postsynaptic cell. Each type of synapse has functional advantages and disadvantages.

Electrical synapse:

The signal is passed through electrical synapse very fast, allowing groups of cells to act in unison. The direct flow of electrical current at gap junctions transmits action potentials in electrical synapses. When the trans-membrane pores of two neighboring cells align, a gap junction is produced. The two cells' membranes are joined together, and the matched pores create a pathway between them. As a result, various chemicals and ions are permitted to flow between the cells. Electrical synapses facilitate bidirectional information flow between cells due to the direct passage of ions and molecules from one cell to another. The function of cardiac myocytes and smooth muscles is dependent on gap junctions.

Chemical synapse:

Chemical synapses allow neurons to integrate information from many presynaptic neurons, determining whether or not the postsynaptic cell will continue to propagate the signal. Multiple chemical synapses send information to neurons, which causes them to respond differently. The majority of synapses in your body are chemical synapses. A synaptic gap or cleft separates the pre- and postsynaptic cells in a chemical synapse. When an action potential is transmitted to the axon terminal, the axon terminals secrete chemical messengers known as neurotransmitters. Neurotransmitter molecules go across the synaptic cleft and bind to receptor proteins on the postsynaptic cell's cell membrane. The neurotransmitter binds to the receptors on the postsynaptic cell, causing a brief shift in the membrane potential of the postsynaptic cell [15].

2.4 Neurotransmitters and Action potential

Neurotransmitters

The chemical messengers of the body are typically referred to as neurotransmitters. They are the chemicals that the nervous system uses to send and receive messages between neurons and between neurons and muscles.

The synaptic cleft is where two neurons communicate with one another (the small gap between the synapses of neurons). The release of neurotransmitters converts electrical messages that have travelled along the axon into chemical signals, generating a specific reaction in the receiving neuron. A neurotransmitter can have one of three effects on a neuron: excitatory, inhibitory, or modulatory.

In the receiving neuron, an excitatory transmitter encourages the formation of an electrical signal known as an action potential, whereas an inhibitory transmitter prevents it. The receptor to which a neurotransmitter binds determines whether it is excitatory or inhibitory.

Neuromodulators are unique in that they are not limited to the synaptic cleft between two neurons and can therefore affect a large number of neurons simultaneously. Neuromodulators, in contrast to excitatory and inhibitory transmitters, influence populations of neurons while functioning at a slower rate [16].

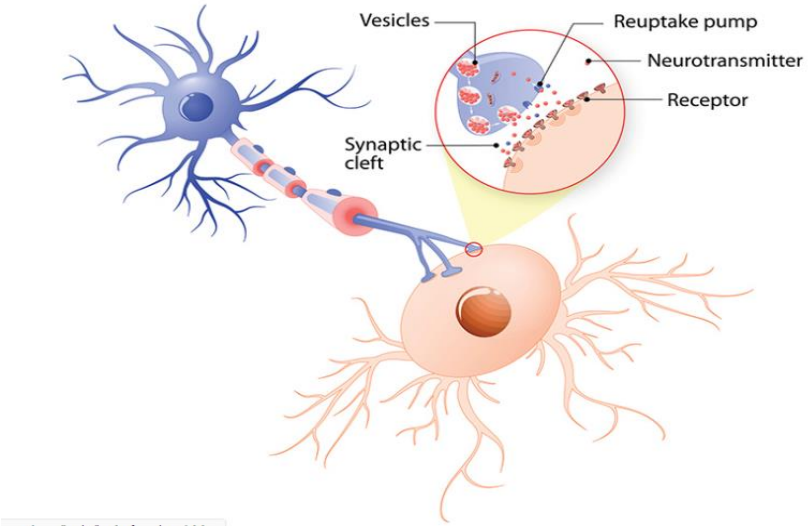

Fig. 2.2 Synapse model

Action Potential

The cell membrane (the border between the interior and outside of a cell) contains many channels that allow positive and negative ions to flow into and out of the cell. The inside of a cell is normally more negative than the exterior; neuroscientists estimate that the inside is roughly -70 mV in comparison to the outside, or that the cell's resting membrane potential is -70 mV. The potential of the membrane isn't constant. It fluctuates regularly, primarily because to inputs from other neurons' axons. Some inputs cause the membrane potential of the neuron to become more positive (or less negative, for example, from -70 mV to -65 mV), whereas others have the reverse effect.

Because they encourage or inhibit the formation of action potentials, these are referred to as excitatory and inhibitory inputs, respectively (the reason some inputs are excitatory and others inhibitory is that different types of neuron release different neurotransmitters; the neurotransmitter used by a neuron determines its effect). The sum total of all excitatory and inhibitory inputs causes the neuron's membrane potential to hit roughly -50 mV (see diagram), which is known as the action potential threshold.

Action potentials are commonly referred to as 'spikes' by neuroscientists, who also remark that a neuron has 'fired a spike' or 'spiked.' The shape of an action potential as recorded with sensitive electrical equipment is referred to by this word [17].

2.5 Communication of Neurons

Neurons communicate with one another via synapses. Neurotransmitter is released from the neuron into the synaptic cleft, a 20–40nm space between the presynaptic axon terminal and the postsynaptic dendrite, when an action potential reaches the presynaptic terminal (often a spine).

The transmitter will attach to neurotransmitter receptors on the postsynaptic side after crossing the synaptic cleft, and depending on the neurotransmitter released (which is dependent on the type of neuron releasing it), specific positive (e.g. Na+, K+, Ca+) or negative ions (e.g. Cl-) will travel through membrane channels.

Synapses can be thought of as converting an electrical signal (the action potential) into a chemical signal in the form of neurotransmitter release, and then switching the signal back into an electrical form as charged ions flow into or out of the postsynaptic neuron after the transmitter binds to the postsynaptic receptor [17].

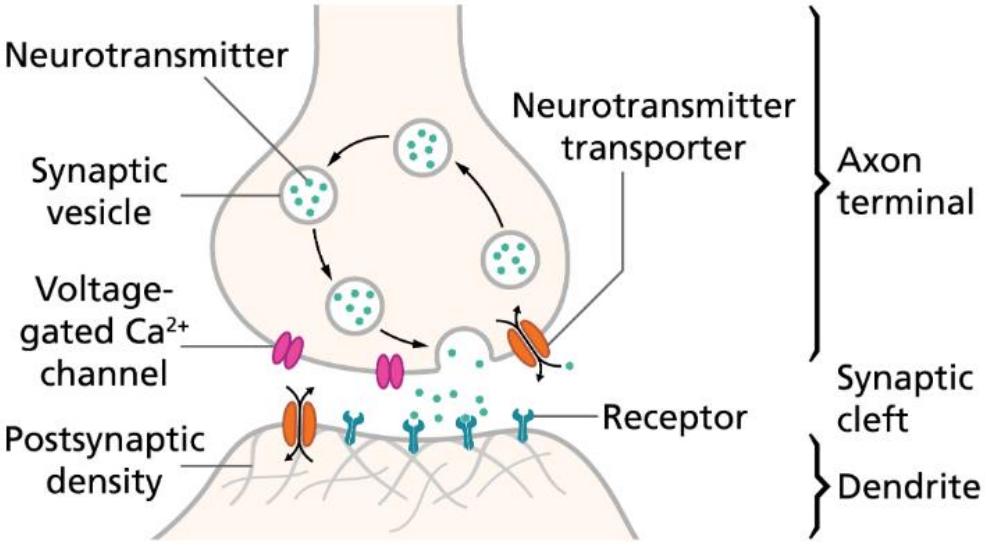

Fig. 2.3 An action potential, or spike, causes neurotransmitters to be released across the synaptic cleft, causing an electrical signal in the postsynaptic neuron

CHAPTER 3

REVIEW OF BRAIN STIMULATION

3.1 Deep Brain Stimulation

Deep brain stimulation (DBS) is a neurosurgical operation that employs electrical stimulation and implanted electrodes to treat movement disorders such as Parkinson's disease (PD), essential tremor, dystonia, and other neurological illnesses. It can also be used to manage obsessive-compulsive disorder and epilepsy symptoms [18]. When drugs are no longer effective or their negative effects interfere with a person's everyday activities, doctors may utilize DBS to treat movement disorders or neuropsychiatric diseases.

- During a surgical operation, surgeons implant one or more small wires (called leads or electrodes) in the brain.
- A tiny pulse generator implanted in the chest provides gentle electrical stimulation to the leads.
- Successful DBS surgery necessitates careful patient selection, precise electrode insertion, and pulse generator modification.
- DBS cannot completely alleviate the symptoms of Parkinson's disease or other illnesses, but it can help patients take fewer medications and have a better quality of life.

Deep brain stimulation (DBS) has changed the treatment of late-stage Parkinson's disease and has shown promise in the treatment of other intractable neuropsychiatric illnesses. Despite over 25 years of clinical experience, many concerns about the neurophysiological basis for therapeutic mechanisms of action remain unanswered. Electrical stimulation therapies in the nervous system are designed to manipulate the opening and closing of voltage-gated sodium channels on neurons, generate stimulation induced action potentials, and then control the release of neurotransmitters in targeted pathways using an applied electric field.

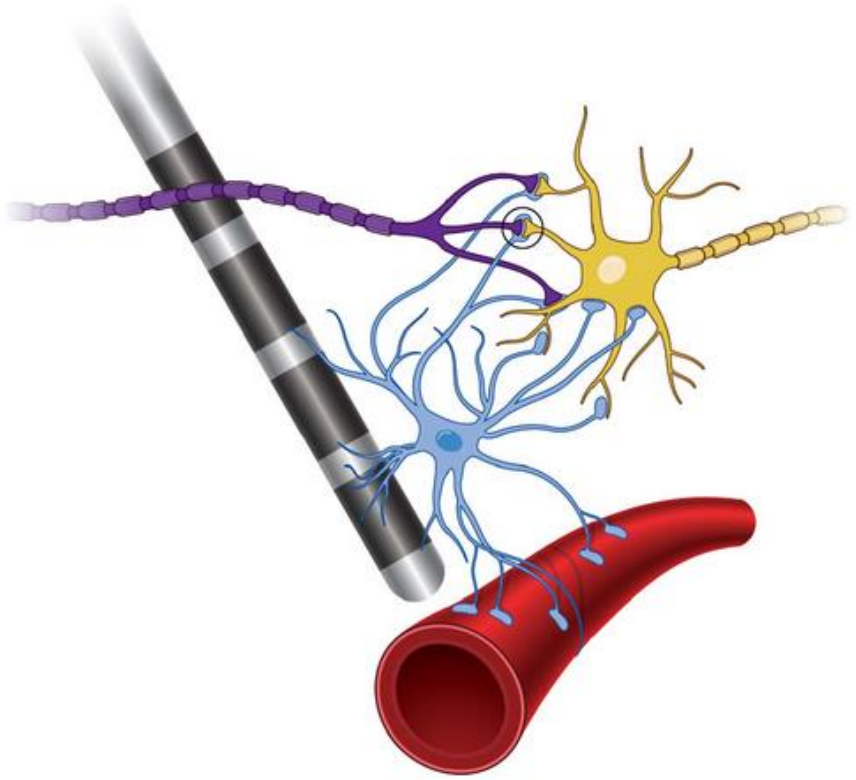

Fig. 3.1 Structural representation of DBS

Deep brain stimulation is a useful clinical tool, although the precise treatment mechanisms are unknown. The most basic concept that can be directly reconciled with experimental recordings of spiking activity in neurons driven by DBS inputs is that high frequency (100 Hz) stimulation-induced synaptic suppression represents the most basic concept that can be directly reconciled with high frequency (100 Hz) stimulation-induced synaptic suppression [19].

Given that therapeutic stimulation methods typically use a constant stimulation frequency, the steady-state PSC generated at the synapse as a function of stimulation frequency is a significant parameter of interest. Low stimulation frequencies (e.g., 10 Hz) can maintain high amplitude PSCs for lengthy periods of time, whereas high stimulation frequencies (e.g., 100 Hz) reduce PSCs immediately after the stimulus train begins.

In most in DBS experiments, communication between the directly stimulated pre-synaptic neuron and a tightly linked post-synaptic neuron does not completely stop. Instead, with high frequency stimulation, signal transmission, which is strong during low frequency stimulation, becomes sporadic and low

fidelity, despite remaining time-locked to the stimulus train. This shows that DBS changes the dynamics of these synaptic connections, and that 100 Hz stimulation acts as a filter, preventing low-frequency oscillatory activity of pre-synaptic neurons from impacting their post-synaptic neurons [20].

The general phenomena of DBS-induced synaptic suppression may be studied most easily at glutamatergic synapses [21, 22], where there is a wealth of experimental data to parameterize synaptic models and post-synaptic neurons can be monitored for synaptically generated APs time-locked to the stimuli. There are several types of glutamatergic synapses, including depressing, facilitating, and pseudo-linear. As a result, we set out to determine how these various synapse types respond to DBS.

Here, Tsodyks-Markram (TM) phenomenological synapse model to represent depressing (D), facilitating (F), and pseudo-linear (P) glutamatergic synapses driven by DBS over a wide range of stimulation frequencies.

3.2 Tsodyks-Markram (TM) model

Short-term synaptic plasticity strongly affects the neural dynamics of cortical networks. The Tsodyks and Markram (TM) model for short-term synaptic plasticity accurately accounts for a wide range of physiological responses at different types of cortical synapses.

To quantify the dynamic behaviour of glutamatergic synapses driven by DBS-induced action potentials, here employed the Tsodyks-Markram (TM) phenomenological model of short-term synaptic plasticity. Short-term depression (related with neurotransmitter depletion) and short-term facilitation (associated with calcium influx into the pre-synaptic terminal) can both be simulated using TM models. The dynamics of the TM model arise from the combination of a depression effect, denoted by normalized variable x, which represents the fraction of neurotransmitter resources that remain available after synaptic transmission, and a facilitation effect modeled by utilization parameter u that represents the fraction of available neurotransmitter resources ready to be used (Fig. 2). As such, u is consumed to produce the postsynaptic current, I. The combination of the depression and facilitation effects, as well as the time delay, D, yields the following differential equations:

$$\dot{u} = -\frac{u}{\tau_f} + U(1 - u^-)\delta(t - t_s - \Delta) \quad (1)$$

$$\dot{x} = -\frac{1 - x}{\tau_d} - u^+ x^- \delta(t - t_s - \Delta) \quad (2)$$

$$\dot{I} = -\frac{I}{\tau_s} + A u^+ x^- \delta(t - t_s - \Delta) \quad (3)$$

where;

- t_s – spike time
- δ – Dirac delta function
- U – Increment of u produced by an incoming spike
- τ_f – decay time constant of variable u
- τ_d – recovery time constant of variable x
- τ_s – decay time constant of variable of I
- A – denotes the synaptic response amplitude that would be produced with the release of all neurotransmitter resources

The specific parameter values for the D, F, and P synapses are listed below, which were previously defined to match the experimentally measured characteristics of intracortical glutamatergic EPSCs.

Synapse	$\tau_f(ms)$	$\tau_d(ms)$	$\tau_s(ms)$	U	$A(\mu s)$
F	670	138	3	0.09	2.5
D	17	671	3	0.5	2.5
P	326	329	3	0.29	2.5

3.3 Obtained synaptic response to DBS

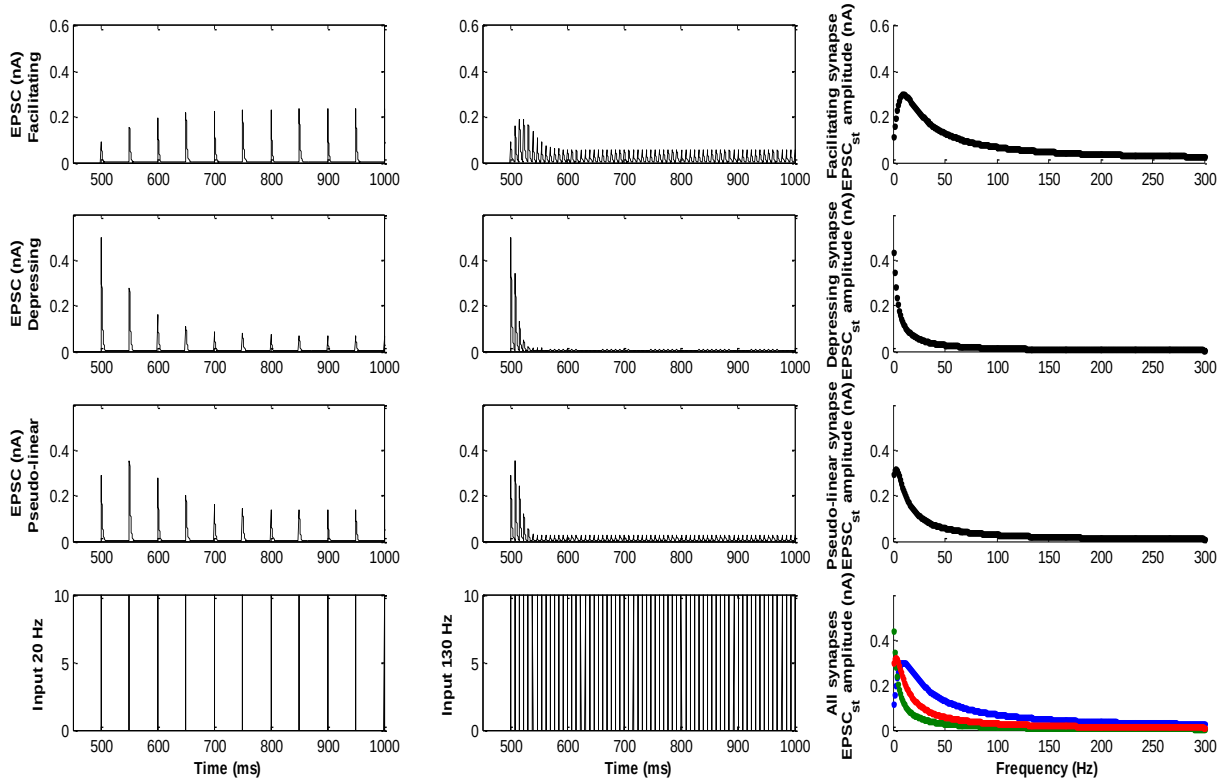

Fig 3.2 shows the EPSC generated by each of the F,D and P synapses for 20HZ and 130Hz.

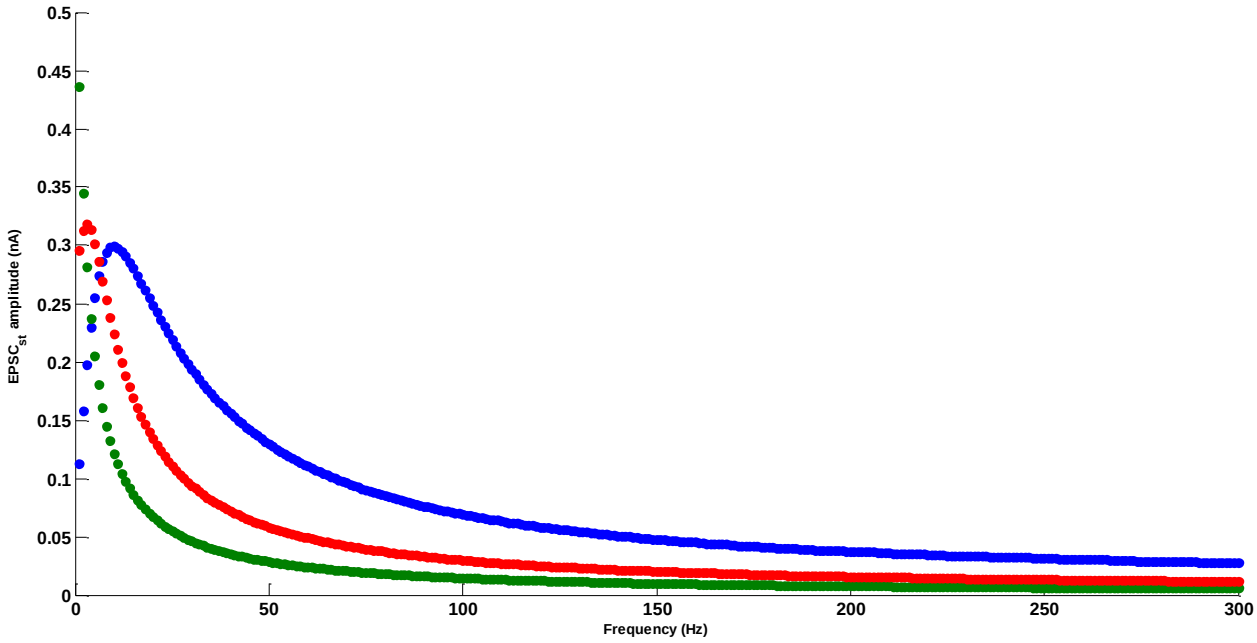

Fig 3.3 EPSC amplitude Vs Frequency plot

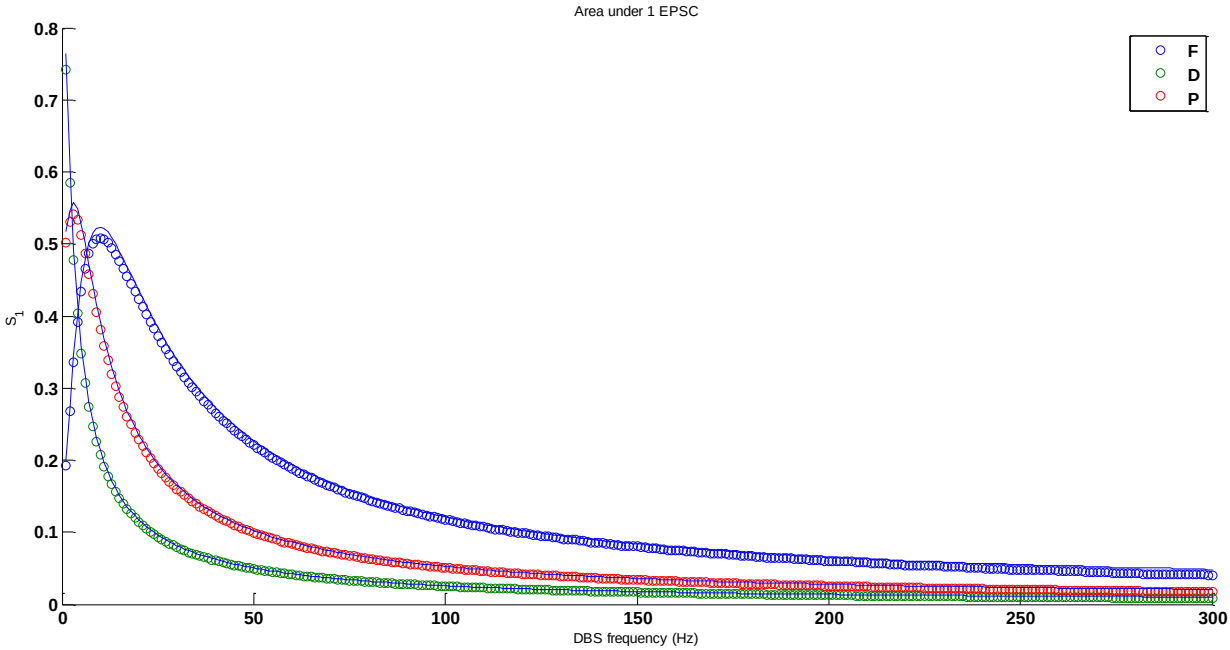

Fig 3.4 Area under 1EPSC

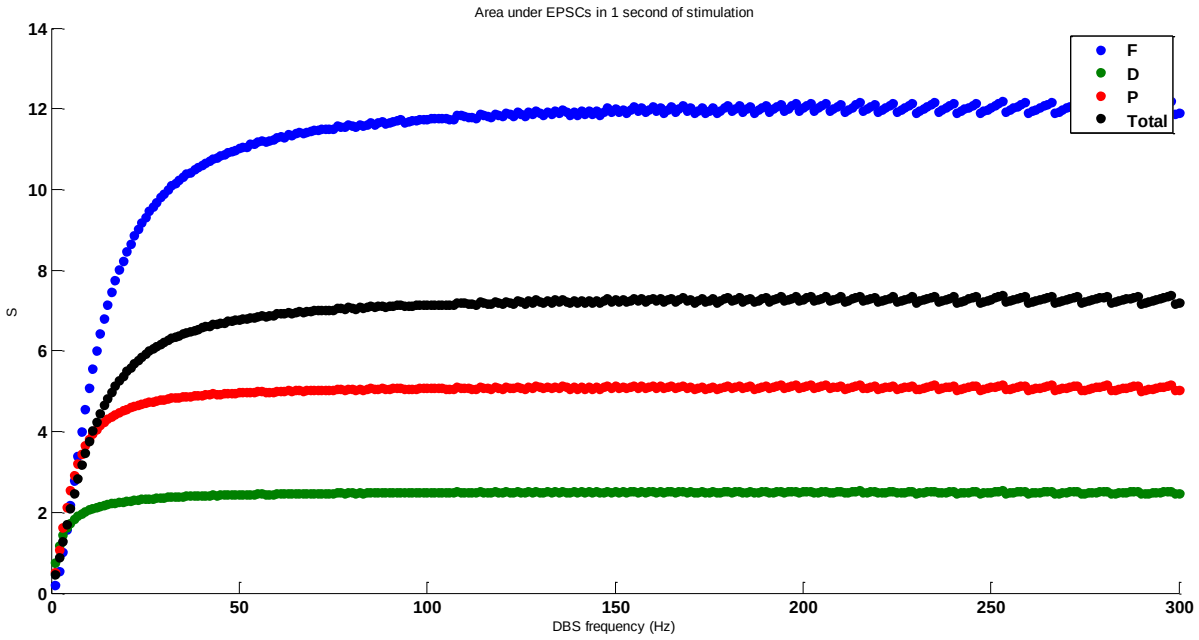

Fig 3.5 Area under EPSCs in 1 second of stimulation

Low frequency stimulation can produce a wide range of EPSCs, depending on the type of synapse (depressing (D), facilitating (F), or pseudo-linear (P)), as well as the timing of when the EPSC is evaluated throughout the stimulus train,

according to simulations of the TM synaptic model. The number of available transmission resources, x, for a D synapse stimulated at 20 Hz decays with a fast time constant. EPSCs are initially very strong, but in the steady-state, they degrade to a modest amplitude.

F synapses stimulated at 20 Hz, on the other hand, have an x that does not decrease rapidly because the utilisation fractions, u, are less. As a result, EPSCs start out small but grow in size with time to reach a larger amplitude in the steady-state. Under high frequency driving, however, both the F and D synapses show a similar tendency of steady-state EPSC suppression. During 130 Hz driving, F synapses have tiny EPSC amplitudes while D synapse EPSCs are essentially zero.

Thus we can conclude that Independent of the synapse type (D, F, P), high frequency driving of the synapse models generates marked EPSC suppression.

CHAPTER 4

THE LIF SPIKING NEURON MODEL

4.1 Introduction

Many neuron models emerged to mimic the functions of a biological neuron, especially the LIF spiking model. It is a simplified and much easier model for hardware implementation and large-scale integration. The primary purpose of an artificial neuron is to mimic the functions of biological neurons in an energy effectiveness and scalability way. The typical LIF model consists of a capacitor and a resistor. The external stimulus is applied to the LIF model until a threshold is reached, and then the action potential is produced. Although the LIF model can reproduce the firing behaviors of neurons after each activation, the previous pulse cannot be retained, and the biological spiking frequency adaptability does not perform very well. To solve these deficiencies, we need to find a new device to promote the LIF neuron model. A memristor is a potential element to emulate the function and behavior of a biological synapse or neuron gets a lot of attention. The non-volatile memristor modulates its conductance due to ion motion, similar to the phenomena in biological neurons and synapses. Therefore, these advantages enable the memristor to become an inevitable choice as a building block between artificial neural networks and biological neural networks.

Even though the LIF neuron model with a memristor had achieved lots of progress in emulating biological neurons, the implementation of retaining the previous pulse and performing the biological spiking frequency adaptability has not been yet explored in the MLIF neuron model.

The LIF spiking circuit model is put forward which is closer to the real biological neuron, as shown in Figure 4.7

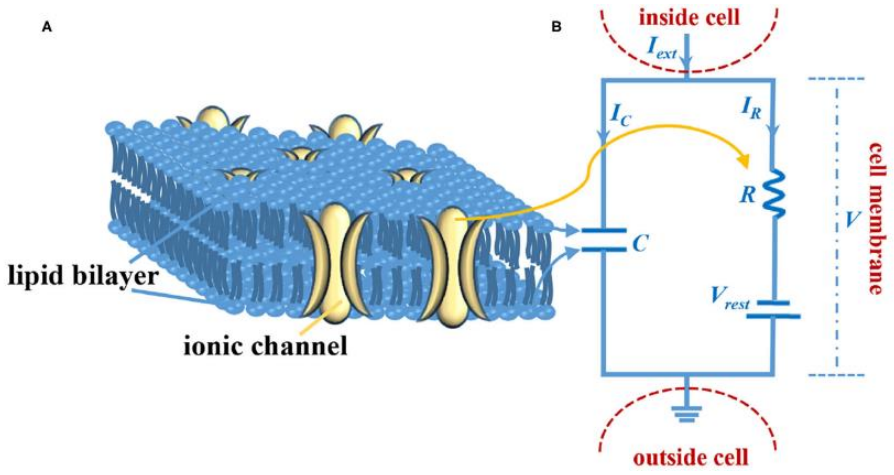

Fig 4.7 The LIF circuit model of the axon membrane. (A) The sketch of the cell membrane. (B) The circuit model of the cell membrane.

The cell membrane consists of the lipid bilayer and the ionic channel (Fig 4.7 A). The lipid bilayer can be represented by a capacitor, and the ionic channel can be characterized by a resistor (Fig 4.7 B). I_{ext} is external stimulus, C is the membrane capacitor, R is the membrane resistor (leaky resistor), V_{rest} is the resting voltage, $V - V_{rest}$ is the resistive voltage, I_c is the current that passes through membrane capacitor, IR is the current that passes through the membrane resistor, and V is the membrane voltage. Current passes through the membrane capacitor:

$$q = CV \tag{1}$$

$$I_c = \frac{dq}{dt} = Cdv/dt \tag{2}$$

Current passes through the membrane resistor:

$$I_R = (V - V_{rest})/R \tag{3}$$

According to Kirchhoff's current law:

$$I_{ext} = I_c + I_R \tag{4}$$

The time constant:

$$\tau = RC \tag{5}$$

The differential equation of the LIF model, which represents the leaky integration process:

$$dt = -(V - V_{rest}) + RI_{ext} \quad (6)$$

Using the finite differential method to solve (6) and compute the membrane potential at a time step of duration Δt:

$$V(t + \Delta t) - V(t) = \frac{\Delta t}{\tau}(-V(t) + V_{rest} + RI_{ext}) \quad (7)$$

4.2 Post-synaptic neuron firing

We used a noisy leaky-integrate-and-fire (LIF) neuron model to evaluate the post-synaptic response to the DBS-driven synaptic inputs. The LIF neuron was parameterized to exhibit an intrinsic tonic firing pattern at 20 Hz. This was achieved by incorporating a bias current, I_e (0.56 nA), background synaptic inputs that arrived stochastically at t_k via a Poissonian process with rate ω_k, and white Gaussian noise, n(t), that had a mean of 0 and variance (σ^2) of 2.5. The LIF neuron also received glutamatergic inputs from DBS-driven synapses, where TM models simulated EPSCs that could also be modulated by a synaptic fidelity coefficient (ω_{sf}). Therefore, the transmembrane potential, v, of the LIF neuron model was defined by the following differential equation:

$$C_m\dot{v} = \frac{E_I - v}{R_m} + I_e + \omega_{sf}EPSC + \sum_{k,t_k} \omega_k \delta(t - t_k) + n(t) \quad (8)$$

Where C_m $(1\,\mu F)$ and R_m $(100\,M\Omega)$ are the membrane capacitance and resistance respectively, and E_I $(-70\,mV)$ is the leak voltage. In eq. (8) EPSC represents the summated post-synaptic currents from all DBS-driven inputs [31].

4.3 Results

Varying DBS frequency

fdbs=60Hz

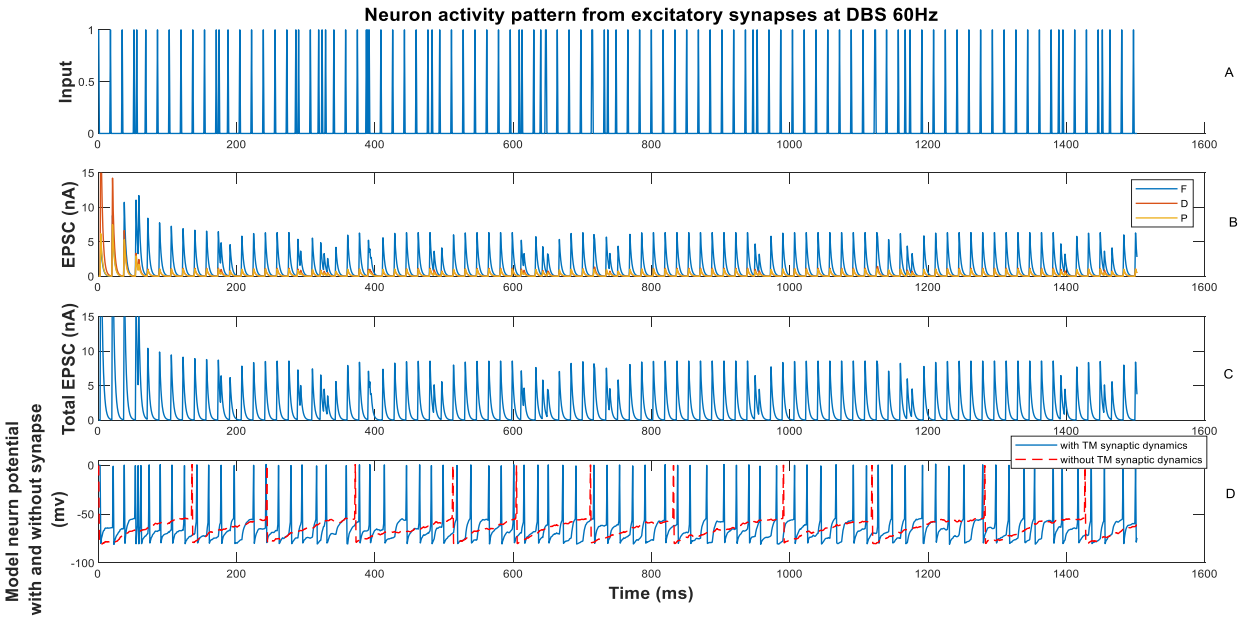

Fig.4.8

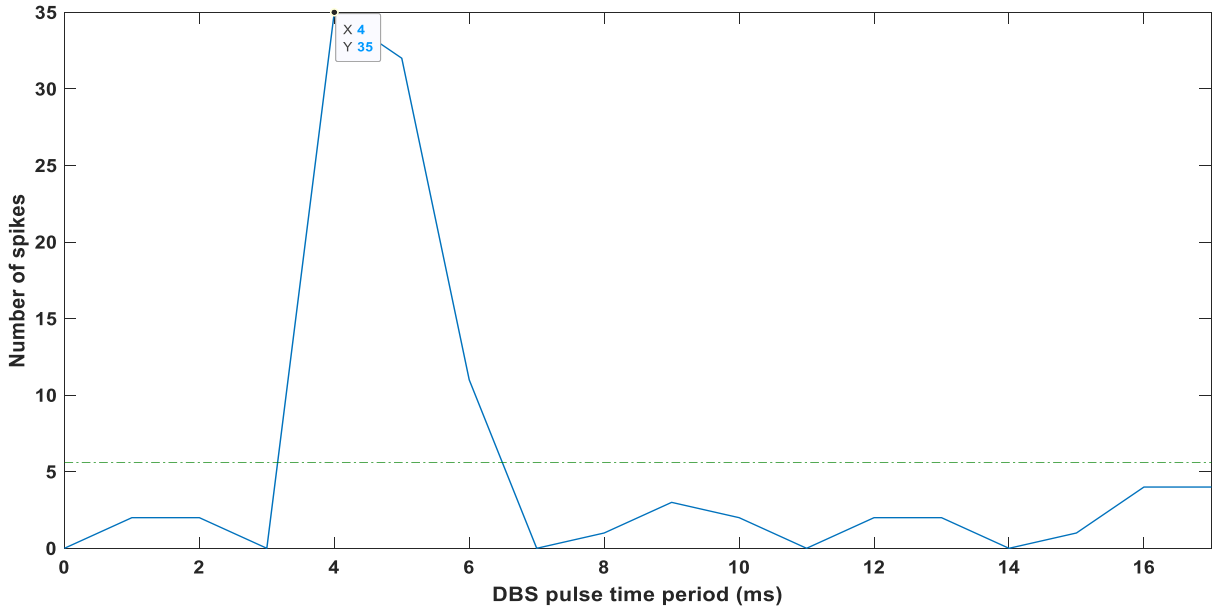

Fig.4.9

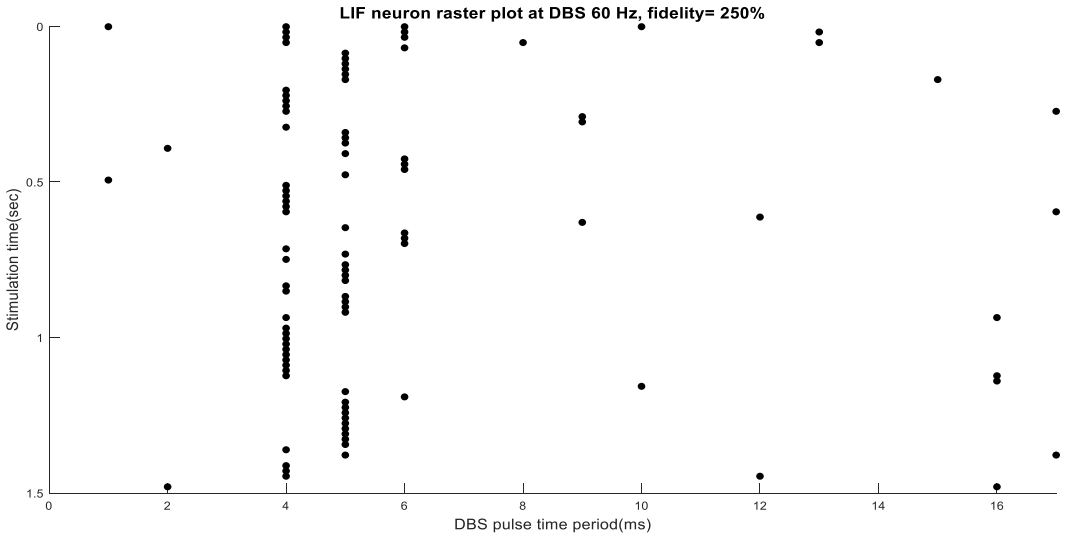

Fig.4.10

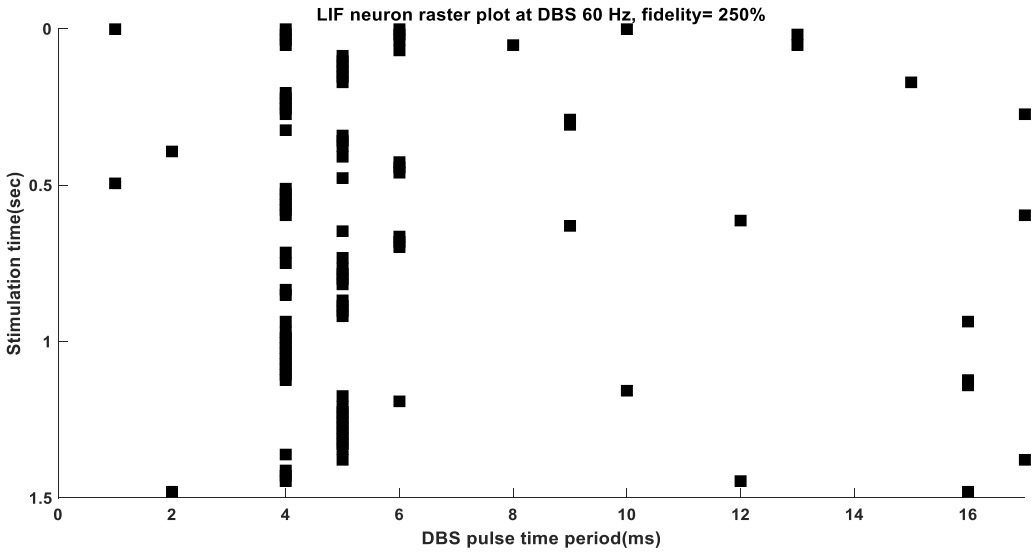

Fig.4.11

Fig. 4.8(A) shows the input frequency, i.e. 60Hz. Fig.4.8(B) depicts EPSC from F, D and P synapses distinctly. Fig. 4.8(C) shows the total EPSC generated from all the synapses F, D and P. Fig.4.8(D) shows the response of neuron when driven by DBS input with or without TM synaptic dynamics.

Fig. 4.9 shows the number of spikes generated versus DBS pulse time period in milliseconds. The maximum no. of spikes generated is 35 at 4ms, whereas the average no. of spikes generated is 5.6.

Fig.4.10 and Fig.4.11 shows stimulus triggered action potentials during DBS. Fig.4.10 shows raster plot of the LIF neuron model without TM synaptic dynamics and Fig. 4.11 with TM synaptic dynamics. Maximum no. of spikes generated lie at DBS pulse time of 4ms.

LIF rate without any synaptic connection = 8.0053 (Hz)

LIF rate with a fraction of synapses during DBS10Hz = 53.3689 (Hz)

LIF rate with all synapses during DBS10Hz = 66.7111 Hz

Elapsed time is 12.924753 seconds.

fdbs=80Hz

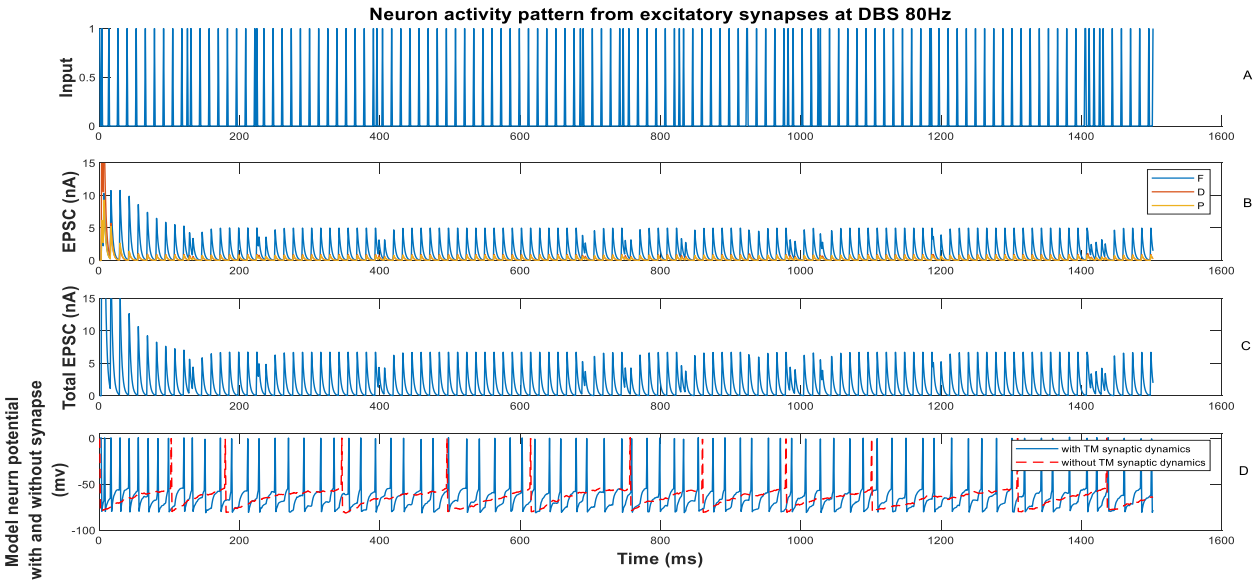

Fig.4.12

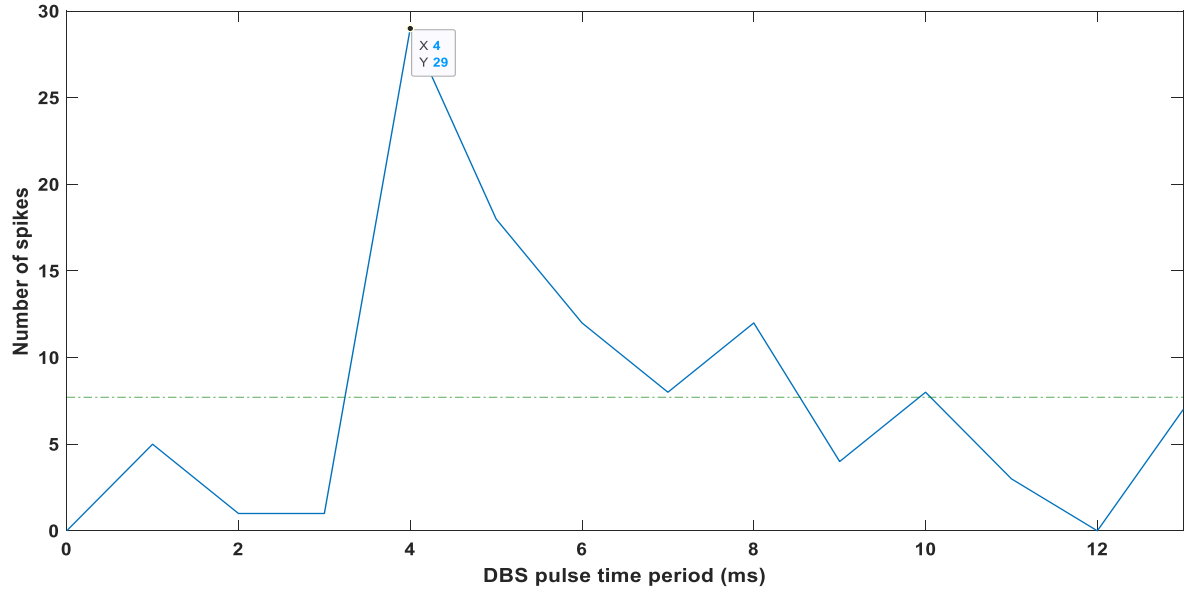

Fig.4.13

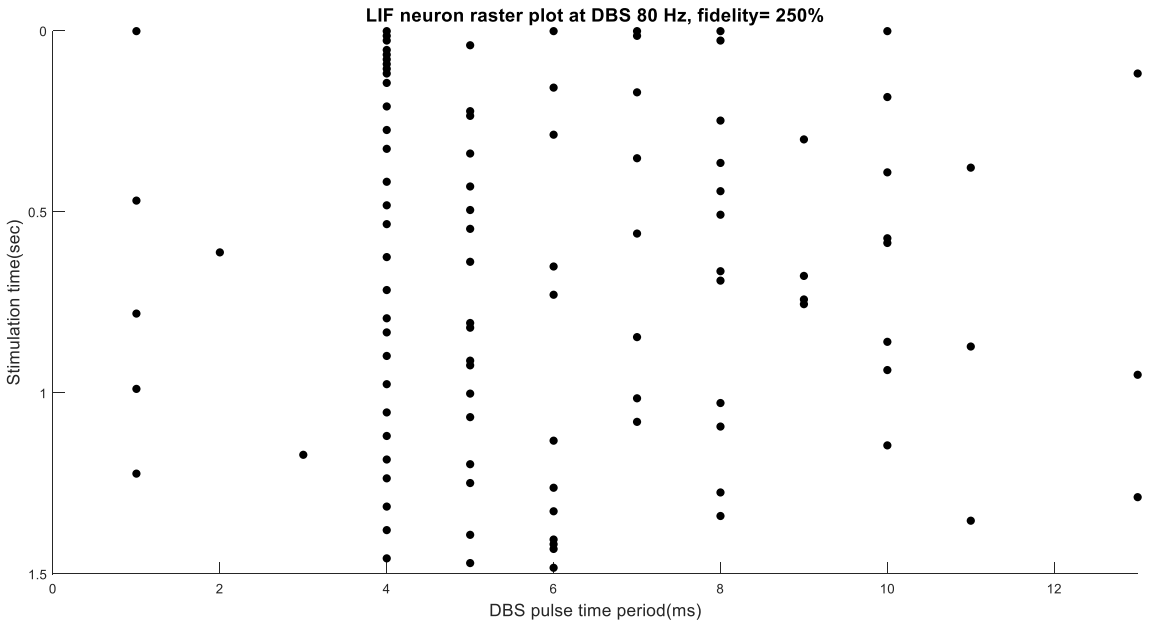

Fig.4.14

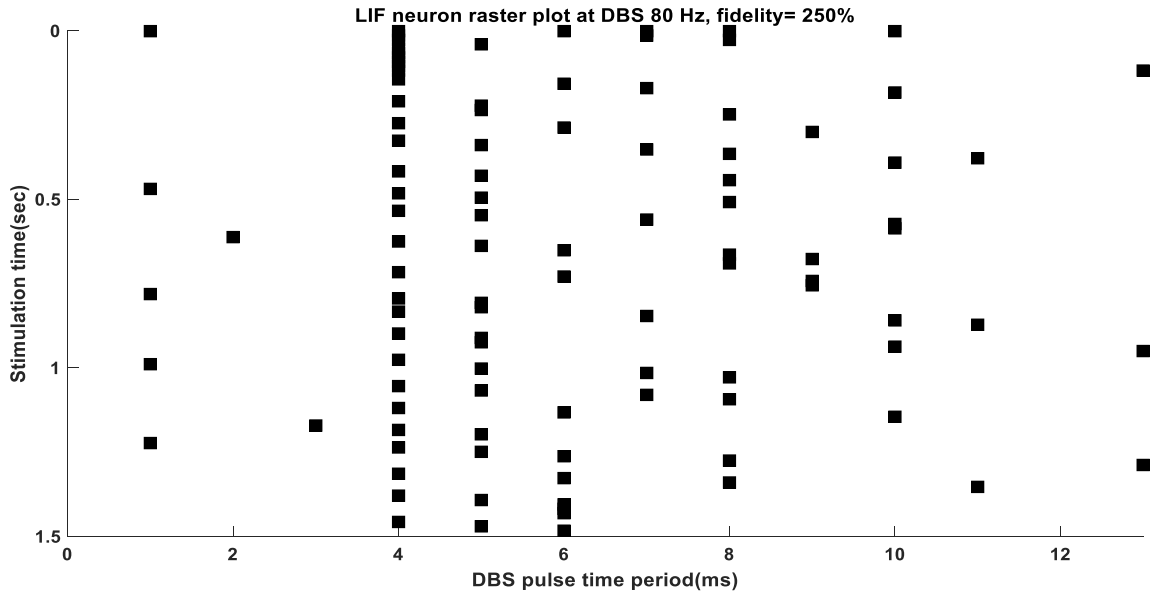

Fig. 4.15

Fig. 4.12(A) shows the input frequency, i.e. 80Hz. Fig.4.12(B) depicts EPSC from F, D and P synapses distinctly. Fig. 4.12(C) shows the total EPSC generated from all the synapses F, D and P. Fig.4.12(D) shows the response of neuron when driven by DBS input with or without TM synaptic dynamics.

Fig. 4.13 shows the number of spikes generated versus DBS pulse time period in milliseconds. The maximum no. of spikes generated is 29 at 4ms, whereas the average no. of spikes generated is 7.7.

Fig.4.14 and Fig.4.15 shows stimulus triggered action potentials during DBS. Fig.4.14 shows raster plot of the LIF neuron model with TM synaptic dynamics and Fig. 4.15 without TM synaptic dynamics. Maximum no. of spikes generated lie at DBS pulse time of 4ms to 5ms.

LIF rate without any synaptic connection = 8.0053 (Hz)

LIF rate with a fraction of synapses during DBS10Hz = 54.036 (Hz)

LIF rate with all synapses during DBS10Hz = 69.3796 Hz

Elapsed time is 10.173028 seconds.

fdbs=130Hz

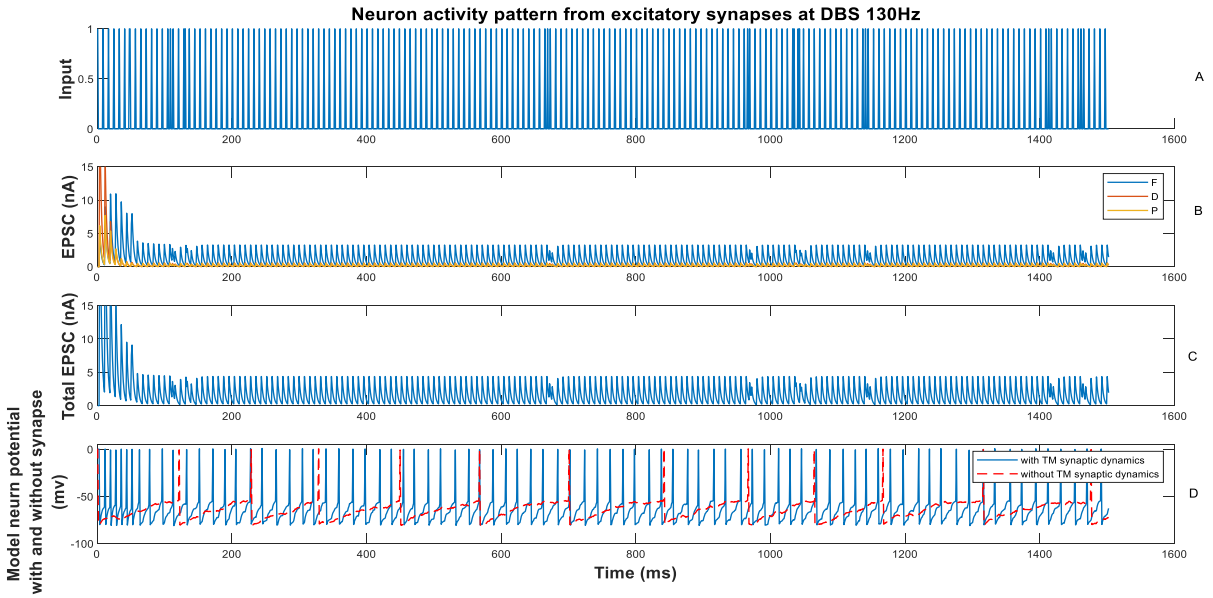

Fig. 4.16

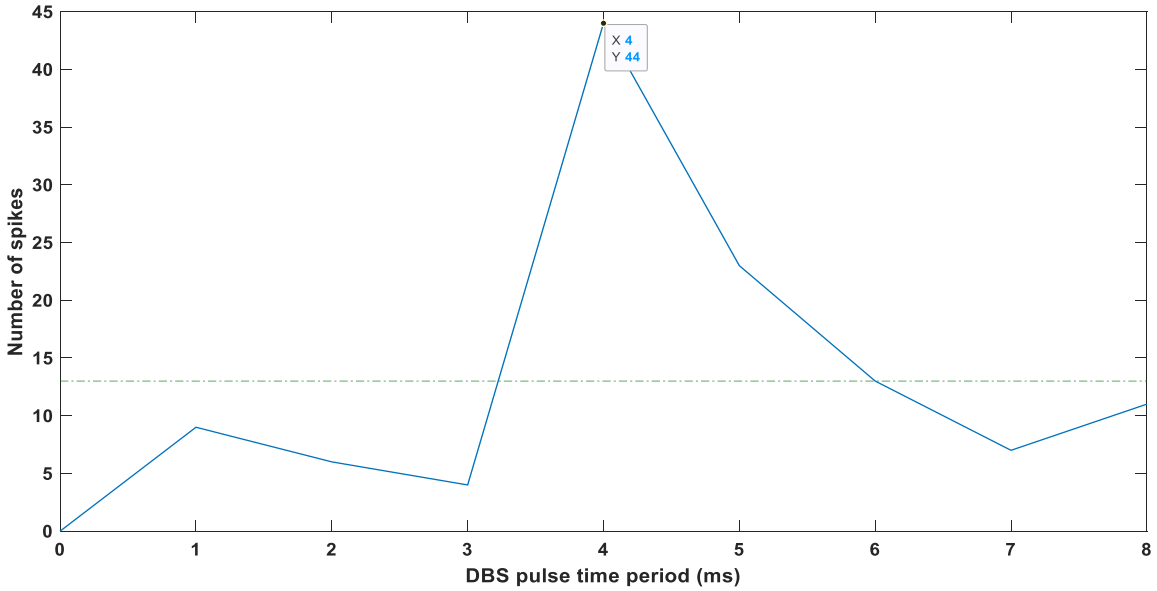

Fig.4.17

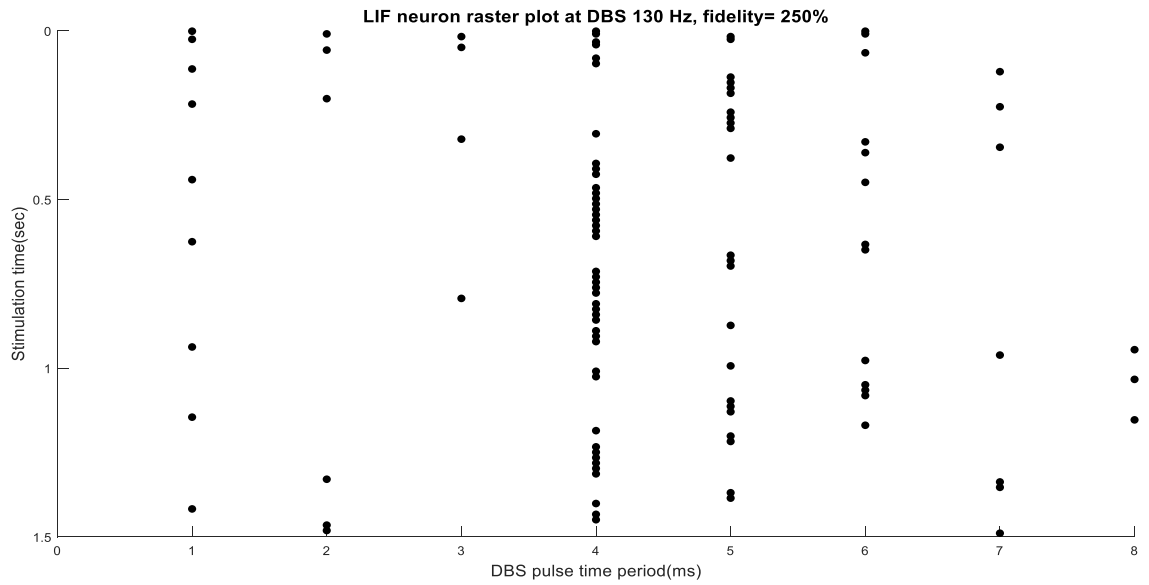

Fig.4.18

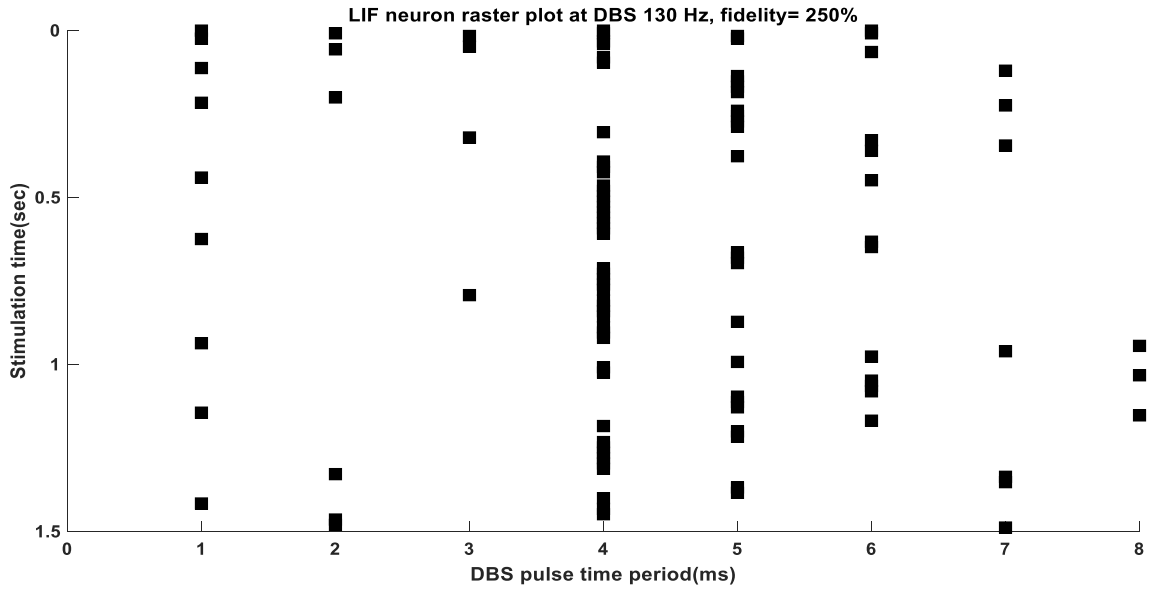

Fig.4.19

Fig. 4.16(A) shows the input frequency, i.e. 130Hz. Fig.4.16(B) depicts EPSC from F, D and P synapses distinctly. Fig. 4.16(C) shows the total EPSC generated from all the synapses F, D and P. Fig.4.16 (D) shows the response of neuron when driven by DBS input with or without TM synaptic dynamics.

Fig. 4.17 shows the number of spikes generated versus DBS pulse time period in milliseconds. The maximum no. of spikes generated is 44 at 4ms, whereas the average no. of spikes generated is 13.

Fig.4.18 and Fig.4.19 shows stimulus triggered action potentials during DBS. Fig.4.18 shows raster plot of the LIF neuron model with TM synaptic dynamics and Fig. 4.19 without TM synaptic dynamics. Maximum no. of spikes generated lie at DBS pulse time of 4ms.

LIF rate without any synaptic connection = 8.6724 (Hz)

LIF rate with a fraction of synapses during DBS10Hz = 56.7045 (Hz)

LIF rate with all synapses during DBS10Hz = 72.7151 Hz

Elapsed time is 15.008347 seconds.

fdbs=150Hz

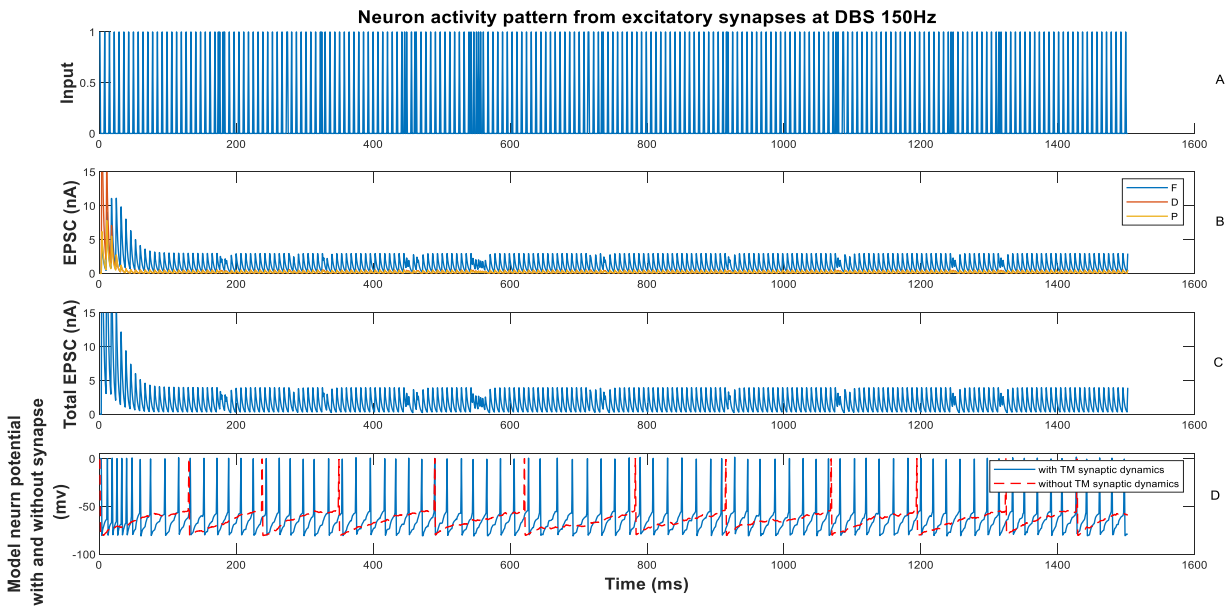

Fig.4.20

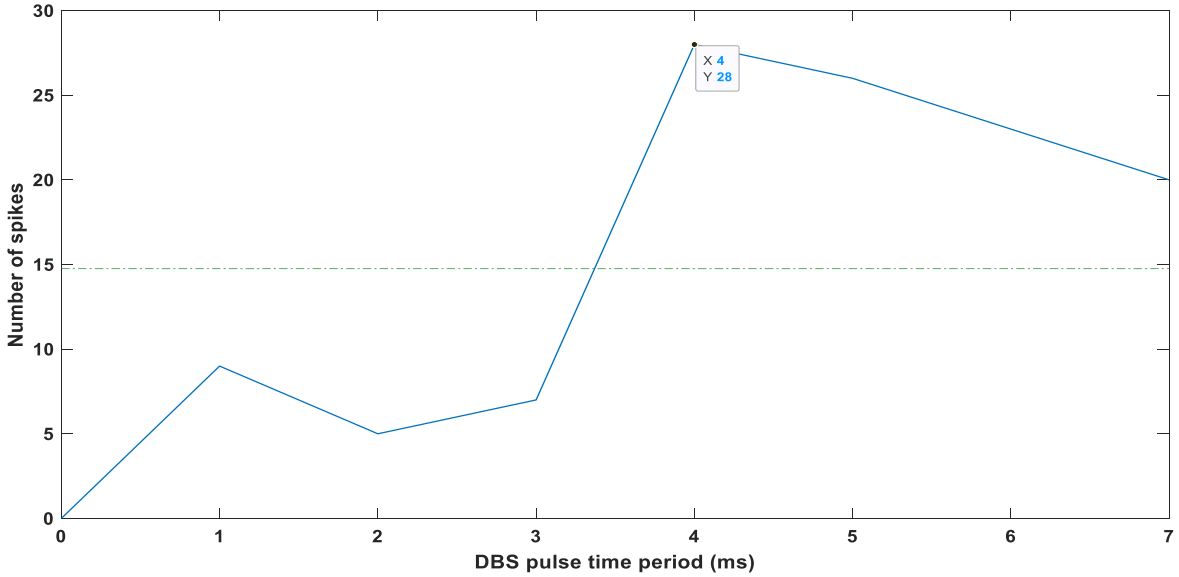

Fig.4.21

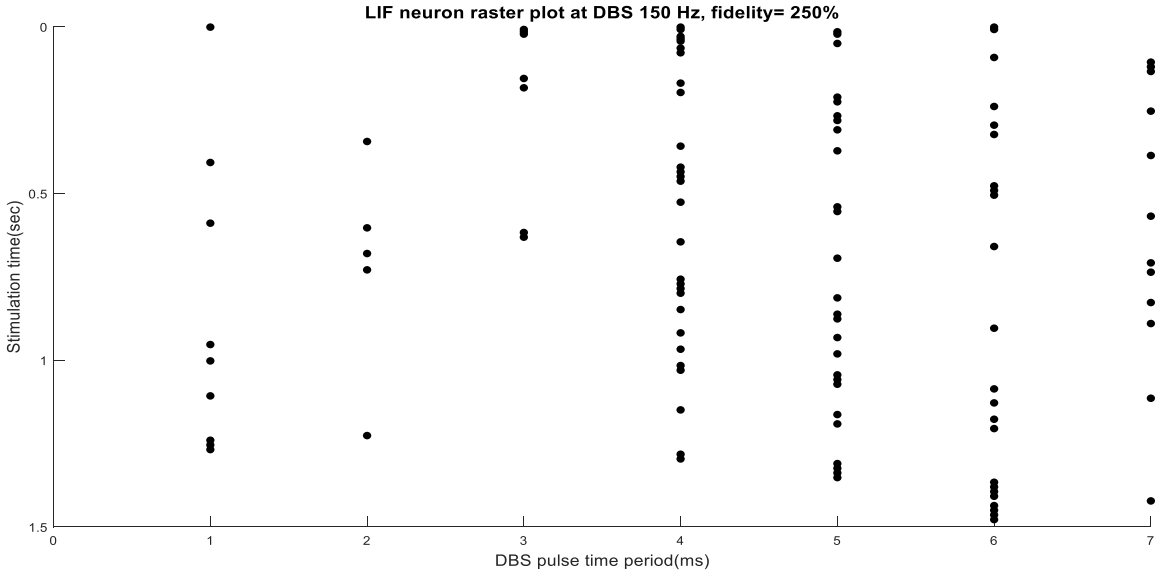

Fig.4.22

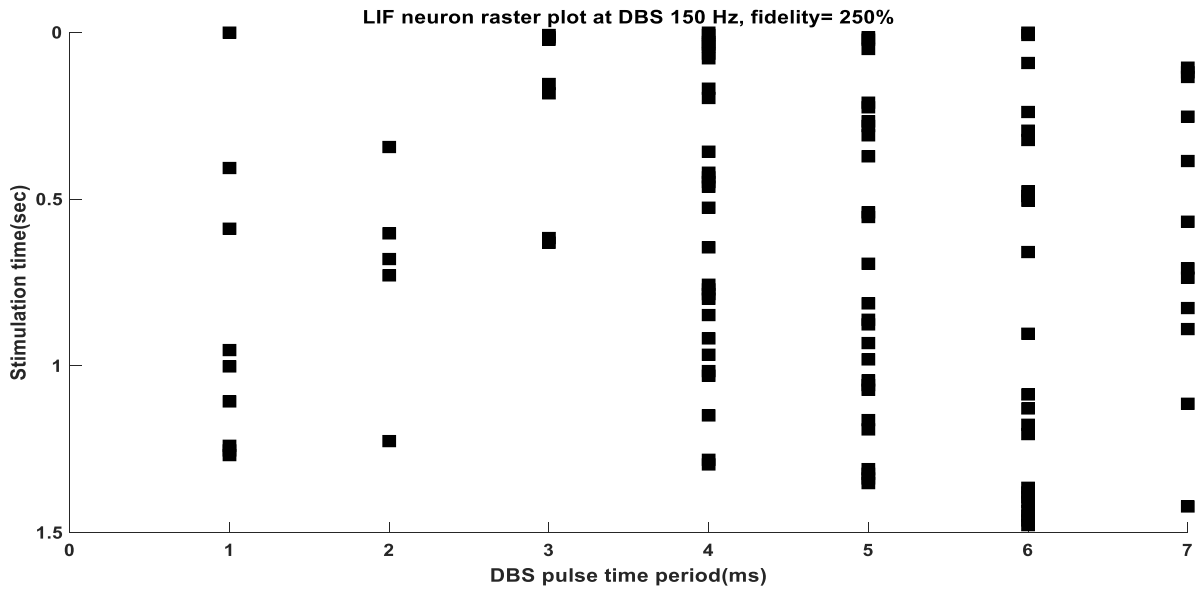

Fig.4.23

Fig. 4.20(A) shows the input frequency, i.e. 150Hz. Fig.4.20(B) depicts EPSC from F, D and P synapses distinctly. Fig. 4.20(C) shows the total EPSC generated from all the synapses F, D and P. Fig.4.20(D) shows the response of neuron when driven by DBS input with or without TM synaptic dynamics.

Fig. 4.21 shows the number of spikes generated versus DBS pulse time period in milliseconds. The maximum no. of spikes generated is 28 at 4ms, whereas the average no. of spikes generated is 14.75.

Fig.4.22 and Fig.4.23 shows stimulus triggered action potentials during DBS. Fig.4.22 shows raster plot of the LIF neuron model with TM synaptic dynamics and Fig. 4.23 without TM synaptic dynamics. Maximum no. of spikes generated lie at DBS pulse time of 4ms.

LIF rate without any synaptic connection = 8.0053 (Hz)

LIF rate with a fraction of synapses during DBS10Hz = 56.7045 (Hz)

LIF rate with all synapses during DBS10Hz = 74.0494 Hz

Elapsed time is 16.477522 seconds.

Fig.4.8 to Fig.4.23 depicts the post synaptic spiking activity of the F, D and P synapses triggered by DBS. It is found that the average number of spikes generated increased as the applied DBS frequency was increased. This implies that as the DBS frequency increases, the spiking activity also increases.

Glutamatergic synaptic inputs were sent to the LIF neuron model, all of which were explicitly triggered by our DBS signal (with a 2 ms AP transmission delay from thalamus). Based on physiologically realistic distributions of synapse types, the various synaptic inputs were classified as F (45), D (38), or P (17). EPSCs were generated simultaneously in the LIF neuron when a single DBS pulse was initiated in these synaptic inputs, thus resulting in a total DBS EPSC that was a mix of F, D, and P components. A single DBS EPSC, generated with the initial conditions of the synapse models, was suprathreshold for the generation of a stimulus evoked AP in the LIF neuron. High frequency driving (130 Hz) of the DBS synaptic input generated an initial burst of APs in the LIF neuron and then as the total DBS EPSC reduced in amplitude to a steady-state value, the inputs provided subthreshold excitatory inputs to the LIF neuron. The overall result of this DBS-driven excitatory current was an increased average firing rate.

CHAPTER 5

DYNAMICS OF MEMRISTIVE LIF MODEL UNDER DEEP BRAIN STIMULATION

5.1 Introduction

A memristor is a two-terminal passive electrical component that serves as a fundamental non-linear circuit element that links charge and magnetic flux. The memristor is a promising device in many analogue and digital applications, particularly memory chips, logic circuits, and neural networks [23].

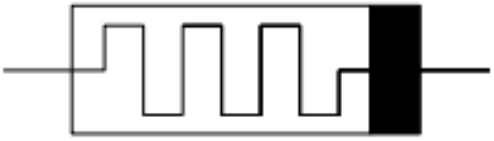

Fig 5.1 Memristor

Three fundamental passive elements such as resistor, capacitor, and inductor are currently used to build electronic circuits. The fourth fundamental element called memristor has recently emerged [24]. Professor Leon O. Chua of the University of California at Berkeley initially described a basic circuit that connects flux to charge in 1971, and it was successfully discovered in 2008 by a team led by Stanley Williams of HP Labs. Members of an HP Lab submitted a paper describing the successful realisation of a nanoscale electronic component whose measured physical attributes can be described by the memristor theory. As illustrated in the figure 2, the HP memristor is a solid state device made up of a nanometer-scale TiO2 thin film with a doped and undoped region sandwiched between two Platinum electrodes.

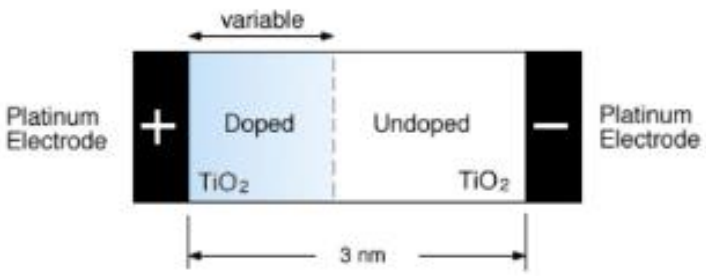

Fig 5.2 Titanium Dioxide Memristor

The new two-terminal passive element is named memristor as it combines the behavior of a memory and a resistor (i.e. memory+resistor). Memristors have shown various outstanding properties, such as good compatibility with CMOS technology, small device area for high-density on-chip integration, non-volatility, fast speed, low power dissipation, and high scalability [25]. One of the basic properties, resistance, of a memristor depends on the magnitude, direction, and duration of the voltage applied across its terminals. Memristor remembers its most recent resistance value when applied voltage was turned off and until the next time when applied voltage is turn on. And has other properties including pinched hysteresis and dynamical-negative resistance that can have significant impact on nanoelectronics.

Many uses for the memristor have been proposed since 2008. Memristors can be utilized in Resistive Random Access Memory (RRAM) cell architectures and Memristor-based Content Addressable Memories (MCAMs) that use a combination of memristor and MOS devices in memory chips. The capacity of the memristor to "memorise" the current pass through it and its direction can be employed efficiently in neural networks to minimize the area and complexity of neuromorphic circuits. A novel form of memristor-based IMPLY logic circuit was developed in the field of logic circuits. Memristor-based logic has the unique capability of being manufactured on the same chip as memory cells. Crossbar-arrays, which are employed in the switching blocks of Field Programmable Gate Arrays, are also designed with memristors (FPGAs) [26]. Thus, although memristors took many years to transform from a purely theoretical derivation into a feasible implementation, these devices has been widely used in applications such as machine learning and neuromorphic computing, as well as non-volatile random-access memory.

Ion motion controls the conductance of the non-volatile memristor, which is analogous to what happens in organic neurons and synapses. As a result of these advantages, the memristor has become an unavoidable choice as a building block for both artificial and organic neural networks.

5.2 Memristor properties

5.2.1 Flux-Charge relation

A charge-controlled memristor is one in which the flux and charge relationship is expressed as a function of charge, whereas a flux-controlled memristor is one in which the flux and charge relationship is expressed as a function of flux [27]. A linear (constant) memristor acts like resistance. If relation is nonlinear, the device behaviour is more complex, thus the memristor's parameter that relates q and φ is not a constant [28].

Memristance M is the missing link between flux and charge. The memristor is said to be charge-controlled with a memristance 'M (q)' given by:

$$M(q) = \frac{d\varphi}{dq}$$

The memristor is said to be flux-controlled with a memductance 'W (φ)' given by:

$$W(\varphi) = \frac{dq}{d\varphi}$$

Therefore it can be derived that:

$$v = M(q).i$$

$$i = W(\varphi).v$$

Memristance has the same unit (Ohm) as resistance, and M(q) is logically a charge controlled resistance. Similarly, the memductance has the unit of conductance [29]. The inverse of memductance is memristance,

$$M = {}^{1}/_{W(\varphi)}$$

The q-φ curve is characterised by a monotonically increasing trend. The memristance M is the slope of this curve (q). As a result, the memristance is

always positive M(q)≥0. A memristor is a passive element if and only if the memristance has a non-negative value, according to the passivity requirement. The instantaneous power dissipated by the memristor is given by:

$$P(i) = M(q)i(t)^2$$

Since M(q)≥0, the wasted power is always positive. As a result, the memristor is a passive device. This means it can't produce or store energy; it can only consume power. A memristor, like a resistor, is entirely dissipative [23].

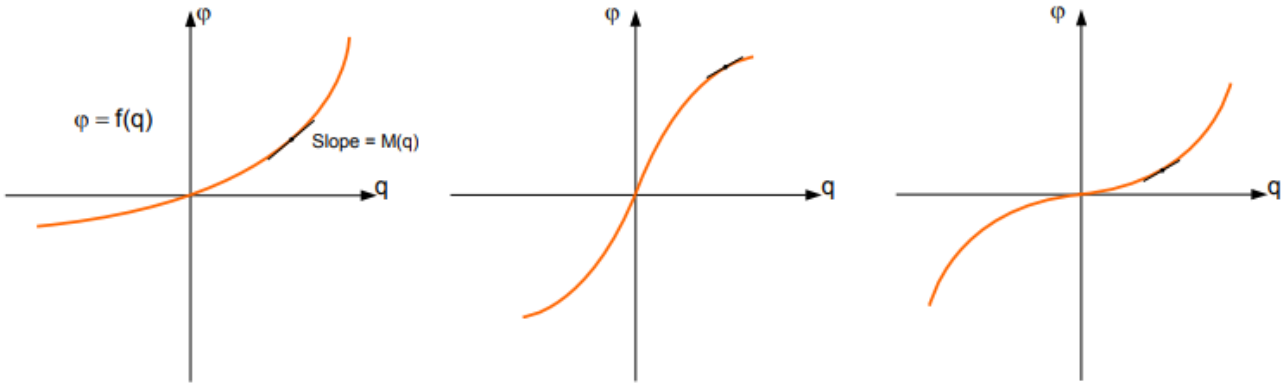

Fig. 5.3 Three examples of charge-flux characteristics of the memristor, which all have monotonically increasing characteristics.

5.2.2 Current-Voltage relation

The current-voltage characteristic of a memristor, which exhibits a pinched hysteresis loop, is its most important feature. The I-V characteristic of the memristor cannot be achieved using any combination of the other three basic components, therefore the memristor is considered a basic component [26]. By applying a periodic signal to a memristor, if the voltage is zero, the current will be zero and vice-versa. So, both voltage v(t) and current i(t) curves always crosses the origin curve. The pinched hysteresis loop's shape will fluctuate with frequency. The hysteresis loop shrinks when the frequency is increased. The memristor will behave like a conventional resistor if the frequency is increased to infinity [23].

The I-V characteristic's slope changes, indicating a changeover between distinct resistance states, with the resistance becoming positive as the applied voltage rises and negative as it falls. Double-loop I-V hysteresis is produced by the symmetrical voltage bias, which can collapse to a straight line at high frequencies [24].

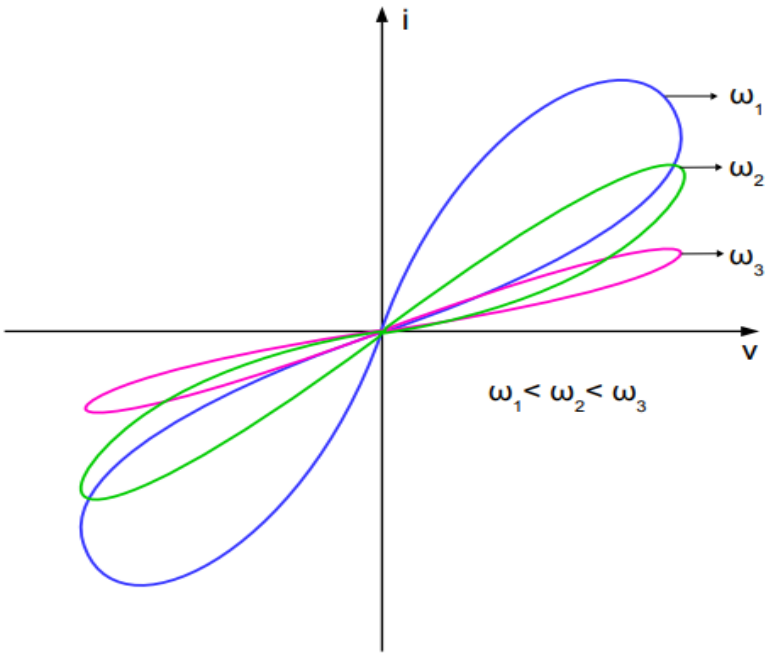

Fig. 5.4 Current-voltage characteristics of the memristor.

5.2.3 Resistance – Time Relation

The resistance versus time characteristic of the memristor is depicted in Fig. 4.5 The instantaneous resistance is in the range $[R_{ON}, R_{OFF}]$. The resistance values depend on the applied voltage. For a sine-wave voltage with period T, the memristance has its extreme (maximum or minimum) values at the following time instances: t = (2n + 1)T/2 [30].

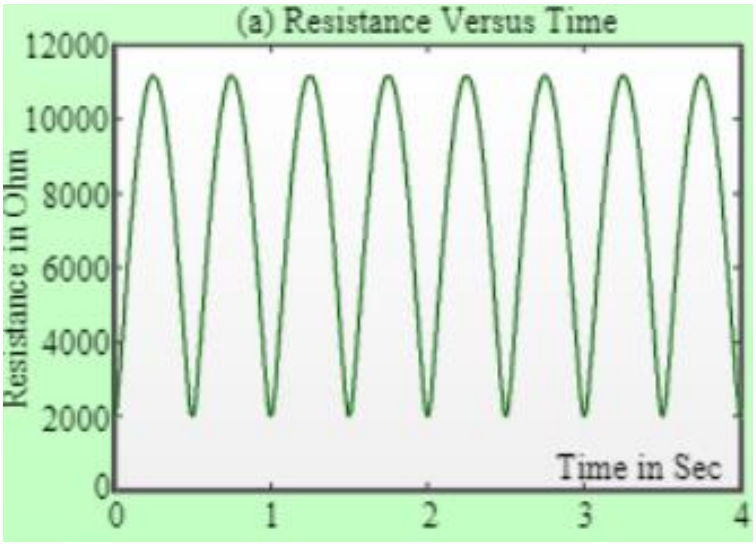

Fig. 5.5 Resistance Versus Time plot of the memristor

5.2.4 Resistance – Voltage Relation

The resistance versus voltage characteristic is depicted in Fig. 4.6. The voltage across the memristor is initially 0 Volt, with a current of 0 Amp and a resistance of R_i [30].

The memristance value also depends on the sign of v(t); in other words, resistance $[R_i, R_{OFF}]$ for v(t) < 0 and $[R_{ON}, R_i]$ for v(t) > 0. This is because current follows voltage, whereas resistance rises as voltage rises. When the voltage drops to zero, the resistance reaches its maximum, R_{OFF} [24].

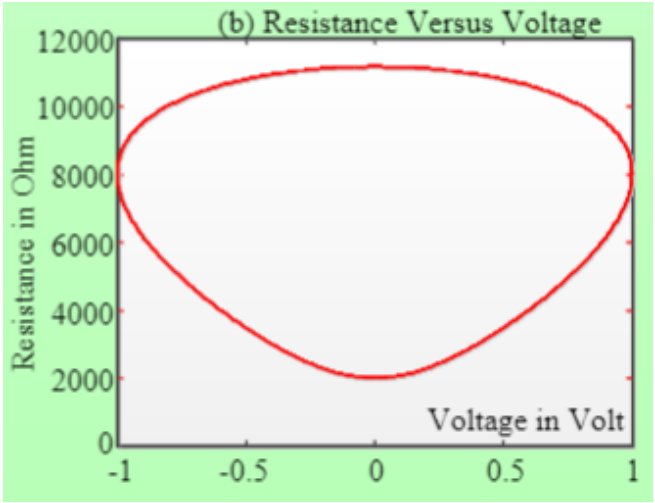

Fig. 5.6 Resistance Versus Voltage plot of the memristor.

5.3 The Memristive LIF (MLIF) spiking neuron model

Considering the LIF spiking model has no memory of the previous spike and the memory advantage of the memristor (can "remember" the charges pass through itself, and it is called non-volatile characteristics) we introduce a memristor to the LIF spiking model, as shown in Figure 4.8.

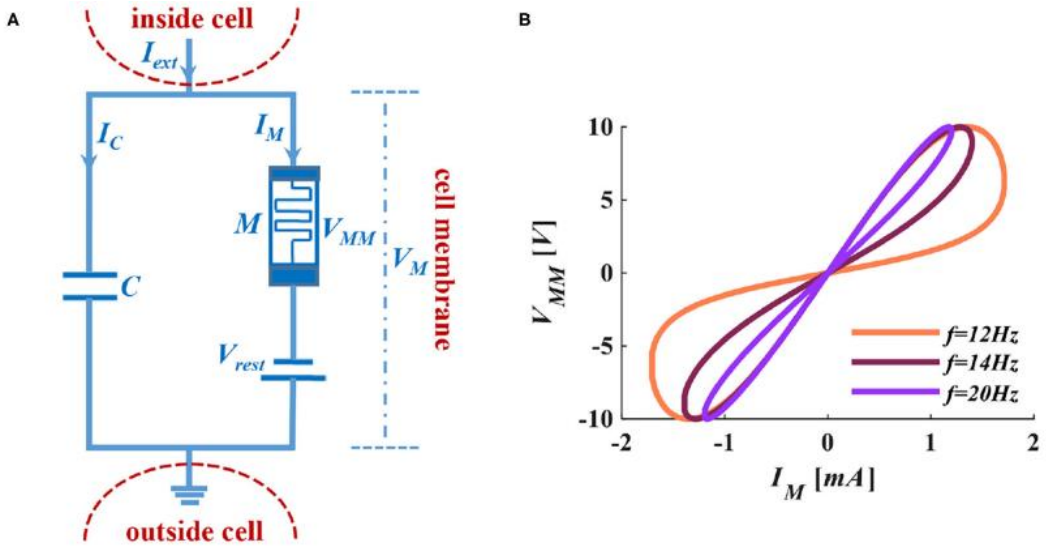

Fig 5.7 The MLIF circuit model and the I-V curve of the memristor. (A) MC membrane circuit of the MLIF model. (B) The pinched hysteresis curve and frequency characteristics of ion channel memristor.

When we apply a sinusoidal voltage to the ion channel memristor, it performs a zero-crossing pinched hysteresis curve. When we adjust the voltage frequency to 100 Hz, the electrical characteristics of the memristor are close to a straight line. The memristor performs the feature of pure resistance. In Figure 4.8 B, the distribution of the curve is in the first and third quadrants, which indicates that the device is passive. The curve has two prominent switching states and keeps a memristance constant without a power supply. It shows that the device is non-volatile.

In the MLIF membrane circuit, the τ is not a constant anymore, and it becomes a function of time. Therefore, $\tau = RC$ is transformed into $\tau_M(t) = M(t)C$. The memristor $M(t)$ is divided into charge-controlled memristor and flux-controlled memristor, and they are the functions of time. According to $q = CV$, we get $q(t) = C(t)V_M$ (V_M is the membrane voltage of the MLIF model, as shown in

Figure 4.8 A), thereby we can rewrite C as $C(t) = q(t)/V_M$, and $\tau_M(t) = M(t)q(t)/V_M$. The charge or discharge time of the capacitor always relates to the accumulation of charge [32].

The charge-controlled memristor:

$$M\big(q(t)\big) =$$

$$\begin{Bmatrix} 20000\,, & q(t) < -0.5 \times 10^{-4} \\ 10^4 + (-1.99) \times 10^8 \times q(t), & q(t) \geq -0.5 \times 10^{-4}\ \ q(t) < 0.5 \times 10^{-4} \\ 100\,, & q(t) \geq 0.5 \times 10^{-4} \end{Bmatrix} \quad (9)$$

And then, we get:

$$\tau_M(t) =$$

$$\begin{Bmatrix} \frac{20000q(t)}{V_M} & \varphi(t) < -0.75 \\ \frac{10^4 q(t)}{V_M} + (-1.99) \times 10^8 \times \frac{q(t)^2}{V_M}, & \varphi(t) \geq -0.75\ and\ \varphi(t) < 0.25 \\ \frac{100q(t)}{V_M}, & \varphi(t) \geq 0.25 \end{Bmatrix} \quad (10)$$

From the above equations, we can get the time constants of charge-controlled memrister.

According to the MLIF membrane circuit and (7), the mathematic expression of the MLIF model can be rewritten as follows:

$$V_M(t + \Delta t) - V_M(t) = \frac{\Delta t}{\tau(t)}(-V_M(t) + V_{rest} + M(t)I_{ext}) \quad (11)$$

In the following experiments, the different stimuli are applied to the MLIF model, and the values of parameters will be set as $C = 2 \times 10^{-9}F$, $R = 10^6\ \Omega$, $V_{rest} = -60\ mV$, $V_{th} = -50\ mV$, $V_{rest} = -80\ mV$

5.4 Results

Varying DBS frequency

fdbs=60Hz

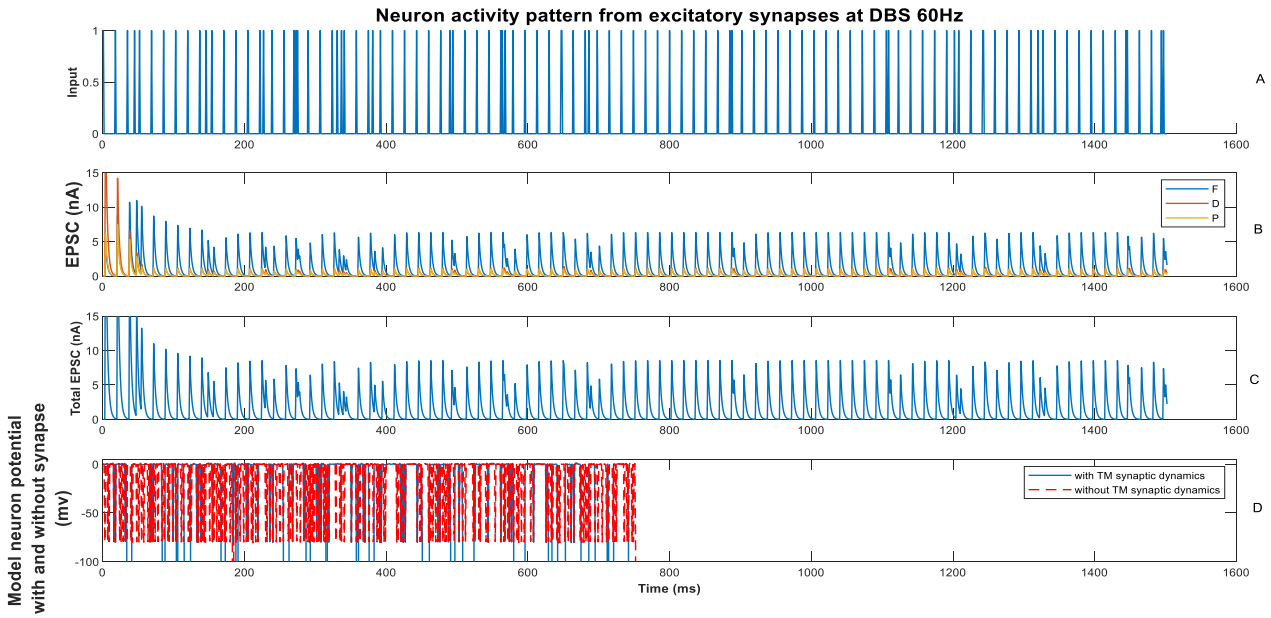

Fig.5.8

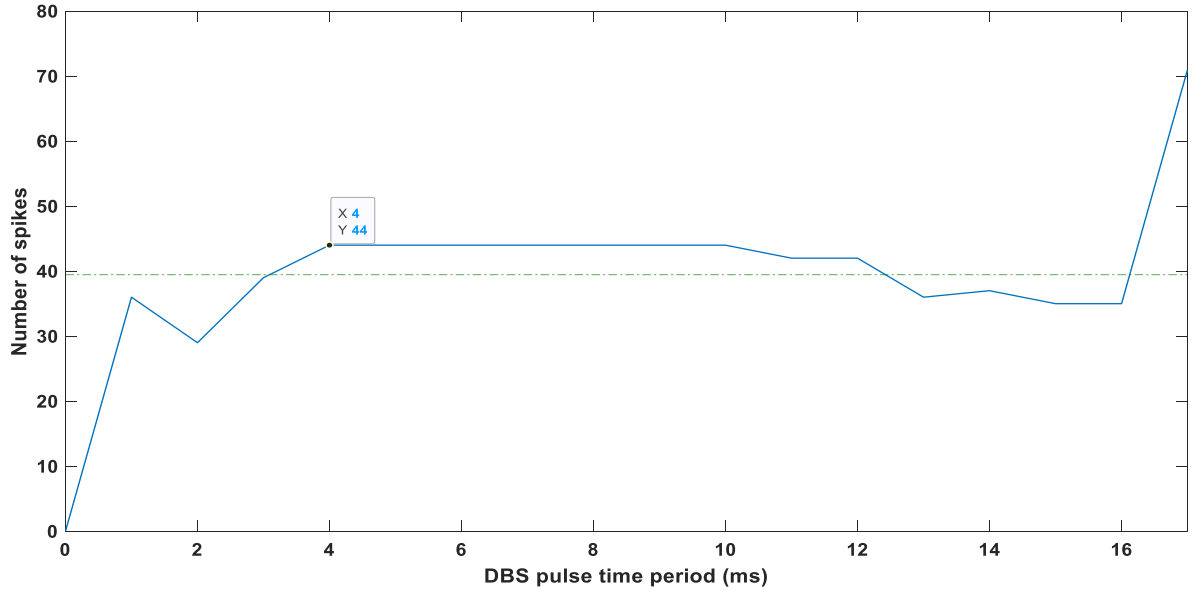

Fig.5.9

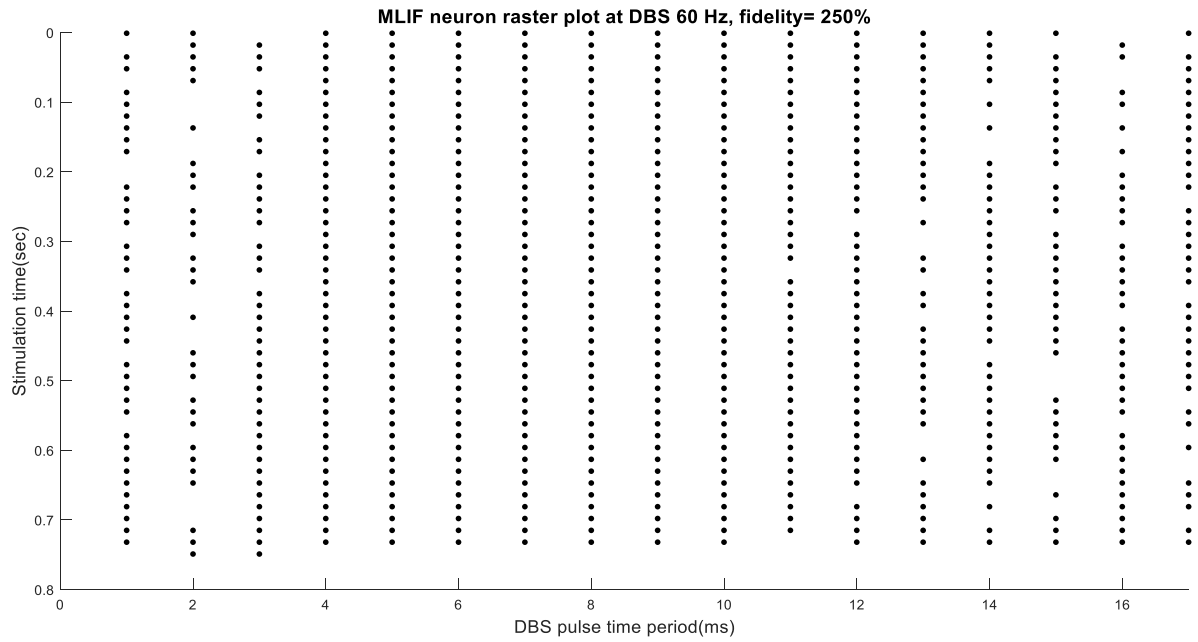

Fig.5.10

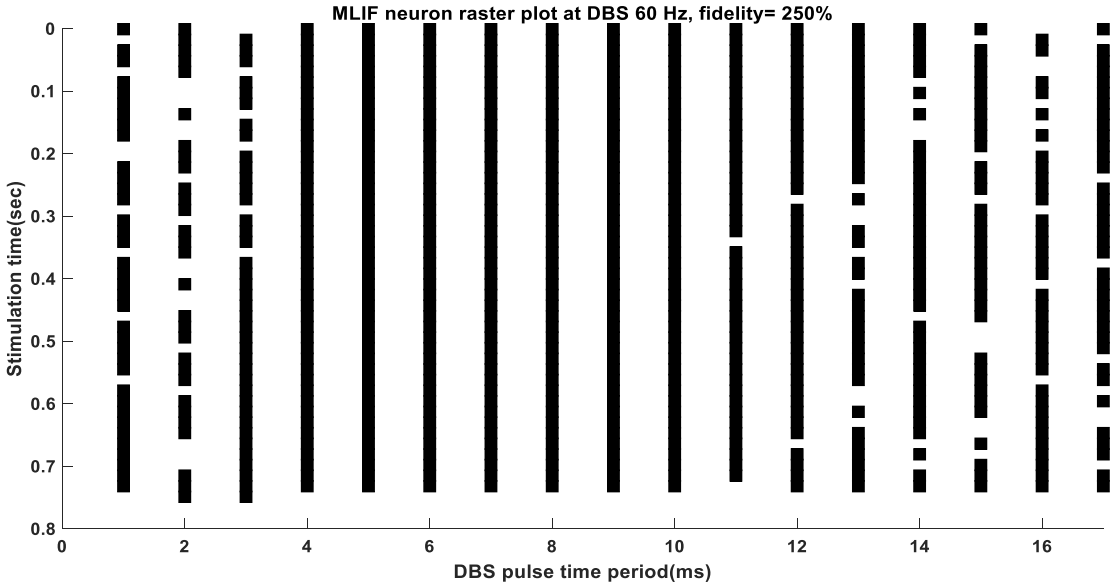

Fig.5.11

Fig.5.8(A) shows the input frequency, i.e. 60Hz. Fig.5.8(B) depicts EPSC from F, D and P synapses distinctly. Fig. 5.8(C) shows the total EPSC generated from all the synapses F, D and P. Fig.5.8(D) shows the response of neuron when driven by DBS input with or without TM synaptic dynamics.

Fig. 5.9 shows the number of spikes generated versus DBS pulse time period in milliseconds. The maximum no. of spikes generated is 44 at 4ms, whereas the average no. of spikes generated is 39.44.

Fig.5.10 and Fig.5.11 shows stimulus triggered action potentials during DBS. Fig.5.10 shows raster plot of the MLIF neuron model with TM synaptic dynamics and Fig. 5.11 without TM synaptic dynamics. Maximum no. of spikes generated lie at DBS pulse time of 4ms.

MLIF rate without any synaptic connection = 381.5877 (Hz)

MLIF rate with a fraction of synapses during DBS10Hz = 360.2402 (Hz)

MLIF rate with all synapses during DBS10Hz = 450.3002 Hz

Elapsed time is 8.107420 seconds.

fdbs=80Hz

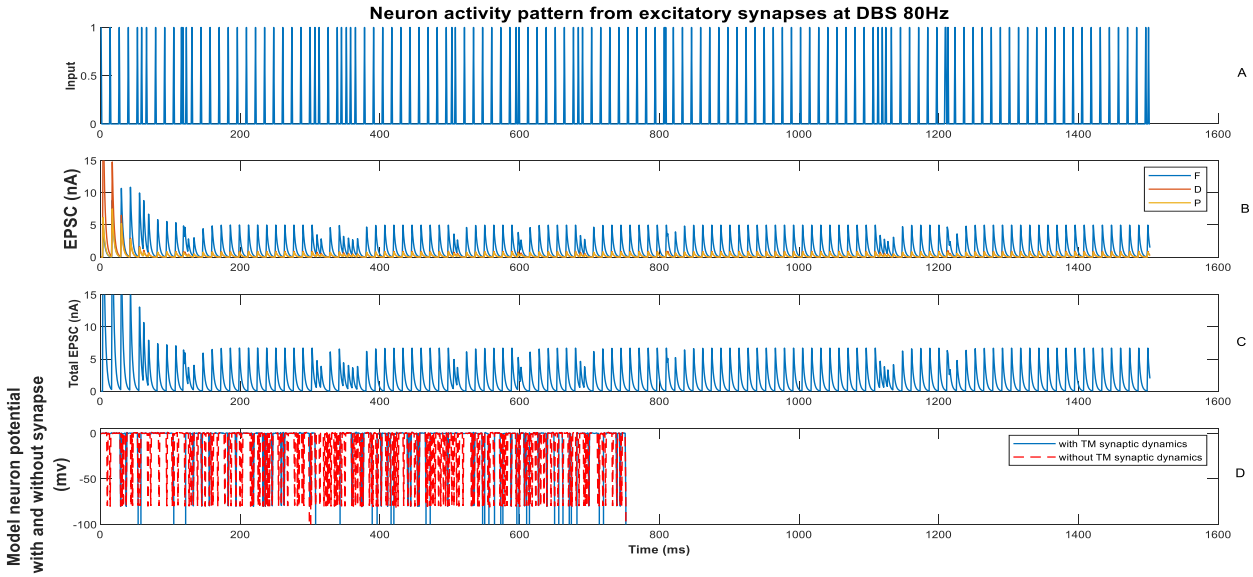

Fig.5.12

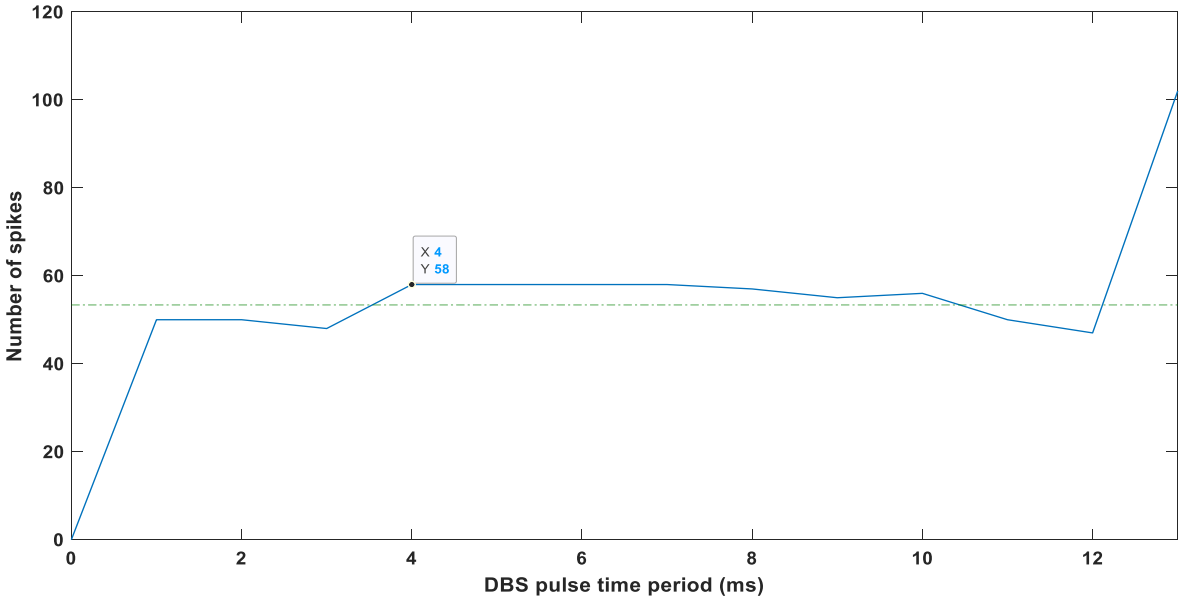

Fig.5.13

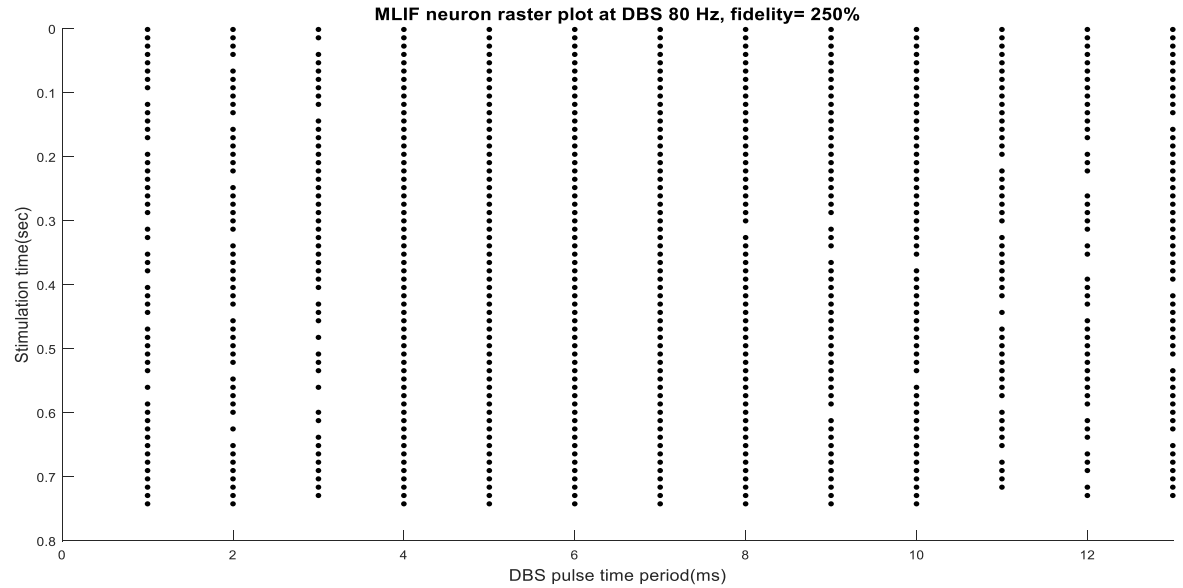

Fig.5.14

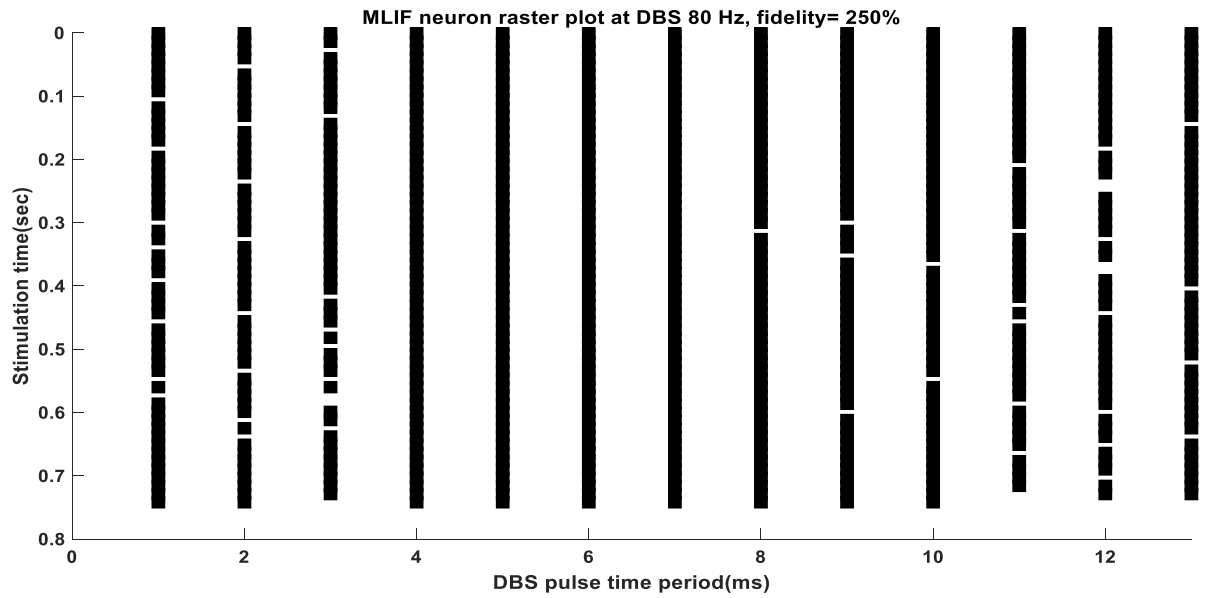

Fig.5.15

Fig.5.12(A) shows the input frequency, i.e. 80Hz. Fig.5.8(B) depicts EPSC from F, D and P synapses distinctly. Fig.5.12(C) shows the total EPSC generated from all the synapses F, D and P. Fig.5.12(D) shows the response of neuron when driven by DBS input with or without TM synaptic dynamics.

Fig. 5.13 shows the number of spikes generated versus DBS pulse time period in milliseconds. The maximum no. of spikes generated is 58 at 4ms, whereas the average no. of spikes generated is 53.36

Fig.5.14 and Fig.5.15 shows stimulus triggered action potentials during DBS. Fig.5.14 shows raster plot of the MLIF neuron model with TM synaptic dynamics and Fig. 5.15 without TM synaptic dynamics. Maximum no. of spikes generated lie at DBS pulse time of 4ms.

MLIF rate without any synaptic connection = 392.2615 (Hz)

MLIF rate with a fraction of synapses during DBS10Hz = 396.9313 (Hz)

MLIF rate with all synapses during DBS10Hz = 465.6438 Hz

Elapsed time is 9.892783 seconds.

fdbs=130Hz

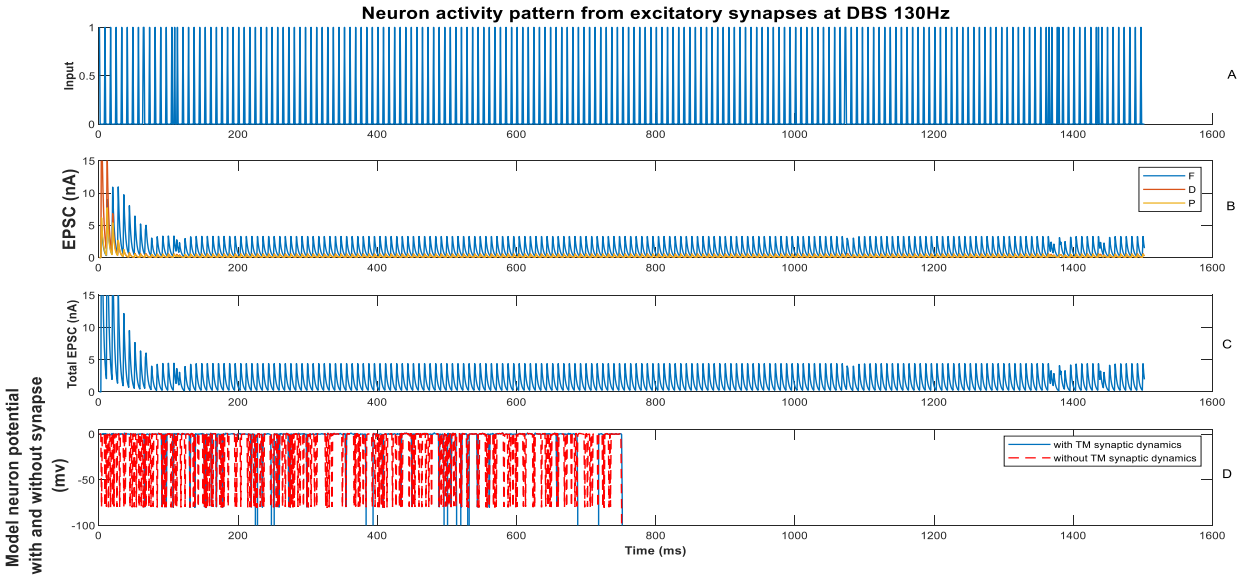

Fig.5.16

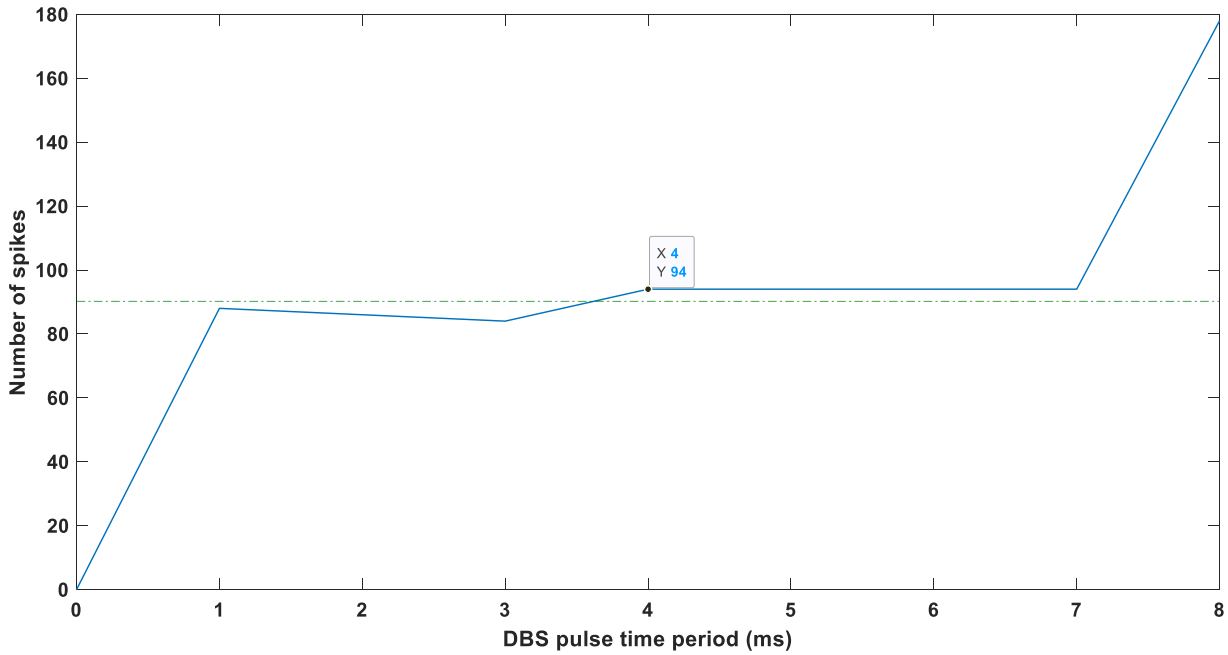

Fig.5.17

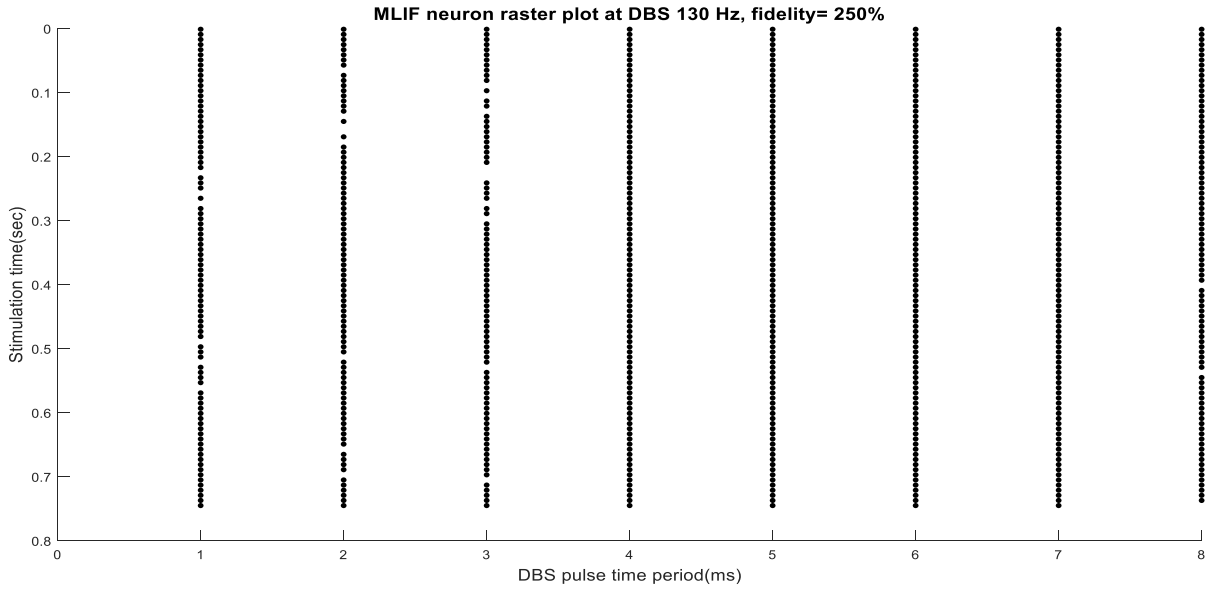

Fig.5.18

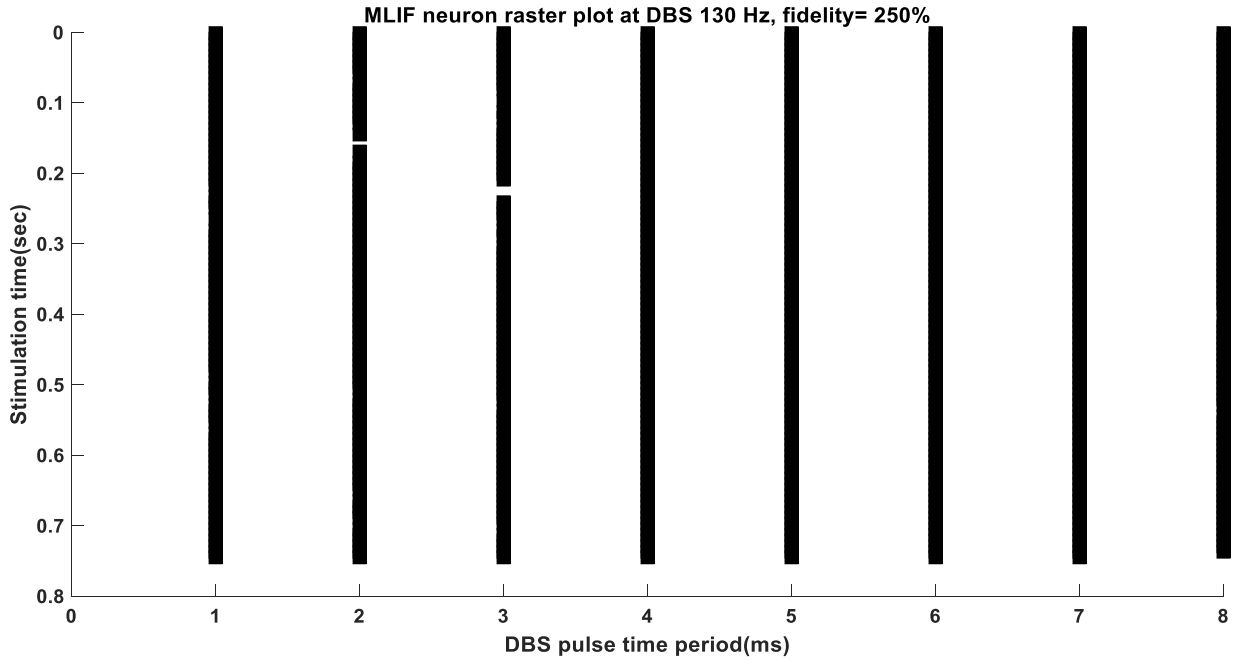

Fig.5.19

Fig.5.16(A) shows the input frequency, i.e. 130Hz. Fig.5.16(B) depicts EPSC from F, D and P synapses distinctly. Fig.5.16(C) shows the total EPSC generated from all the synapses F, D and P. Fig.5.16(D) shows the response of neuron when driven by DBS input with or without TM synaptic dynamics.

Fig. 5.17 shows the number of spikes generated versus DBS pulse time period in milliseconds. The maximum no. of spikes generated is 94 at 4ms, whereas the average no. of spikes generated is 90.22.

Fig.5.18 and Fig.5.19 shows stimulus triggered action potentials during DBS. Fig.5.18 shows raster plot of the MLIF neuron model with TM synaptic dynamics and Fig. 5.19 without TM synaptic dynamics. Maximum no. of spikes generated lie at DBS pulse time of 4ms to 7ms.

MLIF rate without any synaptic connection = 387.5917 (Hz)

MLIF rate with a fraction of synapses during DBS10Hz = 442.2949 (Hz)

MLIF rate with all synapses during DBS10Hz = 483.6558 Hz

Elapsed time is 15.005125 seconds.

fdbs=150Hz

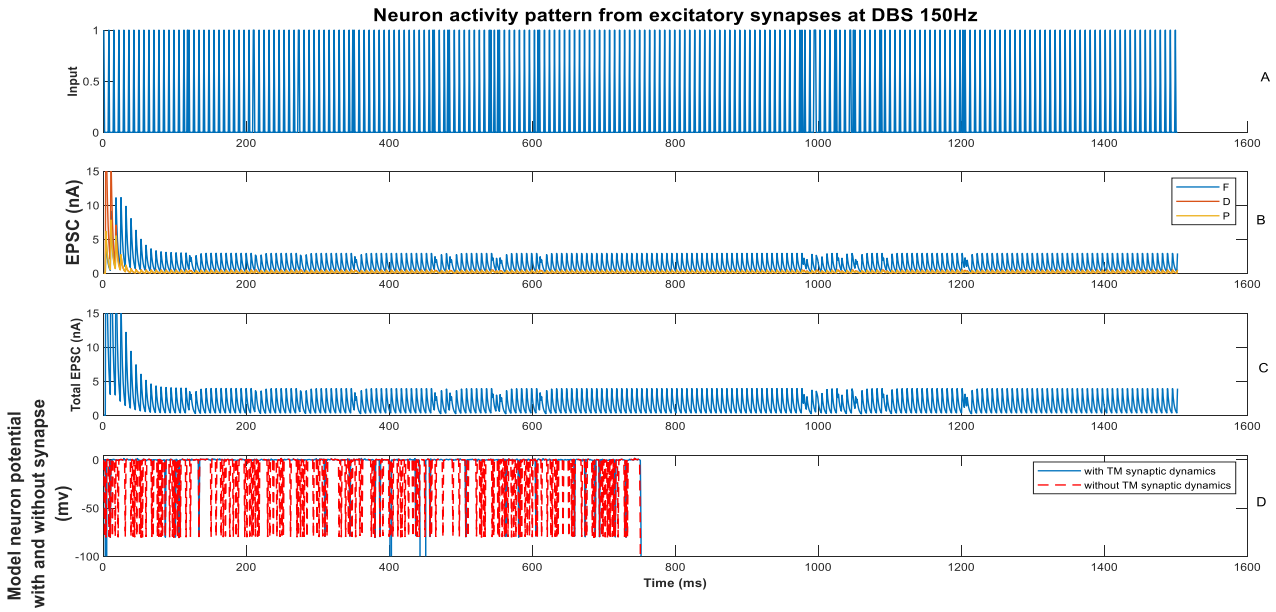

Fig.5.20

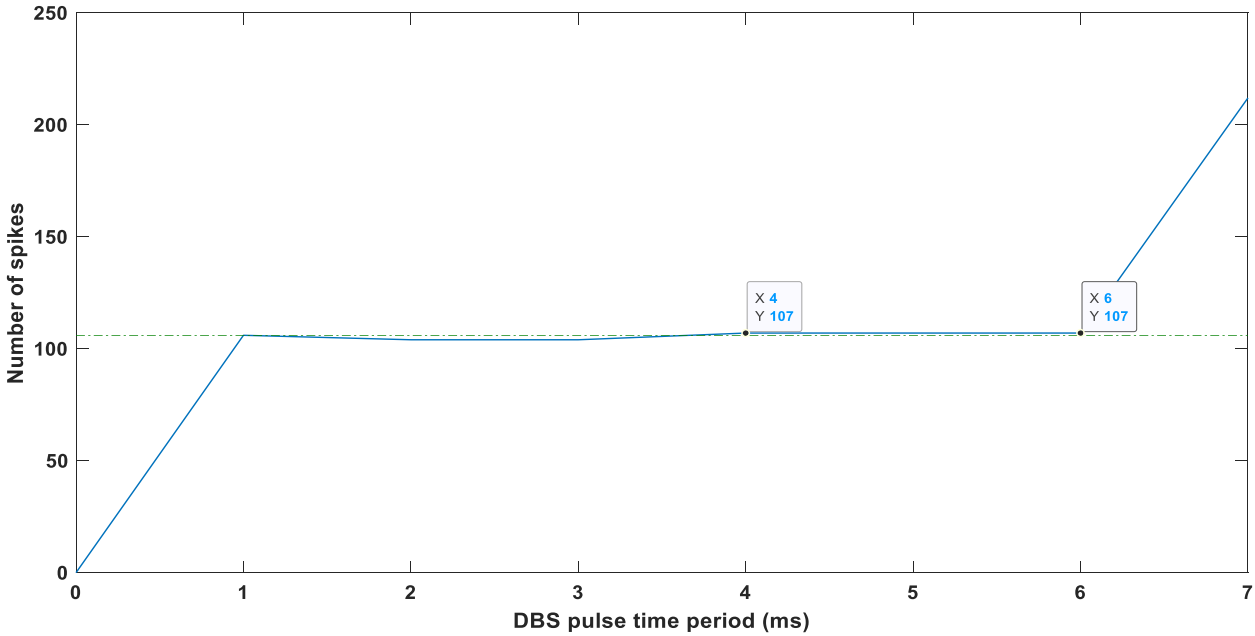

Fig.5.21

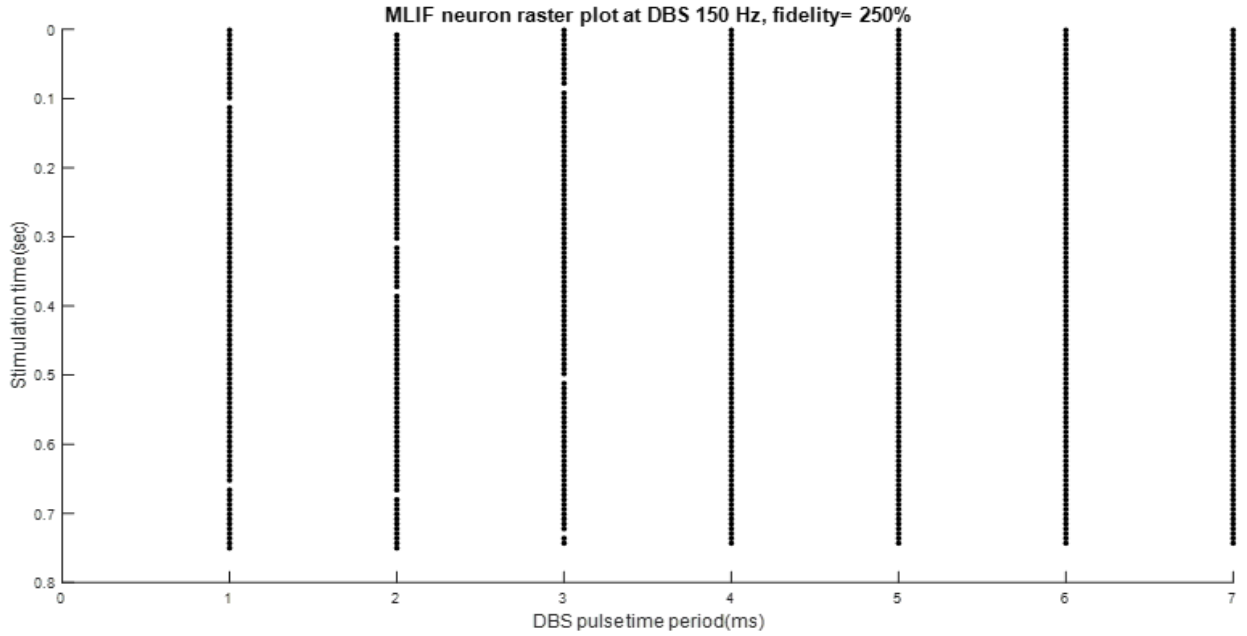

Fig.5.22

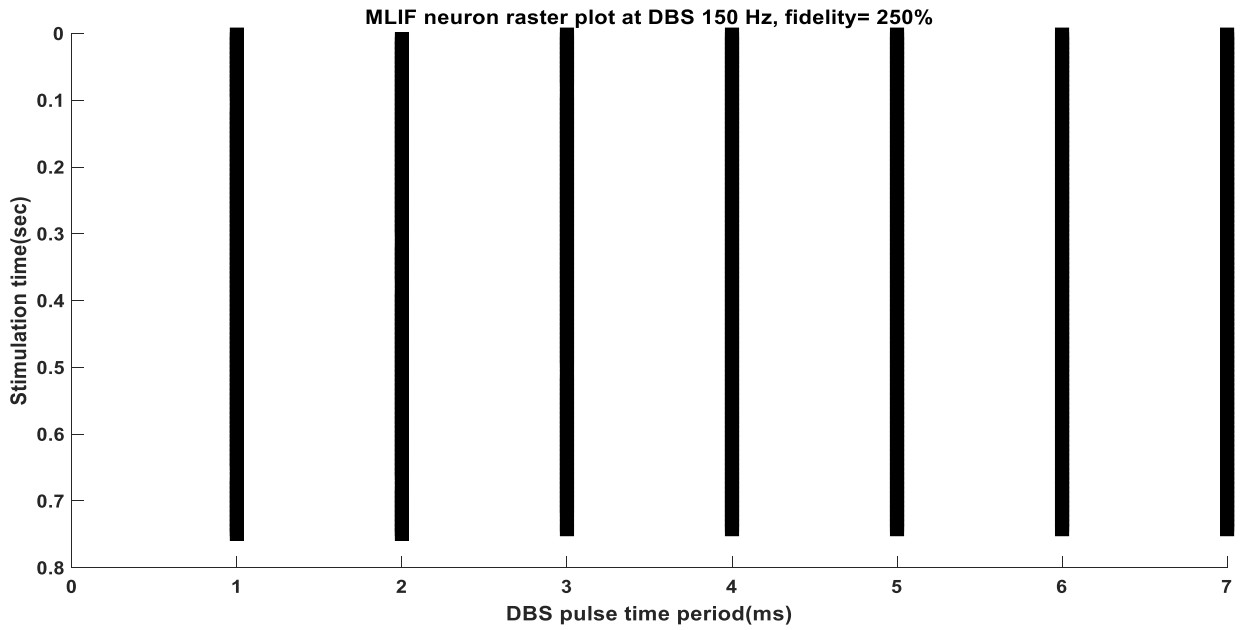

Fig.5.23

Fig.5.20(A) shows the input frequency, i.e. 150Hz. Fig.5.20(B) depicts EPSC from F, D and P synapses distinctly. Fig.5.20(C) shows the total EPSC generated from all the synapses F, D and P. Fig.5.20(D) shows the response of neuron when driven by DBS input with or without TM synaptic dynamics.

Fig. 5.21 shows the number of spikes generated versus DBS pulse time period in milliseconds. The maximum no. of spikes generated is 107 from 4ms to 6ms, whereas the average no. of spikes generated is 105.9.

Fig.5.22 and Fig.5.23 shows stimulus triggered action potentials during DBS. Fig.5.22 shows raster plot of the MLIF neuron model with TM synaptic dynamics and Fig. 5.23 without TM synaptic dynamics. Maximum no. of spikes generated lie at DBS pulse time of 4ms to 6ms.

MLIF rate without any synaptic connection = 392.2615 (Hz)

MLIF rate with a fraction of synapses during DBS10Hz = 479.6531 (Hz)

MLIF rate with all synapses during DBS10Hz = 494.9967 Hz

Elapsed time is 16.452186 seconds.

Fig.5.8 to Fig.5.23 depicts the post synaptic spiking activity of the F, D and P synapses triggered by DBS. It is found that the average number of spikes

generated by the MLIF neuron model increased as the applied DBS frequency was increased. This implies that as the DBS frequency increases, the spiking activity also increases.

Comparing Fig.4.8-4.23 with corresponding frequency plots in Figh.5.8-5.23, we observe that the number of spikes generated is greater when using MLIF neuron model. Hence, MLIF neuron model exhibits increased spiking activity than LIF neuron model.

Varying Noise input

(fdbs=130Hz)

wght=0

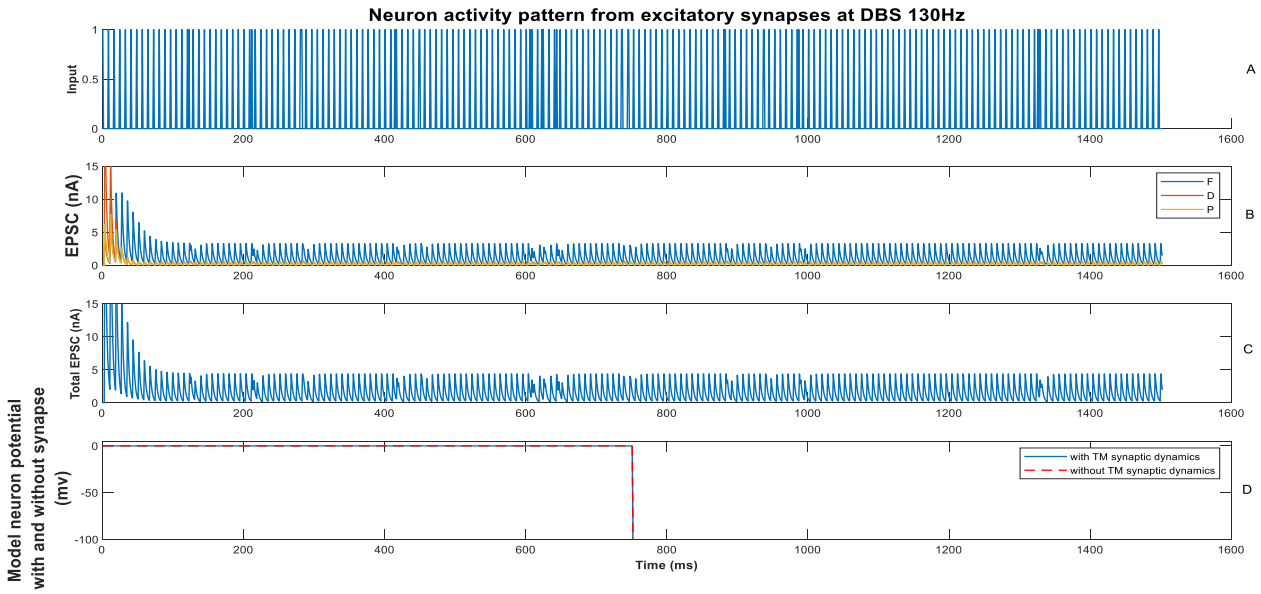

Fig.5.24

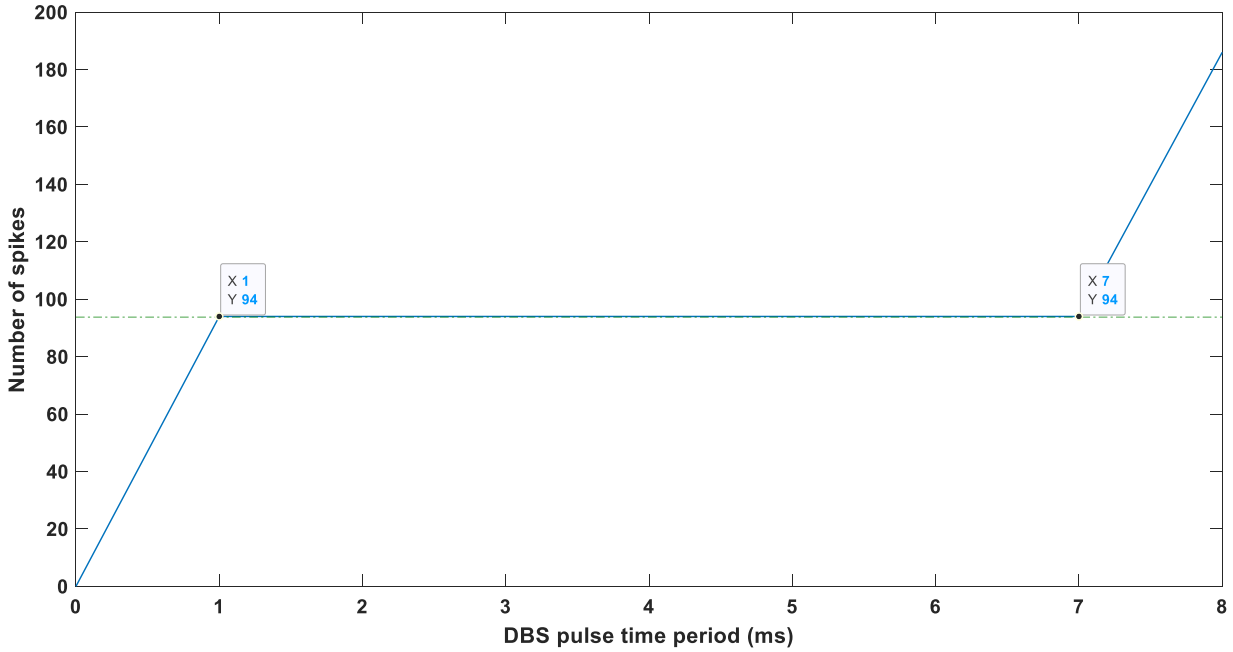

Fig.5.25

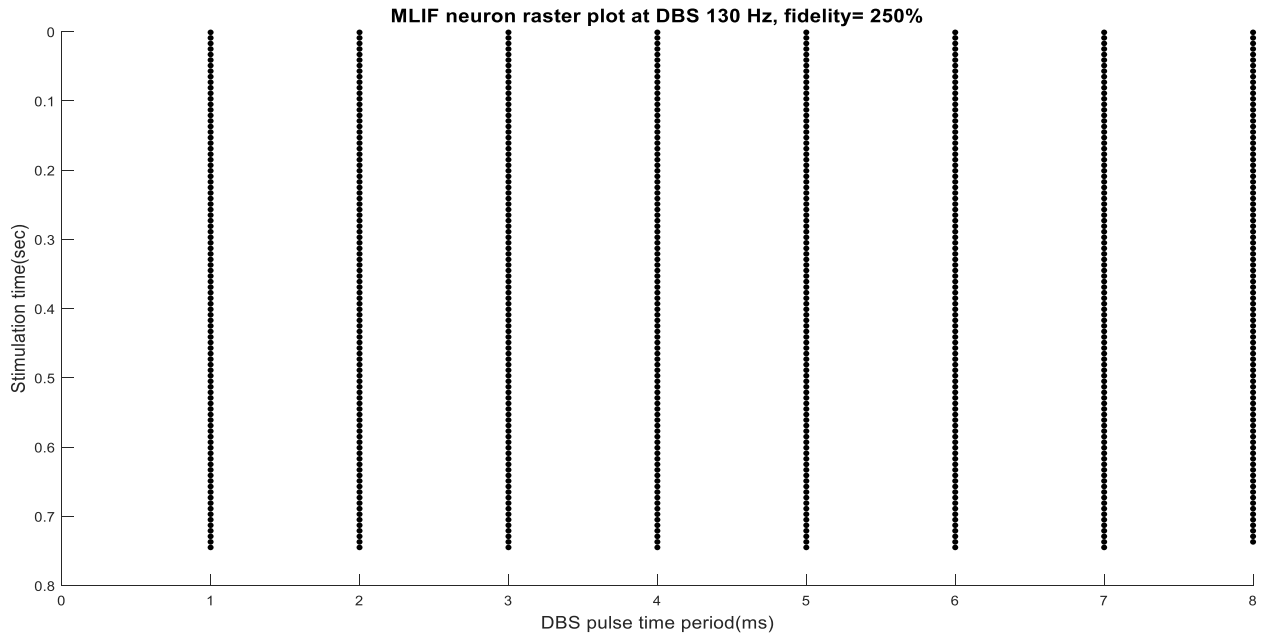

Fig.5.26

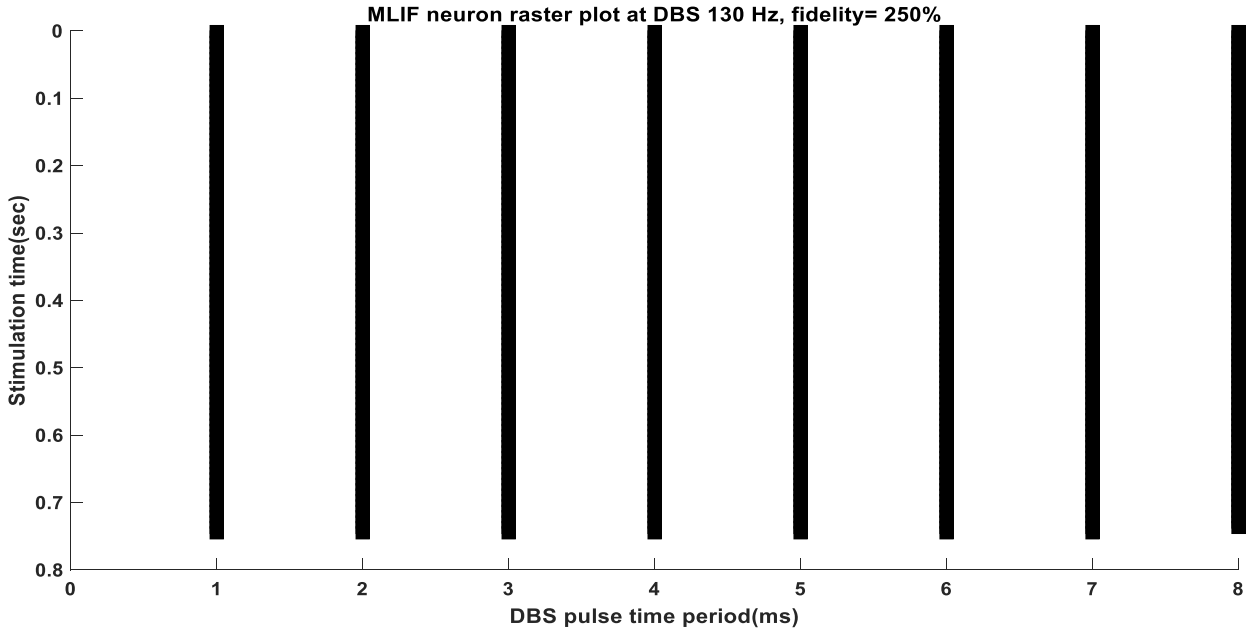

Fig.5.27

Fig.5.24(A) shows the input frequency, i.e. 130Hz. Fig.5.24(B) depicts EPSC from F, D and P synapses distinctly. Fig.5.24(C) shows the total EPSC generated from all the synapses F, D and P. Fig.5.24(D) shows the response of neuron when driven by DBS input with or without TM synaptic dynamics. No noise input is given.

Fig. 5.25 shows the number of spikes generated versus DBS pulse time period in milliseconds. The maximum no. of spikes generated is constant at 94 from 1ms to 7ms, whereas the average no. of spikes generated is 94.

Fig.5.26 and Fig.5.27 shows stimulus triggered action potentials during DBS. Fig.5.26 shows raster plot of the MLIF neuron model with TM synaptic dynamics and Fig. 5.27 without TM synaptic dynamics. Maximum no. of spikes generated lie at DBS pulse time of 1ms to 7ms.

MLIF rate without any synaptic connection = 501.0007 (Hz)

MLIF rate with a fraction of synapses during DBS10Hz = 501.0007 (Hz)

MLIF rate with all synapses during DBS10Hz = 501.0007 Hz

Elapsed time is 17.941460 seconds.

wght=0.5

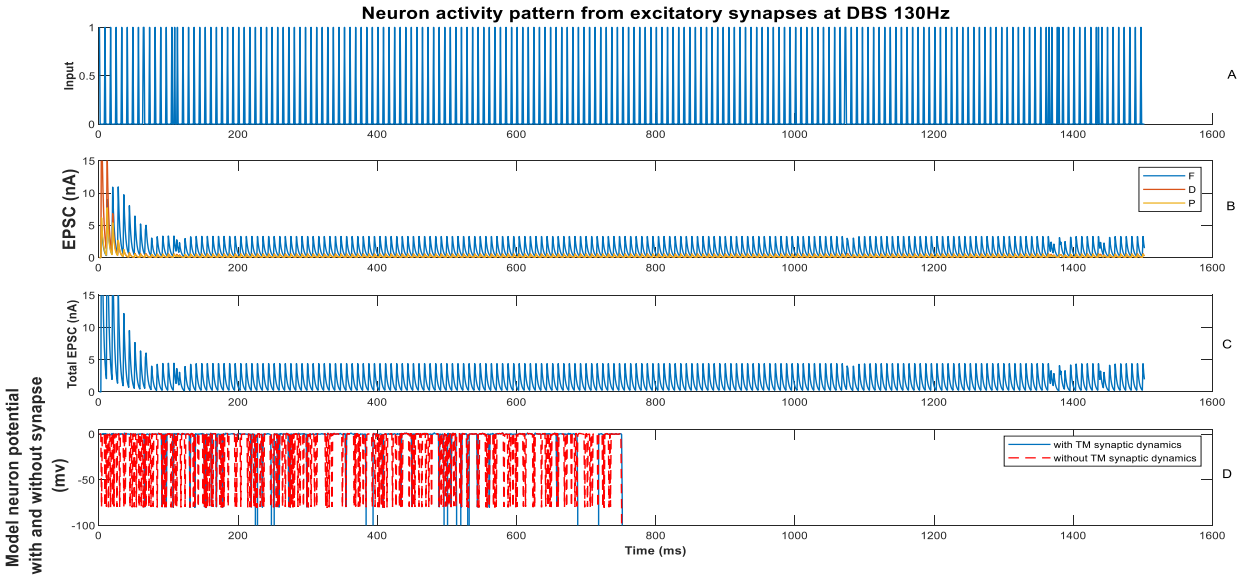

Fig.5.28

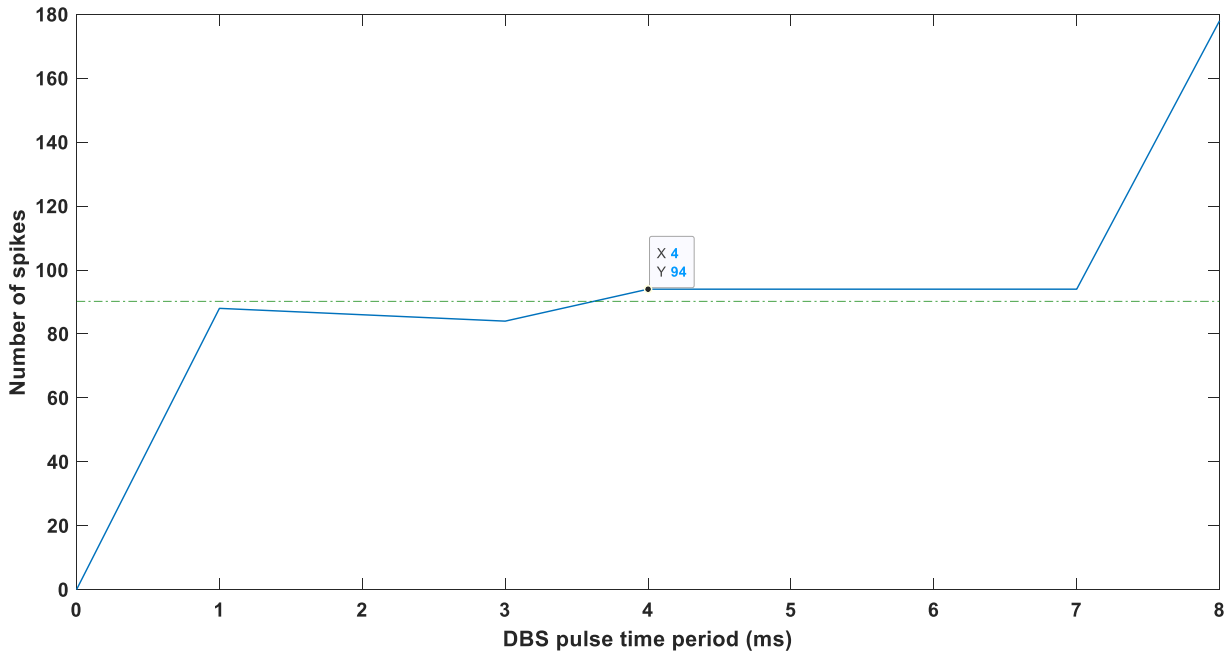

Fig.5.29

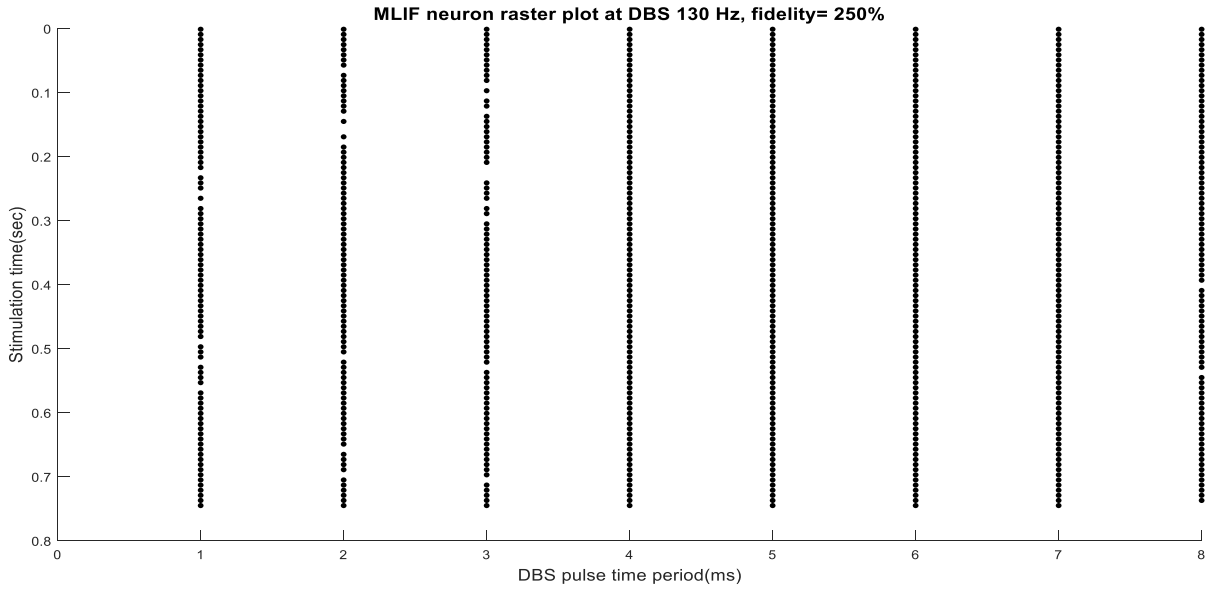

Fig.5.30

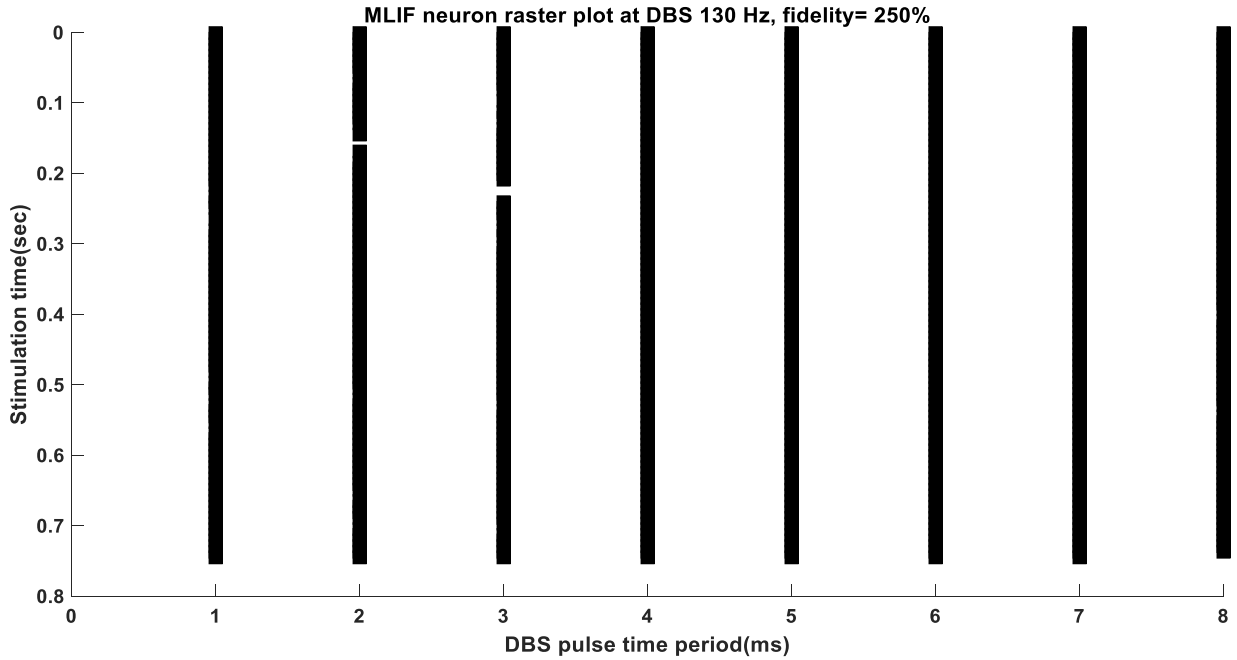

Fig.5.31

Fig.5.28(A) shows the input frequency, i.e. 130Hz. Fig.5.28(B) depicts EPSC from F, D and P synapses distinctly. Fig.5.28(C) shows the total EPSC generated from all the synapses F, D and P. Fig.5.28(D) shows the response of neuron when driven by DBS input with or without TM synaptic dynamics. Noise input given is wght=0.5.

Fig. 5.29 shows the number of spikes generated versus DBS pulse time period in milliseconds. The maximum no. of spikes generated is 94 at 4ms, whereas the average no. of spikes generated is 90.22.

Fig.5.30 and Fig.5.31 shows stimulus triggered action potentials during DBS. Fig.5.30 shows raster plot of the MLIF neuron model with TM synaptic dynamics and Fig. 5.31 without TM synaptic dynamics. Maximum no. of spikes generated lie at DBS pulse time of 4ms to 7ms.

MLIF rate without any synaptic connection = 387.5917 (Hz)

MLIF rate with a fraction of synapses during DBS10Hz = 442.2949 (Hz)

MLIF rate with all synapses during DBS10Hz = 483.6558 Hz

Elapsed time is 15.005125 seconds.

wght=5

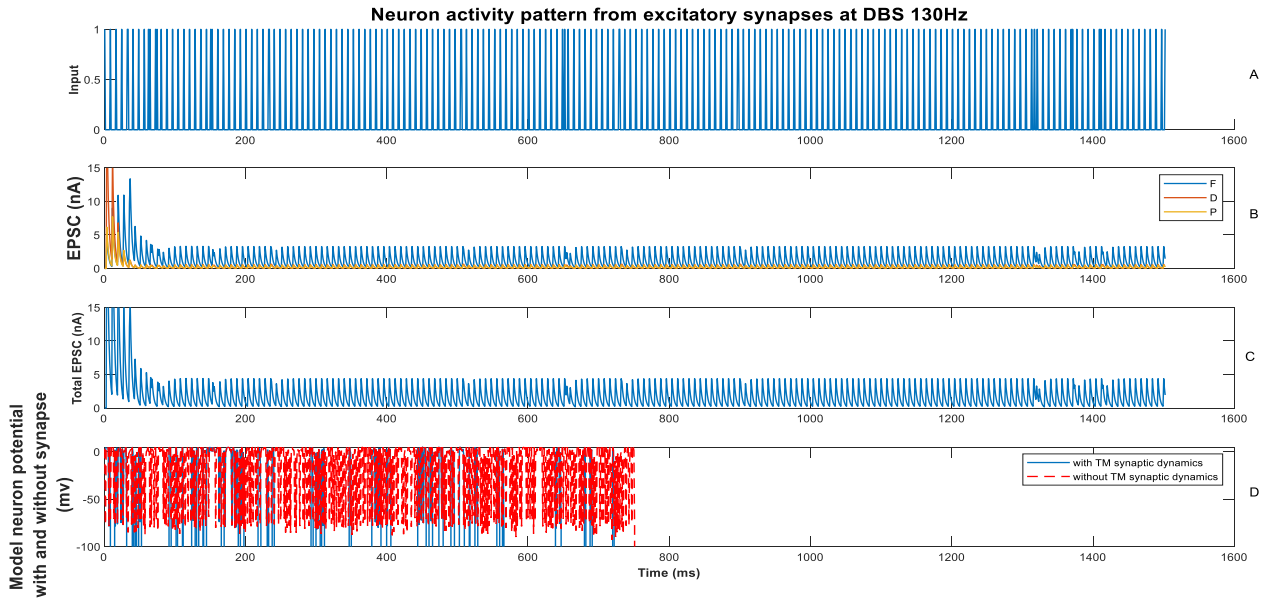

Fig.5.32

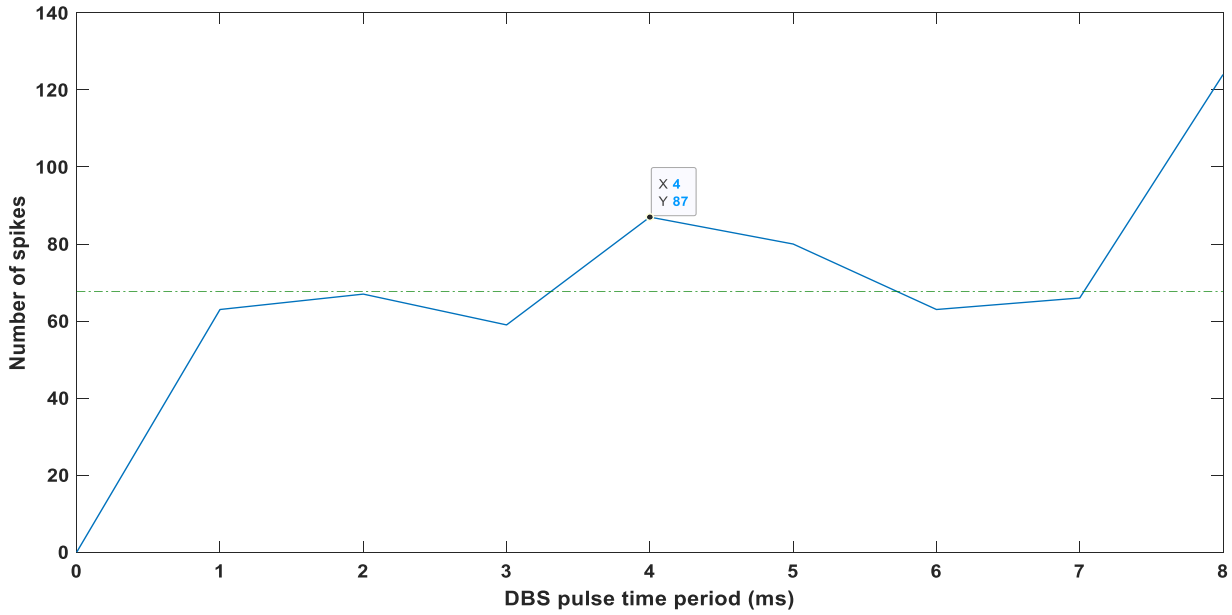

Fig.5.33

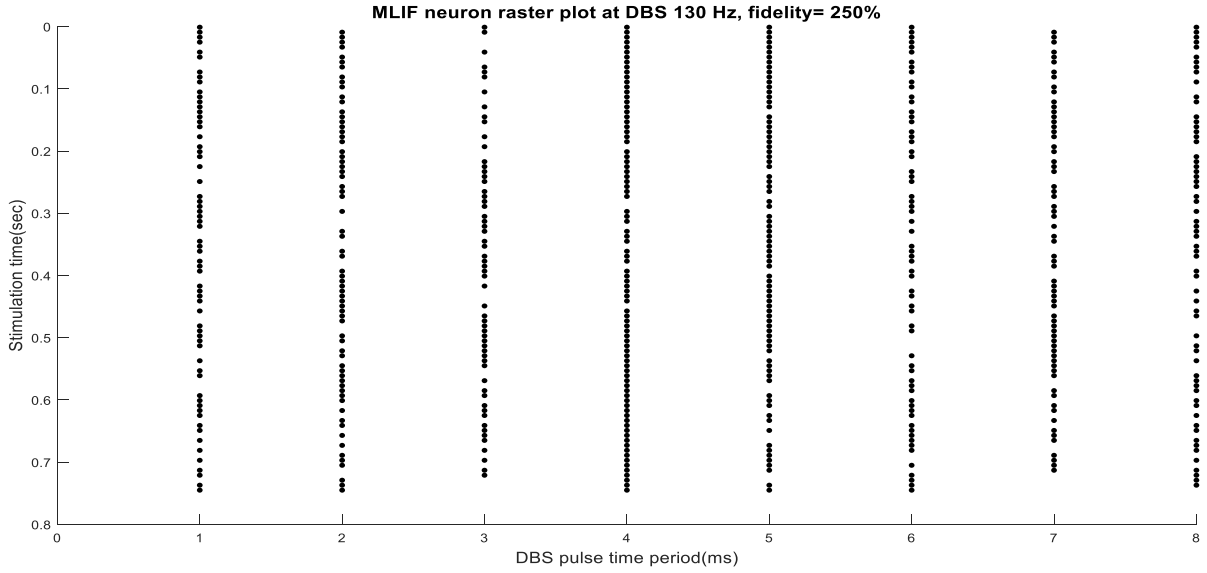

Fig.5.34

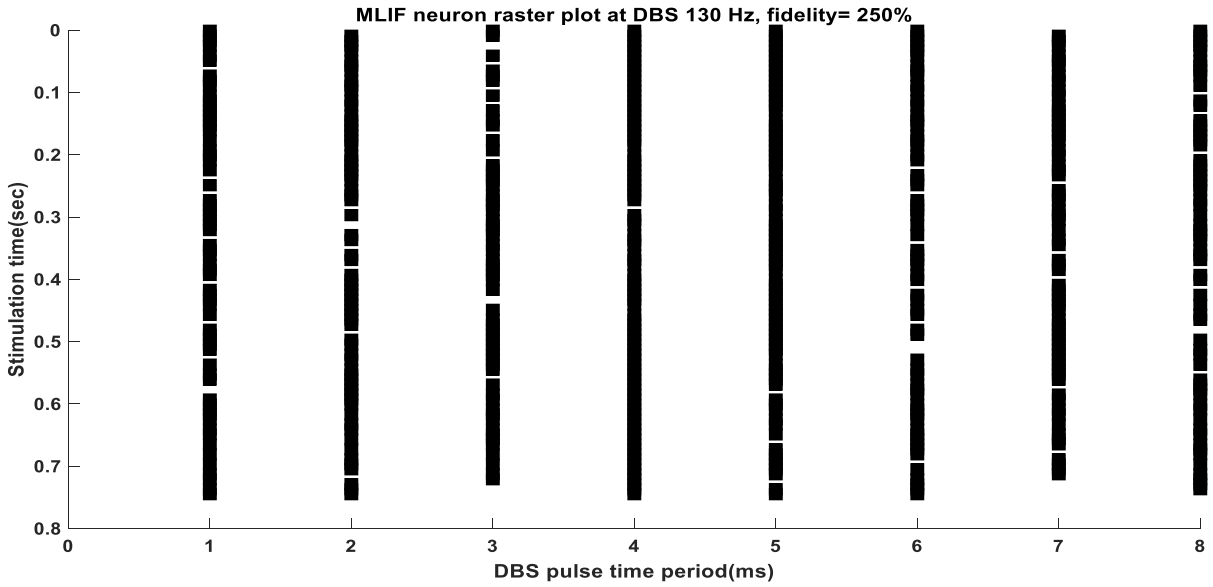

Fig.5.35

Fig.5.32(A) shows the input frequency, i.e. 130Hz. Fig.5.32(B) depicts EPSC from F, D and P synapses distinctly. Fig.5.32(C) shows the total EPSC generated from all the synapses F, D and P. Fig.5.32(D) shows the response of neuron when driven by DBS input with or without TM synaptic dynamics. A high noise input is given as wght=5.

Fig. 5.33 shows the number of spikes generated versus DBS pulse time period in milliseconds. The maximum no. of spikes generated is 87 at 4ms, whereas the average no. of spikes generated is 68.

Fig.5.34 and Fig.5.35 shows stimulus triggered action potentials during DBS. Fig.5.34 shows raster plot of the MLIF neuron model with TM synaptic dynamics and Fig.5.35 without TM synaptic dynamics. Maximum no. of spikes generated lie at DBS pulse time of 4ms.

MLIF rate without any synaptic connection = 334.2228 (Hz)

MLIF rate with a fraction of synapses during DBS10Hz = 112.0747 (Hz)

MLIF rate with all synapses during DBS10Hz = 364.9099 Hz

Elapsed time is 24.509666 seconds.

wght=10

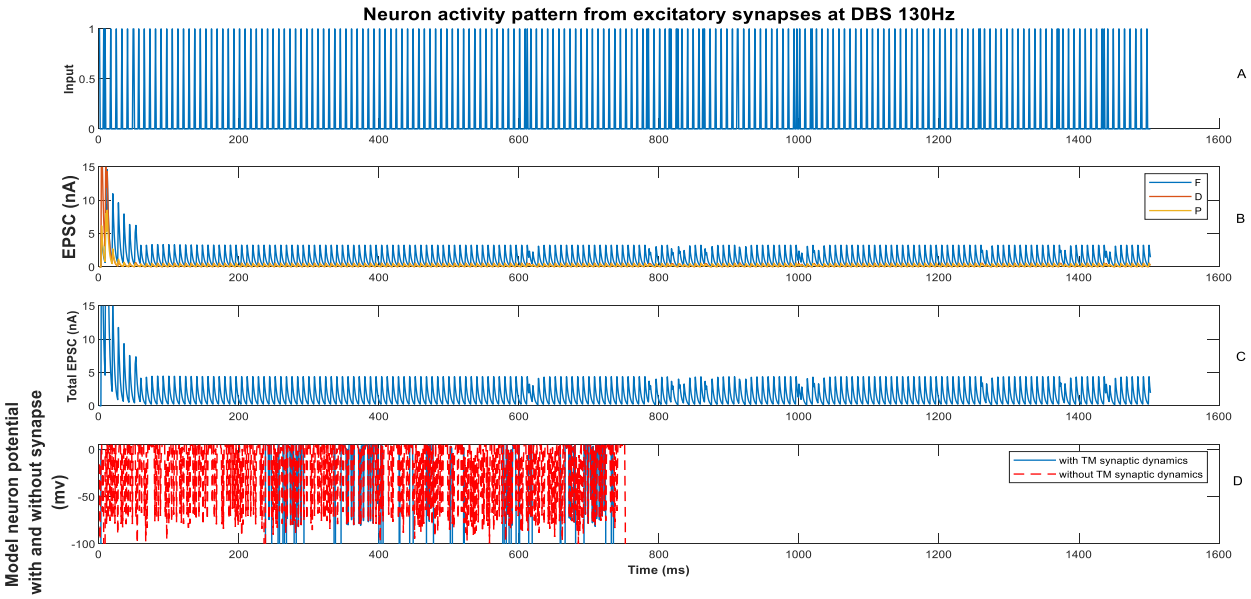

Fig.5.36

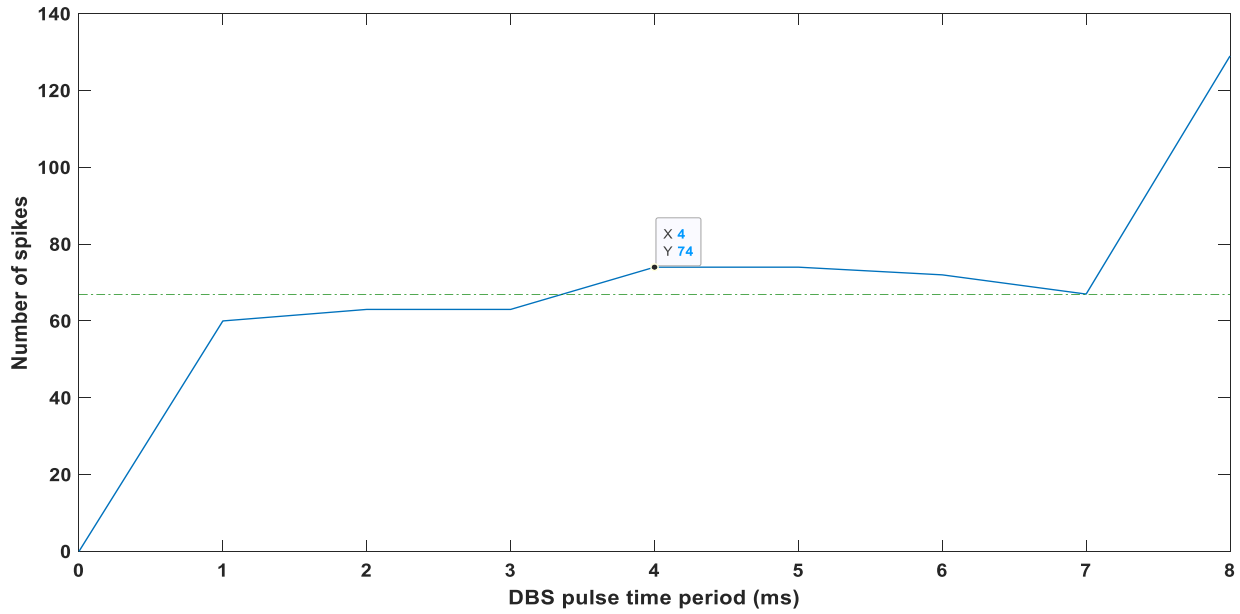

Fig.5.37

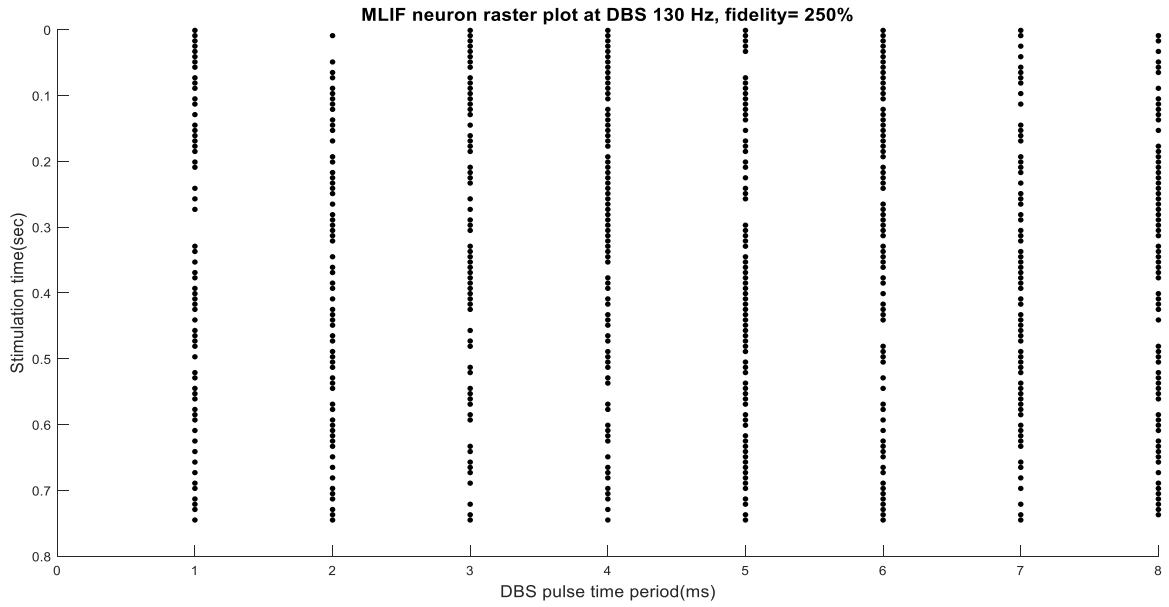

Fig.5.38

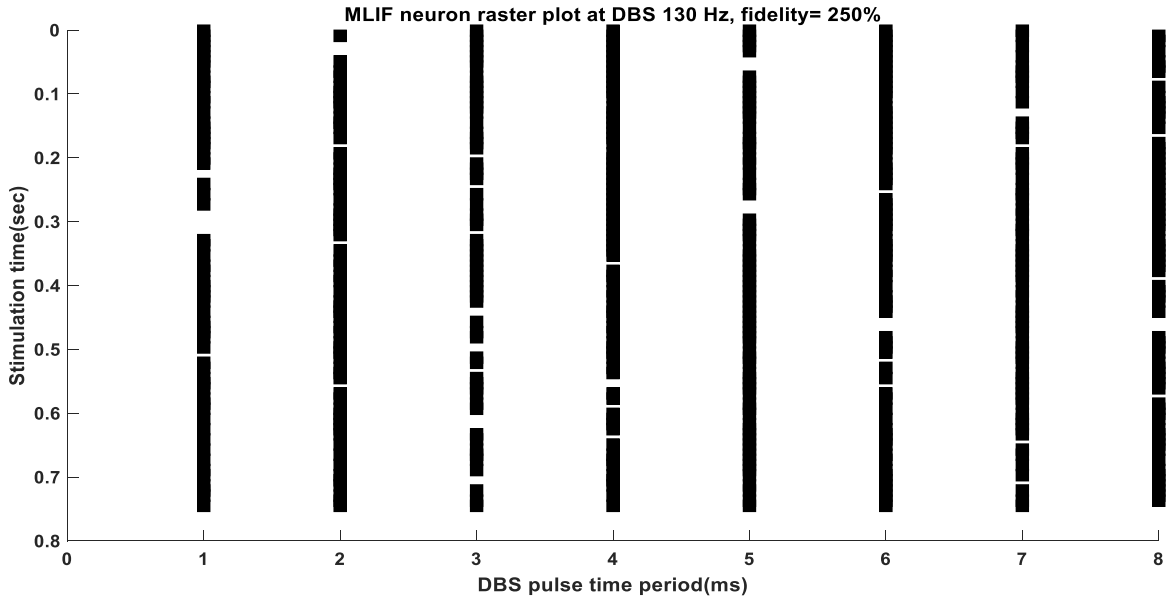

Fig.5.39

Fig.5.36(A) shows the input frequency, i.e. 130Hz. Fig.5.36(B) depicts EPSC from F, D and P synapses distinctly. Fig.5.36(C) shows the total EPSC generated from all the synapses F, D and P. Fig.5.36(D) shows the response of neuron when driven by DBS input with or without TM synaptic dynamics. Noise input is given is wght=10.

Fig. 5.37 shows the number of spikes generated versus DBS pulse time period in milliseconds. The maximum no. of spikes generated is 74 at 4ms, whereas the average no. of spikes generated is 66.

Fig.5.38 and Fig.5.39 shows stimulus triggered action potentials during DBS. Fig.5.38 shows raster plot of the MLIF neuron model with TM synaptic dynamics and Fig.5.39 without TM synaptic dynamics. Maximum no. of spikes generated lie at DBS pulse time of 4ms to 6ms.

MLIF rate without any synaptic connection = 338.8926 (Hz)

MLIF rate with a fraction of synapses during DBS10Hz = 99.3996 (Hz)

MLIF rate with all synapses during DBS10Hz = 362.2415 Hz

Elapsed time is 12.505596 seconds.

Analyzing Fig.5.24-5.39, we observe that as the applied noise input increases, the average number of spikes generated decreases. This implies that, the spiking activity of MLIF neuron model decreases with increasing noise input.

CHAPTER 6

DISCUSSION

The objective of this study was to develop a simple model that could capture the overall characteristics of DBS induced synaptic suppression and the DBS triggered post synaptic spiking. We used the Tsodyks-Markram (TM) phenomenological synapse model to represent depressing, facilitating, and pseudo-linear synapses driven by DBS over a wide range of stimulation frequencies. The EPSCs were then used as inputs to a leaky integrate-and-fire neuron model (LIF) and later to a memristor leaky integrate-and-fire neuron model (MLIF) in order to measure the DBS-triggered post-synaptic spiking activity.

Low frequency stimulation can generate a wide range of EPSCs that depend upon the type of synapse. High frequency driving of the synapse models generate marked EPSC suppression, independent of the synapse type. The average spiking activity increased with increase of applied DBS. The average spiking activity was found to decrease with increase in noise input. The MLIF neuron model was found to exhibit better spiking activity than LIF neuron model. Practically, it is undesirable to expose our body to very high frequency stimulation for DBS treatment to control movement disorders. Thus we prefer MLIF neuron model over LIF neuron model for enhanced spiking activity using a particular DBS frequency. The findings of this study are still theoretical, they do represent a step towards analyzing the consequences of DBS from a synaptic first principles approach. We hypothesize that by first understanding the effects of DBS at the synapse level, we may then extrapolate to network-level effects.

The basic purpose of brain stimulation therapy is to employ electrical pulses to modulate the release of neurotransmitters in specific brain circuits. Low frequency stimulation can be used to enhance neurotransmitter release in directly activated pathways, whereas high frequency stimulation can decrease synaptic communication through the methods described in this project. Furthermore, recent computational research and intraoperative human recordings have proven the importance of synaptic suppression in comprehending and interpreting neural activity patterns recorded during the DBS. We propose that the basic mechanism of DBS is to exploit the

physiological limits of the synaptic machinery to suppress connectivity. A simple model for these processes can help in optimization of DBS pulsing.

The LIF model with the non-volatile memristor is successfully proposed in this study, and we aim to develop the application of memristor in neuroscience. We choose the charge-controlled memristor to combine with the LIF spiking model and get the MLIF spiking model. We examined the firing patterns of LIF and MLIF and found the superiority of MLIF model over LIF model. The simulation results show that the MLIF model has good biological spiking frequency adaptation, higher firing frequency, and rich firing patterns. The MLIF model can reproduce the firing behavior of biological neurons very well.

Recent studies have shown that human skin and other biological tissues are memristors. Many researches have found that human skin exhibits non-volatile memory and that analogue information can actually be stored inside the skin at least for three minutes. Human skin actually contains two different memristor types, one that originates from the sweat ducts and one that is based on thermal changes of the surrounding tissue, the stratum corneum; and information storage is possible in both. Assuming that different physiological conditions of the skin can explain the variations in current responses that we observed among the subjects, it follows that non-linear recordings with DC pulses may find use in sensor applications. A new understanding of skin's electrical properties could have implications for medicine. This can even lead to development of artificially implantable skin.

MATLAB code for TM Model

```
%%%%%% This code generates the excitatory postsynaptic currents of
%%%%%% facilitating, depressing and pseudo-linear excitatory syanpses
%%%%%% based on Tsodyks-Markram synaptic model

clearvars

dt=.1; ti=dt; tf=10000;
t=ti:dt:tf;

% DBS input
fdbs=1:130;
T=ones(1,length(fdbs));
dbsi=500/dt; dbsf=10000/dt;

% I Kernel time constant
taus=1.75; %3

%input spike train
sp=zeros(length(fdbs),length(t));

% Synapse parameters % Each column represents E1, E2 and E3 respectively
tauf=[670,17,326];
taud=[138,671,329];
U=[.09,.5,.29];
% A=[0.0025,0.0025,0.0025];
A=[1,1,1];
n=1;
A=n*A;

% Compute EPSC
u=zeros(length(fdbs),length(t));
x=ones(length(fdbs),length(t));
I=zeros(length(fdbs),length(t));
% It=zeros(length(fdbs),length(t));
EPSC=zeros(length(A),length(fdbs),length(t));
select_time=dbsf-50000:dbsf;
It=zeros(length(fdbs),length(select_time));
M_I=ones(length(A),length(fdbs));
mi=zeros(length(A),1);
M_Iall=ones(length(A),length(fdbs));
area=zeros(length(A),length(fdbs));
area1=zeros(length(A),length(fdbs));
% Sc=zeros(length(A),length(fdbs));

for p=1:3
    for j=1:length(fdbs)
        T(j)=round(1000/fdbs(j)/dt);
        ts=dbsi:T(j):dbsf;
        sp(j,ts)=1/dt;
            for i=1:length(t)-1
                u(j,(i+1)) = u(j,i)+dt*(-(u(j,i)/tauf(p))+U(p)*(1-
u(j,i))*sp(j,i));
                x(j,(i+1)) = x(j,i) + dt*((1/taud(p))*(1-x(j,i)) -
u(j,i+1)*x(j,i)*sp(j,i));
                I(j,(i+1)) = I(j,i) + dt*((-1/taus)*I(j,i) +
A(p)*u(j,i+1)*x(j,i)*sp(j,i));
            end
```

```
        EPSC(p,j,:)= I(j,:);
%         M_Iall(p,j)=max(I(j,:));
        It(j,:)=I(j,select_time);
        M_I(p,j)=max(It(j,:));
%         mi(p)=max(M_Iall(p,j));
%         M_I(p,j)=M_I(p,j)./mi(p);
t1{p,j}=ts(end-1)+1:ts(end);   %last period EPSC curve
It1{p,j}=I(j,t1{p,j});
area1(p,j)=trapz(t1{p,j},It1{p,j})/10;       %area under the EPSC curve for
1 EPSC
area(p,j)=area1(p,j)*j;                      %area under the EPSC curve in
1 second
    end
end

%gain peak frequency
theta=1000/sqrt(tauf(1)*taud(1)*U(1)); %valid only for facilitating synapse

%Make figure
freq1=20; freq2=130;
figure;
ax1=subplot(4,3,1);


plot(t,squeeze(EPSC(1,freq1,:)),'k','LineWidth',1); ylabel({'EPSC
(nA)';'Facilitating'},'FontWeight','bold')
xlim([450 1000]); ylim([0 .6]);

ax2=subplot(4,3,2);
qq=EPSC(1,freq2,:)
ww=squeeze(EPSC(1,freq2,:))
%plot(t,squeeze(EPSC(1,freq2,:)),'k','LineWidth',1); %ylabel({'I_{syn}
(nA)'; 'EPSC'},'FontWeight','bold')
xlim([450 1000]); ylim([0 .6]);

ax3=subplot(4,3,3);
scatter(fdbs,squeeze(M_I(1,:,1)),'k','.'); ylabel({'Facilitating
synapse';'EPSC_{st} amplitude (nA)'},'FontWeight','bold')

hold on
plot((1./fdbs)+.008,'--','LineWidth',1); zoom xon; %ylim([0 .14])
ylim([0 .6]);

ax4=subplot(4,3,4);
plot(t,squeeze(EPSC(2,freq1,:)),'k','LineWidth',1); ylabel({'EPSC
(nA)';'Depressing'},'FontWeight','bold')
xlim([450 1000]); ylim([0 .6]);

ax5=subplot(4,3,5);
plot(t,squeeze(EPSC(2,freq2,:)),'k','LineWidth',1); %ylabel({'I_{syn}
(nA)'; 'EPSC'},'FontWeight','bold')
xlim([450 1000]); ylim([0 .6]);

ax6=subplot(4,3,6);
scatter(fdbs,squeeze(M_I(2,:,1)),'k','.'); ylabel({'Depressing
synapse';'EPSC_{st} amplitude (nA)'},'FontWeight','bold')
ylim([0 .6]);

ax7=subplot(4,3,7);
```

```
plot(t,squeeze(EPSC(3,freq1,:)),'k','LineWidth',1); ylabel({'EPSC
(nA)';'Pseudo-linear'},'FontWeight','bold')
xlim([450 1000]); ylim([0 .6]);

ax8=subplot(4,3,8);
plot(t,squeeze(EPSC(3,freq2,:)),'k','LineWidth',1); %ylabel({'I_{syn}
(nA)'; 'EPSC'},'FontWeight','bold')
xlim([450 1000]); ylim([0 .6]);

ax9=subplot(4,3,9);
scatter(fdbs,squeeze(M_I(3,:,1)),'k','.'); ylabel({'Pseudo-linear
synapse';'EPSC_{st} amplitude (nA)'},'FontWeight','bold')
ylim([0 .6]);

ax10=subplot(4,3,10);
plot(t,sp(freq1,:),'k','LineWidth',1); zoom xon; ylabel(['Input
',num2str(freq1),' Hz'],'FontWeight','bold')
xlim([450 1000]);
xlabel('Time (ms)','FontWeight','bold');

ax11=subplot(4,3,11);
plot(t,sp(freq2,:),'k','LineWidth',1); zoom xon; ylabel(['Input
',num2str(freq2),' Hz'],'FontWeight','bold')
xlim([450 1000]);
xlabel('Time (ms)','FontWeight','bold');

ax12=subplot(4,3,12);
scatter(fdbs,squeeze(M_I(1,:,1)),'.'); zoom xon; hold on;
scatter(fdbs,squeeze(M_I(2,:,1)),'.'); hold on
scatter(fdbs,squeeze(M_I(3,:,1)),'.'); hold on
xlabel('Frequency (Hz)','FontWeight','bold');
ylabel({'All synapses';'EPSC_{st} amplitude (nA)'},'FontWeight','bold')
ylim([0 .6]);

figure
scatter(fdbs,squeeze(M_I(1,:,1)),'filled'); zoom xon; hold on;
scatter(fdbs,squeeze(M_I(2,:,1)),'filled'); hold on
scatter(fdbs,squeeze(M_I(3,:,1)),'filled'); hold on
xlabel('Frequency (Hz)','FontWeight','bold');
ylabel({'EPSC_{st} amplitude (nA)'},'FontWeight','bold')
ylim([0 .5])
set(gca,'FontSize',12,'FontWeight','bold')

%% Integrals
S1=zeros(length(A),length(fdbs));
S=zeros(length(A),length(fdbs));
for j=1:3
for i=1:length(fdbs)
S1(j,i) = -M_I(j,i)*taus*(exp(-T(i)/taus)-1); %The integral of one EPSC at
the steady state
S(j,i) = S1(j,i)*i;
end
end

area1f=area1(1,:);
area1d=area1(2,:);
area1p=area1(3,:);
areaf=area(1,:);
aread=area(2,:);
areap=area(3,:);
```

```
f_weight=.45; d_weight=.38; p_weight=.18;
area_tot=f_weight*areaf+d_weight*aread+p_weight*areap;

figure; title('Area under 1 EPSC'); hold on
for p=1:3
scatter(fdbs,area1(p,:));
hold on
end
legend('F','D','P')
for p=1:3
plot(fdbs,S1(p,:),'Linewidth',1);
hold on
end
xlabel('DBS frequency (Hz)')
ylabel('S_1')
set(gca,'FontSize',12,'FontWeight','bold')

figure; title('Area under EPSCs in 1 second of stimulation'); hold on
for p=1:3
scatter(fdbs,area(p,:),'filled');
hold on
end
scatter(fdbs,area_tot,'filled','k');

legend('F','D','P','Total')
% for p=1:3
% plot(fdbs,S(p,:),'Linewidth',1);
% hold on
% end
% plot(ff,sf,'LineWidth',1)
xlabel('DBS frequency (Hz)')
ylabel('S')
set(gca,'FontSize',12,'FontWeight','bold')
```

MATLAB code for LIF Neuron Model

```
%%%%%% This code computes an LIF neuron activity before and during DBS.
tic
clearvars

% transmission + synaptic delay: td
td=2; %2 ms for trasmission and .5 ms for synaptic delay

dt=1; ti=dt; tf=1500+td;%tf=1500+td;%tf=61000+td; %in mili seconds
t=ti:dt:tf;

% DBS input
fdbs=130;
T=ones(1,length(fdbs));
% dbsi=(100)/dt; dbsf=1100/dt; %in mili seconds
dbsi=(dt)/dt; dbsf=1500/dt;

%Poissonian input
fr=10; %for fr Hz baseline poissonian firing from other cells
[spikes,tsp]=poissonSpikeGen(fr,tf/1000,1,dt/1000);
tp=find(spikes==1);
% ssp=zeros(1,length(t));
% ssp(tp)=1; %uncomment for stochastic model (adding noise to the system)

%noise term
% wght=0;   %no noise
wght=.5; %default noise
% wght=5;   %high noise
kisi=wght*randn(1,length(t));

% I Kernel time constant
taus=3;  %For excitatory synapse

% transmission + synaptic delay: td
td=td/dt; %convert to simulation step scale

%input spike train
sp=zeros(length(fdbs),length(t));

% Synapse parameters % Each column 1,2,3 means F,D,P respectively and each
row means
% Excitatory and inhibitory synapse (1: excitatory, 2: inhibitory)
% In this study we just used the first row, excitstory synapses.
tauf=[670,17,326; 376,21,62];
taud=[138,671,329; 45,706,144];
U=[.09,.5,.29; .016,.25,.32];
A=[.0025,.0025,.0025; .0025,.0025,.0025];
% n=10; A=n*A;  % change the strength of A (order of magnitude of totall
number of synapses)
ie=ones(1,2);
w=1;

fid=2.5; %synaptic fidelity
we=fid*200; wi=0;
% Percentage of excitatory and inhibitory synapses:
```

```
ne=we*[45,38,17]; %original: 45,38,17
% ne=zeros(1,3);
% for 1 synapse n1=1 and so forth (approximately giving 2 pA exc. current)
% ne=10;  % for 10 synapses (approximately giving 20 pA exc. current)
% ne=100; % for 100 synapses (approximately giving 200 pA exc. current)
% ne=1000;% for 1000 synapses (approximately giving 2 nA exc. current)
% ni=wi*[13,10,6];     % for 1 synapse (approximately giving 10 pA
inhibitory current)
ni=wi*[8,76,16]; %ne=ni;
% ni=zeros(1,3);
% ni=10;  % for 10 synapses (approximately giving 100 pA inh. current)
% ni=100; % for 100 synapses (approximately giving 1 nA inh. current)
% ni=1000;% for 1000 synapses (approximately giving 10 nA inh. current)
A=[ne.*A(1,:);ni.*A(2,:)];

% Compute EPSC
u=zeros(length(fdbs),length(t));
x=ones(length(fdbs),length(t));
I=zeros(length(fdbs),length(t));
Iwo=zeros(length(fdbs),length(t));
% It=zeros(length(fdbs),length(t));
PSC=zeros(length(ie),length(A),length(fdbs),length(t));
% IPSC=zeros(length(A),length(fdbs),length(t));

% Compute EPSP (passive mechanism, membrane potential)
tau_memb=40;
r=10^2;   %M Ohm
v=zeros(length(fdbs),length(t));
PSP=zeros(length(ie),length(A),length(fdbs),length(t));
% IPSP=zeros(length(A),length(fdbs),length(t));

% Neuron parameters: (for ~20 Hz base firing .56 and for ~8-10 Hz choose
.26)
Cm= 1; Rm=100; Ie=.26; %(for deterministic model)
% Ie=.16; %subthreshold firing (for noise purpose, stochastic model)
El=-70; Vth=-54;
Vreset=-80;

% % Neuron parameters: (for 62.5 Hz base firing)
% Cm= 1; Rm=100; Ie=1.52; %(for deterministic model)
% % Ie=.18; %subthreshold firing (for noise purpose, stochastic model)
% El=-70; Vth=-54;
% Vreset=-80;

% Compute neuron firing pattern with and without synaptic input:
V=zeros(length(fdbs),length(t));
Vn=zeros(length(ie),length(A),length(fdbs),length(t));
V_all=zeros(length(fdbs),length(t));
% Vn_all=zeros(length(ie),length(A),length(fdbs),length(t));
Vin=zeros(1,length(t));

wk=10; %Poissonian weight
poiss=wk*rand(1,length(sp)).*sp(1,:);
for i=1:length(t)-1
Vin(i+1) = Vin(i) + (dt/Cm)*(((El-Vin(i))/Rm) + Ie + poiss(i) + kisi(i));
if Vin(i+1)>= Vth+kisi(i)
    Vin(i)=0+kisi(i);
    Vin(i+1)=Vreset+kisi(i);
end
end
```

```
for q=1:length(ie)
    if q==1
        w=1;
    else
        w=-1;
    end
for p=1:length(A)
    for j=1:length(fdbs)
        T(j)=round((1000/fdbs(j))/dt);
        dbs=dbsi:T(j):dbsf;
        ts=[tp,dbs]; %uncomment for Poissonian+DBS
%         ts=dbs;      %uncomment for DBS only
        sp(j,ts)=1/dt;
            for i=td+1:length(t)-1
                u(j,(i+1)) = u(j,i) + dt*(-(u(j,i)/tauf(q,p))+U(q,p)*(1-
u(j,i))*sp(j,i-td));
                x(j,(i+1)) = x(j,i) + dt*((1/taud(q,p))*(1-x(j,i)) -
u(j,i+1)*x(j,i)*sp(j,i-td));
                I(j,(i+1)) = I(j,i) + dt*((-1/taus)*I(j,i) +
A(q,p)*u(j,i+1)*x(j,i)*sp(j,i-td));
                Iwo(j,(i+1)) = Iwo(j,i) + dt*((-1/taus)*Iwo(j,i) +
A(q,p)*sp(j,i-td));
                v(j,(i+1)) = v(j,i) + dt*(((-v(j,i)+r*I(j,i)))/tau_memb);
                %Replace I with Iwo for no depletion of synaptic conduction
                V(j,(i+1)) = V(j,i) + (dt/Cm)*(((El-V(j,i))/Rm) +Ie +
w*I(j,i) + poiss(i)+ kisi(i));
                    if  V(j,i+1)>= Vth+kisi(i)
                        V(j,i)=0+kisi(i);
                        V(j,i+1)=Vreset+kisi(i);
                    end
            end
            %replace I with Iwo for no depletion
        PSC(q,p,j,:)= w*I(j,:); %IPSC(p,j,:)= -I(j,:);
        PSP(q,p,j,:)= w*v(j,:); %IPSP(p,j,:)= -v(j,:);
        Vn(q,p,j,:)= V(j,:);

    end
end
end

PSC_exc=sum(PSC(1,:,:,:),2);
PSC_inh=sum(PSC(2,:,:,:),2);
PSC_all=PSC_exc+PSC_inh;

PSP_exc=sum(PSP(1,:,:,:),2);
PSP_inh=sum(PSP(2,:,:,:),2);
PSP_all=PSP_exc+PSP_inh;

for j=1:length(fdbs)
for i=1:length(t)-1
                V_all(j,(i+1)) = V_all(j,i) + (dt/Cm)*(((El-V_all(j,i))/Rm)
+ PSC_all(1,1,j,i) +Ie + poiss(i) + kisi(i));
                    if  V_all(j,i+1)>= Vth+kisi(i)
                        V_all(j,i)=0+kisi(i);
                        V_all(j,i+1)=Vreset +kisi(i);
                    end
end
end
```

```
%% Make figure with arbitrary selection of synapse and DBS frequency
(Figure 4 in the paper)
EI=1;    % Choose 1 for excitatory and 2 for inhibitory
syn=1;   % Choose 1 for F, 2 for D and 3 for P synaptic types
freq=1;  % The desired DBS frequency to be illustrated
figure;
ax1=subplot(4,1,1);
hold on
title(['Neuron activity pattern from excitatory synapses at DBS
',num2str(fdbs),'Hz'],'FontSize',14,'FontWeight','bold')
plot(t,sp(freq,:),'LineWidth',1); zoom xon;
ylabel('Input','FontSize',13,'FontWeight','bold')
ax2=subplot(4,1,2);
plot(t,squeeze(PSC(EI,syn,freq,:)),'LineWidth',1); ylabel('EPSC
(nA)','FontSize',13,'FontWeight','bold')
hold on
plot(t,squeeze(PSC(EI,syn+1,freq,:)),'LineWidth',1); ylabel('EPSC
(nA)','FontSize',13,'FontWeight','bold')
hold on
plot(t,squeeze(PSC(EI,syn+2,freq,:)),'LineWidth',1); ylabel('EPSC
(nA)','FontSize',13,'FontWeight','bold')
legend('F','D','P')
ylim([0 15])
ax3=subplot(4,1,3);
plot(t,squeeze(PSC_all(1,1,freq,:)),'LineWidth',1);
ylabel('Total EPSC (nA)','FontSize',13,'FontWeight','bold')
ylim([0 15])
ax4=subplot(4,1,4);
plot(t,squeeze(Vn(EI,syn,freq,:)),'LineWidth',1);
hold on
plot(t,Vin,'--','Color','r','LineWidth',1);
legend('with TM synaptic dynamics','without TM synaptic dynamics')
ylabel({'Model neurn potential';' with and without synapse';'
(mv)'},'FontSize',13,'FontWeight','bold')
xlabel('Time (ms)','FontSize',13,'FontWeight','bold');
ylim([-100 5])
linkaxes([ax1,ax2,ax3,ax4],'x')
%% Compute firing rate of the LIF neuron without synaptic input:
r_isi_without_syn=(1000/dt)*length(find(Vin(dbsi:dbsf)>=Vth))/((dbsf-
dbsi));
disp(['LIF rate without any synaptic connection =
',num2str(r_isi_without_syn),' (Hz)'])
%% Compute firing rate of the LIF neuron with synaptic input:
r_isi_with_syn=(1000/dt)*length(find(Vn(EI,syn,freq,dbsi:dbsf)>=Vth))/((dbs
f-dbsi));
disp(['LIF rate with a fraction of synapses during
DBS',num2str(freq*10),'Hz = ',num2str(r_isi_with_syn),' (Hz)'])
%% Compute firing rate of the LIF neuron with all synaptic inputs:
r_isi_with_all_syn=(1000/dt)*length(find(V_all(freq,dbsi:dbsf)>=Vth))/((dbs
f-dbsi));
disp(['LIF rate with all synapses during DBS', num2str(freq*10),'Hz =
',num2str(r_isi_with_all_syn),' Hz'])
%% Raster plot (Figure 5 in the paper) and PSTH for 130 Hz:
for q=1
    for sq=1:2
dbsT=round((1000/fdbs(q)/dt));
width=1;
edges=0:width:dbsT;
psth=zeros(1,round(dbsT/width)+1);
figure;
```

```
title(['LIF neuron raster plot at DBS ',num2str(fdbs(q)),' Hz, fidelity=
',num2str(fid*100),'%'],'FontSize',14,'FontWeight','bold');
xlabel('DBS pulse time period(ms)','FontSize',13);
ylabel('Stimulation time(sec)','FontSize',13);
hold on

if sq==1
for i=dbsi:dbsT:dbsf-dbsT
    [xx,zz]=find(V_all(q,(i:i+dbsT))>=Vth);
    hh=hist(zz,edges);
    psth=psth+hh;
scat=scatter(zz*dt,(i*dt/1000)*ones(1,length(xx)),'k','filled'); hold on
end
axis ij
%axis off
xlim([0 dbsT*dt])
%  ylim([0 60])

figure;
plot(edges*dt,psth,'LineWidth',1);
xlabel('DBS pulse time period (ms)')
ylabel('Number of spikes')
xlim([0 dbsT*dt])
hold on
set(gca,'FontSize',14,'FontWeight','bold')
% saveas(fig,['DBS_',num2str(fdbs(q)),num2str(fid),'fidelity'],'jpg')
end

if sq==2
for i=dbsi:dbsT:dbsf-dbsT
    [xx,zz]=find(V_all(q,(i:i+dbsT))>=Vth);
    hh=hist(zz,edges);
    psth=psth+hh;
scat=scatter(zz*dt,(i*dt/1000)*ones(1,length(xx)),121,'k','square','MarkerF
aceColor','k'); hold on
end
axis ij
% axis off
xlim([0 dbsT*dt])
% ylim([42 42.2])
set(gca,'FontSize',14,'FontWeight','bold')
end
    end
end
toc
```

MATLAB code for MLIF Neuron Model

```
%%%%%% This code computes an MLIF neuron activity before and during DBS.
tic
clearvars

% transmission + synaptic delay: td
td=2; %2 ms for trasmission and .5 ms for synaptic delay

dt=1; ti=dt; tf=1500+td;%tf=1500+td;%tf=61000+td; %in mili seconds
t=ti:dt:tf;

% DBS input
fdbs=130;
T=ones(1,length(fdbs));
% dbsi=(100)/dt; dbsf=1100/dt; %in mili seconds
dbsi=(dt)/dt; dbsf=1500/dt;

%Poissonian input
fr=10; %for fr Hz baseline poissonian firing from other cells
[spikes,tsp]=poissonSpikeGen(fr,tf/1000,1,dt/1000);
tp=find(spikes==1);
% ssp=zeros(1,length(t));
% ssp(tp)=1; %uncomment for stochastic model (adding noise to the system)

%noise term
% wght=0;   %no noise
wght=.5; %default noise
% wght=5;   %high noise
kisi=wght*randn(1,length(t));

% I Kernel time constant
taus=3;  %For excitatory synapse

% transmission + synaptic delay: td
td=td/dt; %convert to simulation step scale

%input spike train
sp=zeros(length(fdbs),length(t));

% Synapse parameters % Each column 1,2,3 means F,D,P respectively and each
row means
% Excitatory and inhibitory synapse (1: excitatory, 2: inhibitory)
% In this study we just used the first row, excitstory synapses.
tauf=[670,17,326; 376,21,62];
taud=[138,671,329; 45,706,144];
U=[.09,.5,.29; .016,.25,.32];
A=[.0025,.0025,.0025; .0025,.0025,.0025];
% n=10; A=n*A;  % change the strength of A (order of magnitude of totall
number of synapses)
ie=ones(1,2);
w=1;

fid=2.5; %synaptic fidelity
we=fid*200; wi=0;
% Percentage of excitatory and inhibitory synapses:
ne=we*[45,38,17]; %original: 45,38,17
% ne=zeros(1,3);
```

```
% for 1 synapse n1=1 and so forth (approximately giving 2 pA exc. current)
% ne=10;  % for 10 synapses (approximately giving 20 pA exc. current)
% ne=100; % for 100 synapses (approximately giving 200 pA exc. current)
% ne=1000;% for 1000 synapses (approximately giving 2 nA exc. current)
% ni=wi*[13,10,6];     % for 1 synapse (approximately giving 10 pA
inhibitory current)
ni=wi*[8,76,16]; %ne=ni;
% ni=zeros(1,3);
% ni=10;  % for 10 synapses (approximately giving 100 pA inh. current)
% ni=100; % for 100 synapses (approximately giving 1 nA inh. current)
% ni=1000;% for 1000 synapses (approximately giving 10 nA inh. current)
A=[ne.*A(1,:);ni.*A(2,:)];

% Compute EPSC
u=zeros(length(fdbs),length(t));
x=ones(length(fdbs),length(t));
I=zeros(length(fdbs),length(t));
Iwo=zeros(length(fdbs),length(t));
% It=zeros(length(fdbs),length(t));
PSC=zeros(length(ie),length(A),length(fdbs),length(t));
% IPSC=zeros(length(A),length(fdbs),length(t));

% Compute EPSP (passive mechanism, membrane potential)
tau_memb=40;
r=10^2;   %M Ohm
v=zeros(length(fdbs),length(t));
PSP=zeros(length(ie),length(A),length(fdbs),length(t));
% IPSP=zeros(length(A),length(fdbs),length(t));

% % % Neuron parameters: (for ~20 Hz base firing .56 and for ~8-10 Hz
choose .26)
Cm= 1; Rm=100; Ie=.26; %(for deterministic model)
% Ie=.16; %subthreshold firing (for noise purpose, stochastic model)
El=-70; Vth=-54;
Vreset=-80;



% % % Neuron parameters: (for 62.5 Hz base firing)
% Cm= 1; Rm=100; %Ie=1.52; %(for deterministic model)
% Ie=.18;  %subthreshold firing (for noise purpose, stochastic model)
% El=-70;Vth=-54;
% Vreset=-80;

% Compute neuron firing pattern with and without synaptic input:
V=zeros(length(fdbs),length(t));
Vn=zeros(length(ie),length(A),length(fdbs),length(t));

V_all=zeros(length(fdbs),length(t));
d=linspace(-0.5*10^(-4),0.5*10^(-4),1502);
q1=d.*ones(1,length(t));
tau_m=zeros(1,length(t));
o=linspace(-0.75,0.25,1502);
psi=o.*ones(1,length(t));
M=zeros(1,length(t));
% Vn_all=zeros(length(ie),length(A),length(fdbs),length(t));
Vin=zeros(1,length(t));

wk=10; %Poissonian weight;
poiss=wk*rand(1,length(sp)).*sp(1,:);
for i=1:length(t)-1
```

```
      if q1(i)<(-0.5*10^(-4))
        M(i)=20000;
    elseif q1(i)>=(-0.5*10^(-4)) & q1(i)<(0.5*10^(-4))
        M(i)=10^(4)+(-1.99)*10^(8)*q1(i);
    else
        M(i)=100;
    end
    if psi(i)<(-0.75)
        tau_m(i)=20000*q1(i)/Vin(i);
    elseif psi(i)>=(-0.75) & psi(i)<(0.25)
        tau_m(i)=(10^(4)*q1(i)/Vin(i))+((-1.99)*10^(8)*q1(i)*q1(i))/Vin(i);
    else
        tau_m(i)=100*q1(i)/Vin(i);
    end


Vin(i+1) = Vin(i)+ (dt/tau_m(i))*(El-Vin(i) + M(i)*(Ie+ poiss(i) +
kisi(i)));
if Vin(i+1)>= Vth+kisi(i)
    Vin(i)=0+kisi(i);
    Vin(i+1)=Vreset+kisi(i);
end
end

for q=1:length(ie)
    if q==1
        w=1;
    else
        w=-1;
    end
for p=1:length(A)
    for j=1:length(fdbs)
        T(j)=round((1000/fdbs(j))/dt);
        dbs=dbsi:T(j):dbsf;
        ts=[tp,dbs]; %uncomment for Poissonian+DBS
%         ts=dbs;      %uncomment for DBS only
        sp(j,ts)=1/dt;
            for i=td+1:length(t)-1
                u(j,(i+1)) = u(j,i) + dt*(-(u(j,i)/tauf(q,p))+U(q,p)*(1-
u(j,i))*sp(j,i-td));
                x(j,(i+1)) = x(j,i) + dt*((1/taud(q,p))*(1-x(j,i)) -
u(j,i+1)*x(j,i)*sp(j,i-td));
                I(j,(i+1)) = I(j,i) + dt*((-1/taus)*I(j,i) +
A(q,p)*u(j,i+1)*x(j,i)*sp(j,i-td));
                Iwo(j,(i+1)) = Iwo(j,i) + dt*((-1/taus)*Iwo(j,i) +
A(q,p)*sp(j,i-td));
                v(j,(i+1)) = v(j,i) + dt*(((-v(j,i)+r*I(j,i)))/tau_memb);
                %Replace I with Iwo for no depletion of synaptic conduction
                V(j,(i+1)) = V(j,i) + (dt/tau_m(i))*(El-Vin(i) +
M(i)*(w*I(j,i) +Ie+ poiss(i) + kisi(i)));
                    if  V(j,i+1)>= Vth+kisi(i)
                        V(j,i)=0+kisi(i);
                        V(j,i+1)=Vreset+kisi(i);
                    end
            end
            %replace I with Iwo for no depletion
        PSC(q,p,j,:)= w*I(j,:); %IPSC(p,j,:)= -I(j,:);
        PSP(q,p,j,:)= w*v(j,:); %IPSP(p,j,:)= -v(j,:);
        Vn(q,p,j,:)= V(j,:);
```

```
    end
end
end

PSC_exc=sum(PSC(1,:,:,:),2);
PSC_inh=sum(PSC(2,:,:,:),2);
PSC_all=PSC_exc+PSC_inh;

PSP_exc=sum(PSP(1,:,:,:),2);
PSP_inh=sum(PSP(2,:,:,:),2);
PSP_all=PSP_exc+PSP_inh;

for j=1:length(fdbs)
for i=1:length(t)-1
                V_all(j,(i+1)) = V_all(j,i) + (dt/tau_m(j,i))*(El-
V_all(j,i)+ M(j,i)*(PSC_all(1,1,j,i) +Ie+ poiss(i) + kisi(i)));
                    if  V_all(j,i+1)>= Vth+kisi(i)
                        V_all(j,i)=0+kisi(i);
                        V_all(j,i+1)=Vreset +kisi(i);
                    end
end
end

%% Make figure with arbitrary selection of synapse and DBS frequency
(Figure 4 in the paper)
EI=1;    % Choose 1 for excitatory and 2 for inhibitory
syn=1;   % Choose 1 for F, 2 for D and 3 for P synaptic types
freq=1;  % The dseired DBS frequency to be illustrated
figure;
ax1=subplot(4,1,1);
hold on
title(['Neuron activity pattern from excitatory synapses at DBS
',num2str(fdbs),'Hz'],'FontSize',14,'FontWeight','bold')
plot(t,sp(freq,:),'LineWidth',1); zoom xon;
ylabel('Input','FontWeight','bold')
ax2=subplot(4,1,2);
plot(t,squeeze(PSC(EI,syn,freq,:)),'LineWidth',1); ylabel('EPSC
(nA)','FontSize',13,'FontWeight','bold')
hold on
plot(t,squeeze(PSC(EI,syn+1,freq,:)),'LineWidth',1); ylabel('EPSC
(nA)','FontSize',13,'FontWeight','bold')
hold on
plot(t,squeeze(PSC(EI,syn+2,freq,:)),'LineWidth',1); ylabel('EPSC
(nA)','FontSize',13,'FontWeight','bold')
legend('F','D','P')
ylim([0 15])
ax3=subplot(4,1,3);
plot(t,squeeze(PSC_all(1,1,freq,:)),'LineWidth',1);
ylabel('Total EPSC (nA)','FontWeight','bold')
ylim([0 15])
ax4=subplot(4,1,4);
plot(t,squeeze(Vn(EI,syn,freq,:)),'LineWidth',1);
hold on
plot(t,Vin,'--','Color','r','LineWidth',1);
legend('with TM synaptic dynamics','without TM synaptic dynamics')
ylabel({'Model neuron potential';' with and without synapse';'
(mv)'},'FontSize',13,'FontWeight','bold')
xlabel('Time (ms)','FontWeight','bold');
ylim([-100 5])
linkaxes([ax1,ax2,ax3,ax4],'x')
```

```
%% Compute firing rate of the LIF neuron without synaptic input:
r_isi_without_syn=(1000/dt)*length(find(Vin(dbsi:dbsf)>=Vth))/((dbsf-
dbsi));
disp(['MLIF rate without any synaptic connection =
',num2str(r_isi_without_syn),' (Hz)'])
%% Compute firing rate of the LIF neuron with synaptic input:
r_isi_with_syn=(1000/dt)*length(find(Vn(EI,syn,freq,dbsi:dbsf)>=Vth))/((dbs
f-dbsi));
disp(['MLIF rate with a fraction of synapses during
DBS',num2str(freq*10),'Hz = ',num2str(r_isi_with_syn),' (Hz)'])
%% Compute firing rate of the LIF neuron with all synaptic inputs:
r_isi_with_all_syn=(1000/dt)*length(find(V_all(freq,dbsi:dbsf)>=Vth))/((dbs
f-dbsi));
disp(['MLIF rate with all synapses during DBS', num2str(freq*10),'Hz =
',num2str(r_isi_with_all_syn),' Hz'])
%% Raster plot (Figure 5 in the paper) and PSTH for 130 Hz:
for q=1
    for sq=1:2
dbsT=round((1000/fdbs(q)/dt));
width=1;
edges=0:width:dbsT;
psth=zeros(1,round(dbsT/width)+1);
figure;
title(['MLIF neuron raster plot at DBS ',num2str(fdbs(q)),' Hz, fidelity=
',num2str(fid*100),'%'],'FontSize',14,'FontWeight','bold');
xlabel('DBS pulse time period(ms)','FontSize',13);
ylabel('Stimulation time(sec)','FontSize',13);
hold on

if sq==1
for i=dbsi:dbsT:dbsf-dbsT
    [xx,zz]=find(V_all(q,(i:i+dbsT))>=Vth);
    hh=hist(zz,edges);
    psth=psth+hh;
scat=scatter(zz*dt,(i*dt/1000)*ones(1,length(xx)),16,'k','filled'); hold on
end
axis ij
% axis off
xlim([0 dbsT*dt])
% ylim([0 60])

figure;
plot(edges*dt,psth,'LineWidth',1);
xlabel('DBS pulse time period (ms)')
ylabel('Number of spikes')
xlim([0 dbsT*dt])
hold on
set(gca,'FontSize',14,'FontWeight','bold')
% saveas(fig,['DBS_',num2str(fdbs(q)),num2str(fid),'fidelity'],'jpg')
end

if sq==2
for i=dbsi:dbsT:dbsf-dbsT
[xx,zz]=find(V_all(q,(i:i+dbsT))>=Vth);
hh=hist(zz,edges);
psth=psth+hh;
scat=scatter(zz*dt,(i*dt/1000)*ones(1,length(xx)),121,'k','square','MarkerF
acecolor','k'); hold on
end
axis ij
% axis off
```

```
xlim([0 dbsT*dt])
% ylim([42 42.2])
set(gca,'FontSize',14,'FontWeight','bold')
end
    end
end
toc
```

REFERENCES:

[1] Guanrong Chen, Jorge L. Moiola, “An overview of bifurcation, chaos and nonlinear dynamics in control systems”, Journal of the Franklin Institute, Volume 331, Issue 6, 1994, ISSN 0016-0032.

[2] Duane Q. Nykamp, “The idea of a dynamical system”, mathinsight.org

[3] Hiroki Sayama, Introduction to the Modeling and Analysis of Complex Systems, chapter 3,2015,ISBN 13: 9781942341093

[4] Victor Kamdoum Tamba, Francois Kapche Tagne, Arsene Loic Mbanda Biamou, Manuela Corazon Nkeing, Armand Nzeukou Takougang,Chapter 7 - Hidden extreme multistability generated from a novel memristive two-scroll chaotic system, Editor(s): Christos Volos, Viet-Thanh Pham, In Advances in Nonlinear Dynamics and Chaos (ANDC), Mem-elements for Neuromorphic Circuits with Artificial Intelligence Applications,Academic Press,2021,Pages 147-164,ISBN 9780128211847.

[5] Huzaifa Kapasi, Modeling Non-Linear Dynamic Systems with Neural Networks,Towards Data Science,2020.

[6] S. Simrock, “Control Theory III”, CERN Accelerator School, 2007.

[7] S. Chartier, P. Renaud, and M. Boukadoum, ‘A nonlinear dynamic artificial neural network model of memory’, *New Ideas in Psychology*, vol. 26, no.2, pp. 252–277, Aug. 2008, doi: 10.1016/j.newideapsych.2007.07.005.

[8] G. Nicolis, *NON-LINEAR SYSTEMS*, Thermopedia, 2011, doi:10.1615/AtoZ.n.nonlinear_systems.

[9] P. Mellodge, ‘Characteristics of Nonlinear Systems’, *A Practical Approach to Dynamical Systems for Engineers*, Elsevier, 2016, pp. 215–250. doi: 10.1016/B978-0-08-100202-5.00004-8.

[10] G. Espinosa-Paredes, ‘Nonlinear BWR dynamics with a fractional reduced order model’, *Fractional-Order Models for Nuclear Reactor Analysis*, Elsevier, 2021, pp. 247–295. doi: 10.1016/B978-0-12-823665-9.00007-9.

[11] H. Fathabadi, ‘Behavior of Limit Cycles in Nonlinear Systems’, International Journal of Information and Electronics Engineering, Vol. 2, No. 4, July 2012, doi: 10.7763/IJIEE.2012.V2.152.

[12] E. Ott, C. Grebogi and J. A. Yorke, “Controlling chaos”, Phys. Rev. Lett., Vol. 64, pp. 1196-1199, 1990.

[13] E. A. Jackson, “Perspectives of Nonlinear Dynamics”, Vols 1 and 2, Cambridge University Press, New York, 1990.
[14] Brain Basics: The Life and Death of a Neuron | National Institute of Neurological Disorders and Stroke
[15] Synapses | Anatomy and Physiology I
[16] What are neurotransmitters? - Queensland Brain Institute - University of Queensland
[17] https://qbi.uq.edu.au/brain-basics/brain/brain-physiology/action-potentials-and-synapses
[18] Neurosurgical-Conditions-and-Treatments/Deep-Brain-Stimulation, American Association of Neurological Surgeons.
[19] Deep brain stimulation mechanisms: the control of network activity via neurochemistry modulation – McIntyre, Journal of Neurochemistry - Wiley Online Library, 2016.
[20] https://www.ncbi.nlm.nih.gov/pmc/articles/PMC6851468/ - Search
[21] Anderson TR, Hu B, Iremonger K, Kiss ZH. Selective attenuation of afferent synaptic transmission as a mechanism of thalamic deep brain stimulationinduced tremor arrest. J Neurosci 2006;26(3):841e50.
[22] Milosevic L, Kalia SK, Hodaie M, Lozano AM, Popovic MR, Hutchison WD. Physiological mechanisms of thalamic ventral intermediate nucleus stimulation for tremor suppression. Brain 2018;141(7):2142e55
[23] V. Keshmiri, ‘A Study of the Memristor Models and Applications’, Linkoping University, 2014
[24] Mohanty, Saraju, Memristor: From Basics to Deployment. Potentials, IEEE, 32. 34-39, 2013 10.1109/MPOT.2012.2216298.
[25] W. Xu, J. Wang, and X. Yan, ‘Advances in Memristor-Based Neural Networks’, Frontiers in Nanotechnology, vol. 3, 2021, doi: 10.3389/fnano.2021.645995.
[26] Nafea, Sherief & Dessouki, Ahmed & El-Rabaie, El-Sayed. (2015). Memristor Overview up to 2015. 24. 79-106. 10.21608/mjeer.2015.64132.
[27] B. Widrow, “An Adaptive ADALINE Neuron Using Chemical MEMISTORS,” no. 1553–2, 1960.
[28] Ho Yenpo & Huang, Garng & Li, Peng. (2011). Dynamical Properties and Design Analysis for Nonvolatile Memristor Memories. Circuits and Systems I: Regular Papers, IEEE Transactions on. 58. 724 - 736. 10.1109/TCSI.2010.2078710.
[29] Frank Y. Wang, “Memrister for introductory physics”, Preprint arXiv:0808.0286.2008

[30] A. G. Radwan, M. A. Zidan, and K. N. Salama, “On The Mathematical Modeling Of Memristors,” inProceedings of the International Conference on Microelectronics, 2010, pp. 284 –287 .
[31] Farokhniaee AmirAli-g, McIntyre CC, Theoretical principles of deep brain stimulation induced synaptic suppression, Brain Stimulation, https://doi.org/10.1016/j.brs.2019.07.005
[32] Fang X, Liu D, Duan S and Wang L (2022) Memristive LIF Spiking Neuron Model and Its Application in Morse Code. Front. Neurosci. 16:853010.doi: 10.3389/fnins.2022.8530